84

SUR/FIN

American Electroplaters' Society
SUR/FIN '84

71st Annual Technical Conference

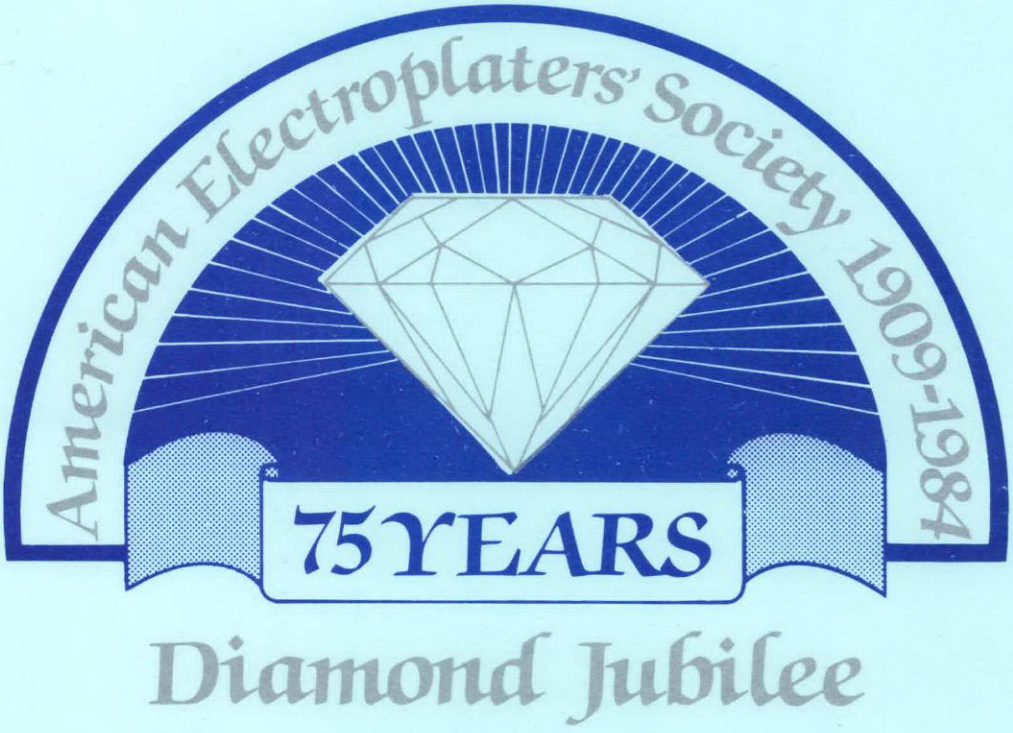


July 16-19, 1984
New York Hilton
New York, NY

## Session G - Light Metals Finishing II

AMERICAN ELECTROPLATERS' SOCIETY, INC.

71ST ANNUAL TECHNICAL CONFERENCE - NEW YORK CITY

LIGHT METALS FINISHING II

SESSION G

Page No.

Recovery of Phosphoric Acid by Ion Exchange and Evaporation.....G-1

Craig Brown, Eco-Tec Limited, Pickering, Ontario, Canada

Impact of Formation Time and Current Density on Barrier Anodizing Quality..G-2

Dr. S. K. Doss and G. A. Condas, IBM Corp., San Jose, CA

Film Growth on Aluminum Alloys During AC Anodizing in Sulphuric and Oxalic Acid Solutions.....G-3

Dr. J. Zahavi, H. Kerbel and O. Korotkina, Israel Institute of Metals, Technion, Haifa, Israel

Corrosion Studies With The Rotated Aluminum Electrode (R.Al.E.).....G-4

Dr. W. E. Dalton, St. John's University, Jamaica, NY

A Continuous Flow Caustic Etch Regeneration Process.....G-5

Raymond J. Meyer, Aluminum Company of America, Alcoa Center, PA

New Chemical Polishing Process of Aluminum Without the Use of Toxic Nor Nutritious Compositions and Fumes.....G-6

Dr. Sakae Tajima, Environmental and Resources Research Institute (NRI), Tokyo University of Agriculture and Tokyo City University, Japan

G-1

# Light Metals Finishing II
# Session G

## Recovery of Phosphoric Acid by Ion Exchange and Evaporation

Craig Brown
Eco-Tec Limited
Pickering, Ontario, Canada

# RECOVERY OF PHOSPHORIC ACID BY ION EXCHANGE AND EVAPORATION

by: Craig Brown P.Eng.
Eco-Tec Limited,
925 Brock Rd. S.,
Pickering, Ontario,
Canada L1W 2X9.

## 1.0 Phosphoric Acid Aluminum Bright Dips

Concentrated phosphoric acid based solutions are used to chemically polish aluminum prior to sulfuric acid anodizing. The cost of this phosphoric acid represents a significant portion of the total finishing cost.

Aluminum phosphate accumulates during use because of etching of the metal and reaches optimum at Al=15-45 g/l. Up to 15 grams of aluminum are etched for each square meter of work processed. Excessive buildup of aluminum contamination in the bath is not usually a serious problem however, since the high dragout rate of these highly viscous solutions provides a natural means of removing the aluminum.

In order to re-coup part of the dragout loss, most aluminum finishers operate a countercurrent rinse system to yield a 35% acid solution from the first rinse which can be sold for fertilizer. To increase the recovery efficiency, a few installations have utilized vacuum evaporators to allow increased rinsewater flows and to concentrate the rinse water to about 70%. The evaporator concentrate cannot be recycled to the bright dip bath since this would "close the loop" on the aluminum contamination and quickly foul the bath.

Cation exchange can be utilized to remove the aluminum contamination from the rinsewater prior to evaporative concentration. Over the years several systems have been installed of this type, however no systems employing conventional cation exchange technology are believed to be operating successfully today.

The principle problems associated with these ion exchange systems have been: 1) excessive regenerant consumption with the attendant high waste disposal expense, 2) excessive phosphoric acid product dilution and 3) large physical size.

The reciprocating flow ion exchange or "Recoflo" technique has been used effectively for the recovery of a wide variety of metal finishing chemicals over the last dozen or so years. Through its use of fine mesh resins, countercurrent regeneration, low exchange loadings and short resin beds, this patented

technique has overcome many of the limitations of conventional ion exchange technology in this type of application. The results of a laboratory program to determine the feasibility of utilizing this technology for phosporic acid recovery were presented to this conference in 1982.

## 2.0 The Recoflo Phosphoric Acid Recovery System

There are three major components in the recovery system: the decationizer unit or "DCU", the acid purification unit or "APU" and the evaporator.

### 2.1 The DCU

The DCU is employed to remove the aluminum contamination from the phosphoric acid rinsewater.

There are four basic steps in the DCU operating cycle:(see fig. 1)

1. Product

Phosphoric acid rinsewater (DCU feed) is pumped from a feed reservoir into the bottom of the bed. Aluminum and other cationic metals such as copper are removed by the cation exchange resin according to equation (1).

$$3RH + AlPO_4 \text{ ----½ } R_3Al + H_3PO_4 \qquad (1)$$

where 'R' represents cation resin.

First emerging from the top of the bed is the void of water. This solution, containing a small amount of phosphoric acid, due to mixing at the water/feed interface, is recycled to the rinse tank. Next emerges the purified phosphoric acid product which is ultimately concentrated by evaporation and recycled.

2. Feed Displacement Void

Water is introduced into the top of the bed, displacing the entrained void of partially purified feed solution from the bottom of the bed back into the feed reservoir. A small excess of water is required to accomplish this, resulting in dilution of the feed in the reservoir and ultimately the product.

3. Regeneration

Sulfuric acid regenerant is pumped into the top of the bed to regenerate the resin according to equation (2).

$$2R_3Al + H_2SO_4 \text{ (excess)} \text{ ----½ } 6RH + Al_2(SO_4)_3 + H_2SO_4 \text{ (residual)} \quad (2)$$

An excess of sulfuric acid beyond the stoichiometric quantity is required to effectively elute the aluminum from the resin.

Emerging from the bottom of the bed first is the void of entrained water followed by the spent regenerant or eluate. The liquid leaving the bottom of the bed is split into dilute and concentrated fractions.

4. Regenerant Wash

Water is pumped into the top of the bed to wash the regenerant from the resin bed. Emerging from the bottom of the bed is the void of spent regenerant or eluate followed by a very dilute acid solution containing the remaining traces of sulfuric acid left on the resin. This solution is split into dilute and concentrated fractions as before. The volume of the total concentrated fraction collected during the regeneration and regenerant wash steps is equal to to the volume of fresh regenerant solution originally admitted to the bed.

An acid purification unit or APU is employed to reclaim the residual sulfuric acid in the concentrated fraction of the eluate/wash.

The total DCU cycle takes about 40 minutes.

## 2.2 APU Operating Cycle

The APU cycle consists of two basic steps: (see fig. 2)

1. Upstroke

Acid feed solution (ie. the DCU eluate/wash fraction) is pumped from the acid reservoir into the bottom of the resin bed. Utilizing the acid retardation principle, the APU resin "sorbs" the free sulfuric acid present and rejects the aluminum sulfate. This can be represented by equation (3).

$$RH_2O + H_2SO_4 + Al_2(SO_4)_3 \text{ ----½ } RH_2SO_4 + Al_2(SO_4)_3 + H_2O \quad (3)$$

After the void of water is displaced from the top of the bed, the deacidified aluminum sulfate byproduct solution is collected.

2. Downstroke

Water is pumped into the top of the resin bed. The water desorbs the acid from the resin according to equation (4).

$$RH_2SO_4 + H_2O \text{ ----½ } RH_2O + H_2SO_4 \qquad (4)$$

After the void of acid feed solution is displaced from the bottom of the bed back to the feed reservoir, the purified acid product is collected.

The total APU cycle takes about 5 minutes.

## 2.3 Evaporator Operation

The evaporator is the forced circulation, vacuum type. The evaporator basically consists of a steam fired shell and tube reboiler, a separator, a circulation pump, a shell and tube surface condenser, vacuum pump and cooling tower (not shown).

Phosphoric acid is pumped from the separator into the bottom of the reboiler where it is heated inside the tubes to the boiling point. The boiling liquid leaving the reboiler enters the side of the separator. The water vapor disengages from the liquid, rising through a demister pad located in the top of the separator and over to the condenser. Water vapor condenses inside the tubes of the condenser, collecting in a receiving chamber in the bottom section of the condenser. A condensate pump removes the condensed water from the evaporator. A vacuum pump removes any noncondensable gases present (ie. air) and maintains a vacuum on the unit. The condenser cooling water is recirculated through a cooling tower.

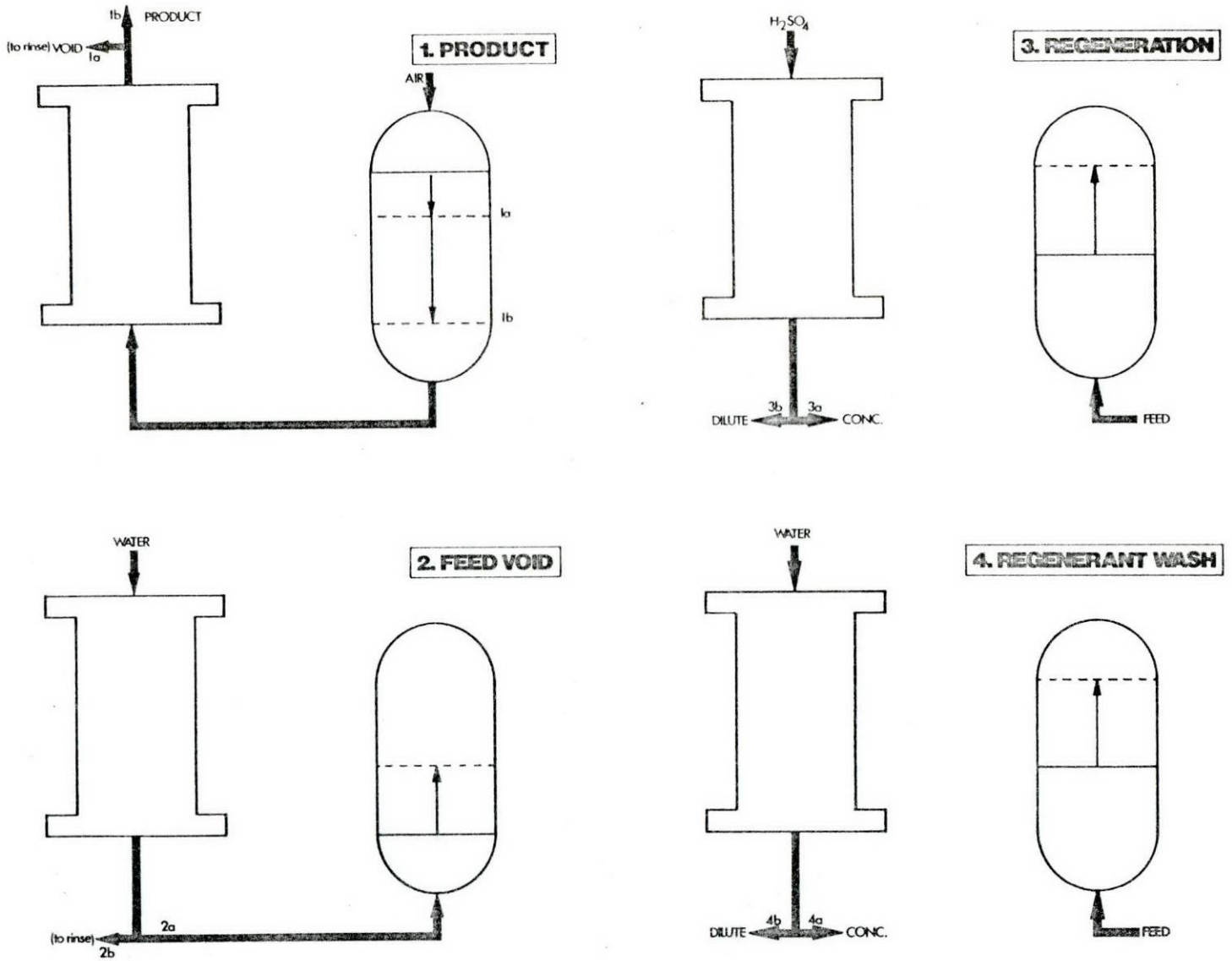


Fig. 1: DCU Operating CYCLE

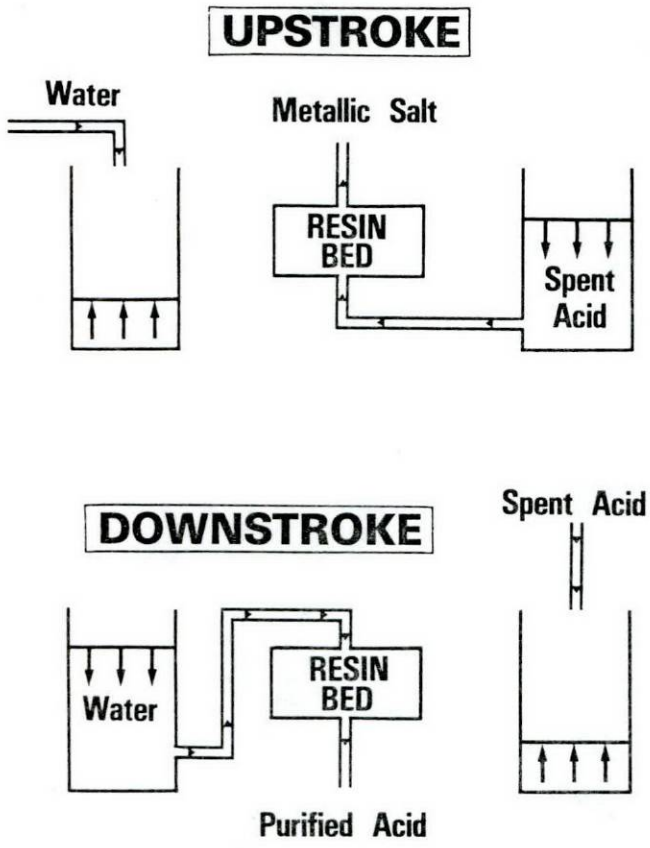


Fig. 2: APU Operating Cycle

## 3.0 System Layout and Operation

The basic layout of the system is shown in fig. 3. The bright dip bath is followed by two or three recovery rinses. To ensure a good quality final rinse prior to anodizing one or two polishing rinses should ideally be employed following the recovery rinses.

The concentration in R1 is maintained at a predetermined concentration in the 10-20% $H_3PO_4$ range by transferring rinsewater to the feed reservoir (not shown) which is located between R1 and the DCU.

The rinsewater is pumped from the feed rinsewater through the DCU. The purified phosphoric acid rinsewater produced by the DCU is then passed to the evaporator where it is concentrated up to about $H_3PO_4$ = 80%. The condensed water from the evaporator is reused in the rinse tanks, which are allowed to counterflow forward.

The DCU is regenerated with sulfuric acid. The dilute eluate/washwater fraction from the DCU flows to waste. The concentrated fraction flows to the APU. The purified sulfuric acid from the APU is refortified with virgin sulfuric acid and held for reuse by the DCU. The aluminum sulfate byproduct from the APU flows to waste.

The overflow from the polishing rinse tank flows to waste.

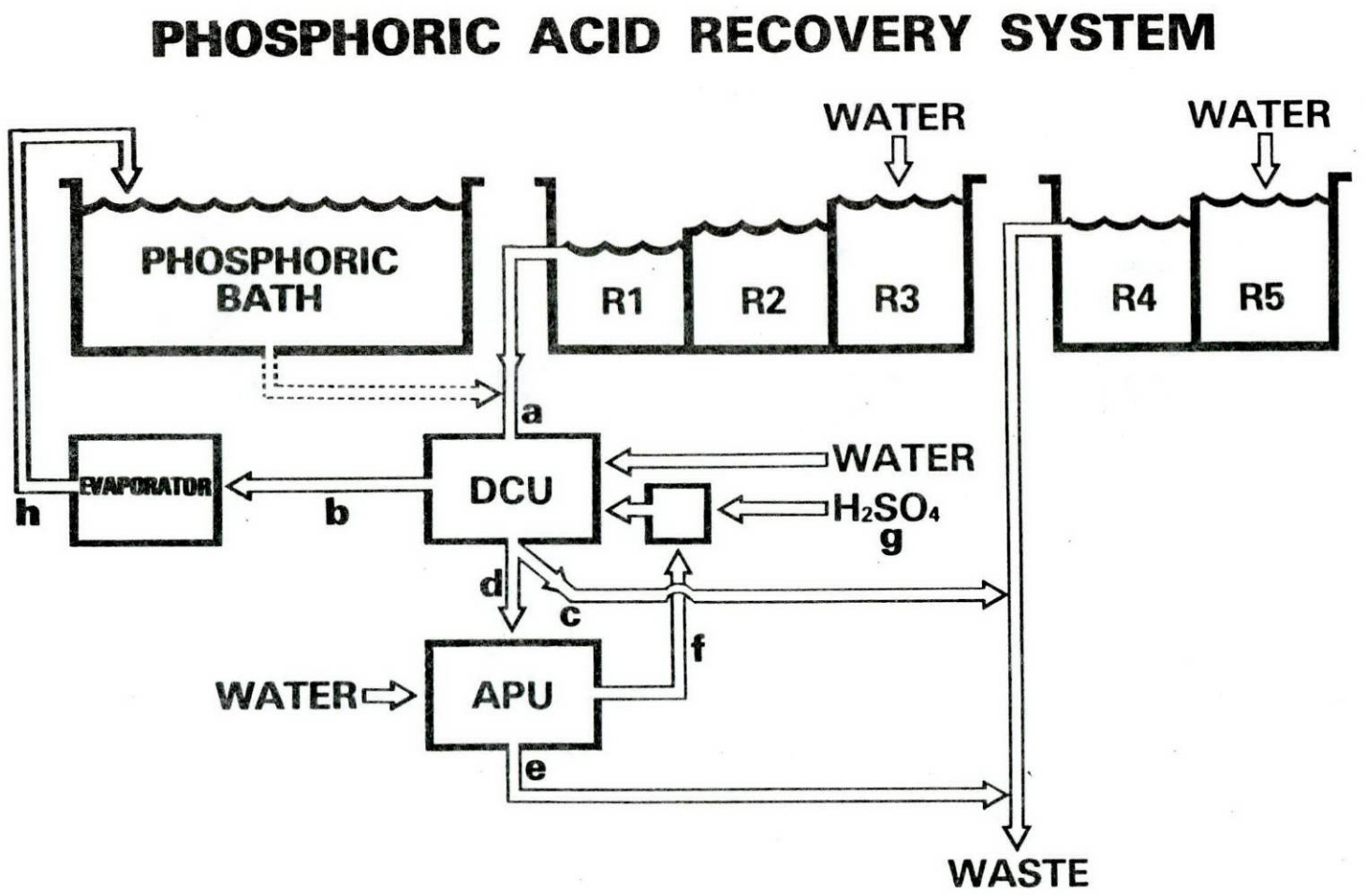


FIG. 3: SYSTEM LAYOUT

## 4.0 Field Installations

By January 1984 five installations based upon the system oulined above were in operation.

### #1. Kyoritsu Alumi, Japan

The first Recoflo phosphoric acid recovery system was started up in Japan at the Kyoritsu Alumi Co. Ltd. in March 1980. The plant was subject to severe restrictions on phosphorus discharge since the factory effluent ultimately was discharged to a lake. (See fig. 4).

This is a particularly challenging application since the bath employed is made up with approximately equal volumes of concentrated sulfuric and phosphoric acids. This made things difficult for three reasons: 1. the high acidiy of the rinsewater due to the prescence of sulfuric acid does not favor uptake of the aluminum onto the cation resin. 2. the recovered acid product has to be evaporated to a very high degree, resulting in a very high boiling point elevation. 3. the recovered acid is very corrosive, requiring special materials of construction.

The Kyoritsu system basically consists of a DCU with a 41 cm (16 inch) diameter by 61 cm (24 inch) high resin bed , an APU with a 61 cm (24 inch ) by 61 cm high resin bed and a two stage vacuum evaporator. A photgraph of the installed ion exchange equipment is shown in fig. 5.

The first stage of the evaporator is as discussed above. The separator is rubber lined steel. The reboiler is graphite. This type of unit cannot sufficiently concentrate the recovered product, however. The final concentration is done in a second stage with a hot-oil fired, mechanically agitated, glassteel reactor-type vessel.

The system has encountered no major problems since startup. The original resin is still in service and has seen only minor reductions in operating effiency over three years service. The phosphate recovery efficiency of the system was measured at 98.8% after 1 year and remains at greater than 98% after three years of operation. The APU free sulfuric acid recovery efficiency was measured at 91.9% after 1 year and is approximately 86.7% after 3 years.

Typical results for this system after 3 years operation are shown in Table I.

Table I: Kyoritsu Alumi- Typical Results

| | DCU feed (g/L) | DCU product (g/L) | EVAP conc (g/L) |
|---|---|---|---|
| total $H_3PO_4$ | 117 | 92.4 | ca 720 |
| total $H_2SO_4$ | 148.9 | 129.4 | ca 1008 |
| Al | 10.8 | 3.6 | 28-36 |

#2. Large U.S. Extruder

The second system was started up at a large U.S. extruder in September 1982. The installation is shown in fig. 5. The system employs a DCU and an APU with 91 cm (36 inch) diameter by 61 cm (24 inch) high beds each. The evaporator is manufactured in 316L stainless steel, has a 122cm (48 inch) diameter separator and has a nominal evaporative capacity of 1360 (360 GPH). The evaporator is shown in fig. 6.

Tests performed over a 5 day period shortly after startup indicated that the system was recovering approximately 93% of the phosphoric acid fed to it from the rinse system. Tests performed by plant personnel during the subsequent year of operation confirmed this figure. This is fairly consistent with the lab results. This loss occurs because of uptake of phosphate on the DCU resin with the aluminum. This sorbed phosphate is not liberated from the resin until the resin is regenerated with sulfuric acid. Our hypothesis is that a cationic aluminum phosphate complex exists in the rinsewater which exchanges on to the resin. It is interesting to note that this does not occur to the same degree with the phosphoric/sulfuric acid rinsewater treated at Kyoritsu. Apparently the complex is much weaker at lower pH's.

Prior to installation of the recovery system the plant had been consuming 0.27 kg of $H_3PO4$ per kg of aluminum processed. Subsequent to installation of the the recovery this figure dropped to 0.06 kg/kg which represents a 78% decrease in phosphoric acid purchases. According to the plant engineer, this reduction was not as large as originally anticipated for several reasons.

1. Only two recovery rinses are employed, so that dragout losses from the second rinse are significant.
2. There are several leaks in the recovery rinse tanks. Continuous operation of the line has not permitted shutdown for repair.

3. There was a change in the profile of the product mix (ie. a higher surface area and dragout to weight ratio).
4. There were some inconsistencies in the accounting procedures involved with inventory of the recovered acid.

Nevertheless the reduction is impressive.

The sulfuric acid consumption has been measured as 0.285 kg of 66 Be $H_2SO4$ per kg of 80% $H_3PO4$. It is felt that based upon the laboratory investigations that this can be reduced through fine tuning of the operating conditions of the system. It was observed that the lime consumption in the central plant waste treatment system has doubled with utilization of the recovery system. This is reasonable, considering the quantity of acid consumed by the system.

The only serious mechanical problem to date has been corrosion of the heat exchanger tubes in the evaporator reboiler after one year of continuous operation. Detailed examination of the tubes revealed that the corrsion was restricted to the weld area. Analysis of the metal in this area indicated that it was not in fact 316L. To be safe, the exchanger was replaced with alloy 20 stainless steel, although it appears that the original choice of 316L was the correct one.

Occasional problems have been experienced with the plastic diaphragm valves supplied with the system. These are being replaced with more reliable valves.

A very high concentration of suspended solids has been observed in the rinsewater feeding the system. A two stage cartridge filter system is employed with a 10 micron nominal followed by a 1 micron nominal filter. The 10 micron cartridges are changed twice each week and the 1 micron cartridges are changed weekly (7 days per week, 24 h/day operation). More economical means of filtration are currently being investigated.

To maximize rinse capture efficiency, the system is operated to hold the concentration of phosphoric acid in the rinse tanks as low as possible. This tends to increase steam consumption on the evaporator, however. There are some side benefits to this improved rinse quality. The reduction in phosphate dragout has prolonged the life of the nitric acid desmut and the sulfuric acid anodize baths. For example, the anodize bath life was increased from 3 weeks to 9 weeks. This represents an annual savings of over 7500 litres (2000 gallons) per year of concentrated sulfuric acid as well as the associated waste disposal costs.

Table II show some typical results obtained from this installation.

Table II: Large U.S. Extruder: Typical Results

| | DCU feed (g/L) | DCU prod (g/L) | APU feed (g/L) | APU prod (g/L) | APU waste (g/L) |
|---|---|---|---|---|---|
| $H_3PO_4$ (tot) | 179.4 | 138.7 | 12.5 | 7.2 | 5.93 |
| $H_2SO_4$ (free) | 148.9 | 129.4 | 112.7 | 100.5 | 16.2 |
| Al | 6.03 | 0.57 | 9.0 | 0.8 | 7.0 |

#3. Production Plating, Adel , Georgia

Approximately six years ago, Production Plating installed a phosphoric acid bright dip rinsewater recovery system consisting of a continuous countercurrent cation exchange unit and a vacuum evaporator. After working out the initial bugs in the system, it functioned well. It was found however that the spent sulfuric acid regenerant required excessive quantities of lime for neutralization and generated large amounts of calcium sulfate (gypsum) sludge which had to be disposed of offsite. The cost of neutralization and disposal seriously adversly affected the economics of the recovery system.

An APU with a 91 cm (36 inch) diameter by 61 cm (inch) high bed was started up in April 1983 to reclaim the free sulfuric acid present in the spent regenerant from the existing ion exchange unit. The unit is shown in fig. 7, installed along-side another APU installed for purification of the sulfuric acid anodizing baths.

Tests indicate that approximately 90% of the free acid in the spent ion exchange regenerant fed to the APU are being recovered.

Its interesting to note that the continuous cation exchange resin bed is approximately 30 cm (12 inch) diameter by 9140 cm (30 feet) high. A Recoflo DCU bed to accomplish this job would be 91 cm (36 inch) diameter by 61 cm (2 feet) high.

#4. Large Continuous Anodizer of Lithographic Plates

Aluminum coil stock is anodized in dilute phosphoric acid for manufacturing lithographic plates. Dragout can be controlled through use of rollers however aluminum contamination in the anodizing bath is a serious problem. The aluminum must be held at very low levels.

This plant previously installed a conventional cation exchanger for aluminum removal. An evaporator was also installed to remove water added to the bath when the phosphoric acid is rinsed from the ion exchanger. Although it was effective in controlling the aluminum contamination, this system had a number of problems. It required excessive amounts of sulfuric acid regenerant and a large amount of phosphoric acid was lost from the system. After several years of operation reliability of the ion exchange unit became a problem and the decision was made to replace it with a Recoflo DCU / APU system.

The Recoflo units were commissioned in December 1983. To date no problems have been experienced. The consumption of concentrated phosphoric acid was 604-756 L (160-200 gallons) per day with the old system. The consumption has been reduced to approximately 151 L (40 gallons) per day with installation of the new system

Phosphoric acid anodizing baths are extremely sensitive to sulfate contamination. A very small amount of sulfate contamination has been noted with both ion exchange systems, probably as a result of inadequate rinsing of the resin after regeneration. The excess sulfate is removed by precipitation with barium carbonate.

#5. General Extrusions

This system consists of a DCU with a 91 cm (36 inch) diameter by 61 cm (24 inch) high bed, an APU with a 76 cm (30 inch) diameter by 61 cm (24 inch) high bed, and a 862 L/h (228 GPH) evaporator with a 107 cm (42 inch) diameter separator. The installation which is shown in fig. 7, was fully operational in November 1983.

The performance is comparable with the large extruder discussed above, with the following exceptions:

1. The reduction in phosphoric acid purchases is greater, probably because three recovery rinses are employed and there are no tank leaks. No virgin phosphoric acid purchases were required for the first six weeks of operation.

2. More reliable diaphragm valves were employed in the original designs, so that this has not been a problem.

The system was designed so that the rinsewater is diverted to a large storage tank when the recovery system is being serviced. This stored rinsewater is then drained back into the system when service is complete. Initially, a considerable amount of solids were present in the bottom of this storage tank. These

solids, which were exceedingly fine, quickly clogged and penetrated the DCU filters and clogged the DCU resin bed. This necessitated removal and cleaning of the resin. The filtration situation is currently being monitored very closely.

Table III: General Extrusions: Typical Results

| | $H_3PO_4$ (g/L) | Al (g/L) |
|---|---|---|
| BATH | 1340 | 26.8 |
| R1 | 153.9 | NA |
| R2 | 19.1 | NA |
| R3 | 8.7 | NA |
| DCU feed | 140.5 | 2.45 |
| DCU product | 127.1 | 0.014 |
| EVAP conc | 1365 | 0.174 |

## 5.0 Summary

A new system for the recovery of phosphoric acid from aluminum bright dip rinsewaters and anodizing baths, based on Recoflo ion exchange, has been field proven. The system has demonstrated a significant improvement over other ion exchange systems with respect to equipment size, regenerant consumption and phosphoric acid recovery efficiency.

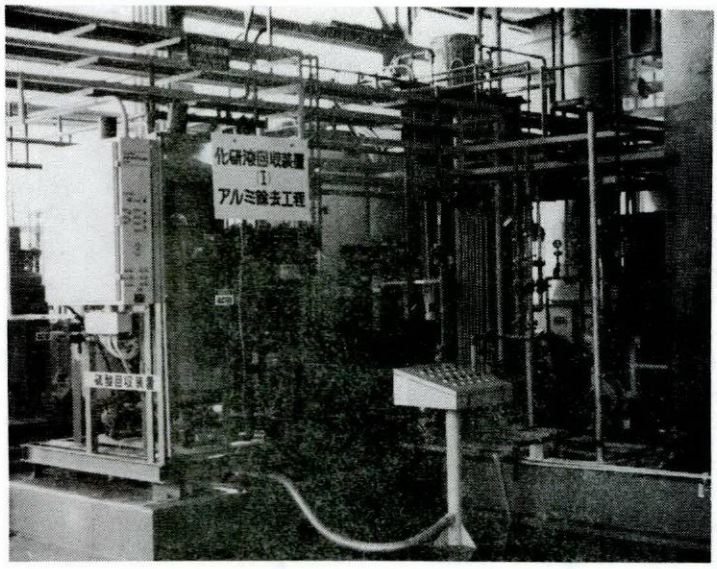


Fig. 4: DCU at Kyoritsu Alumi Co., Japan

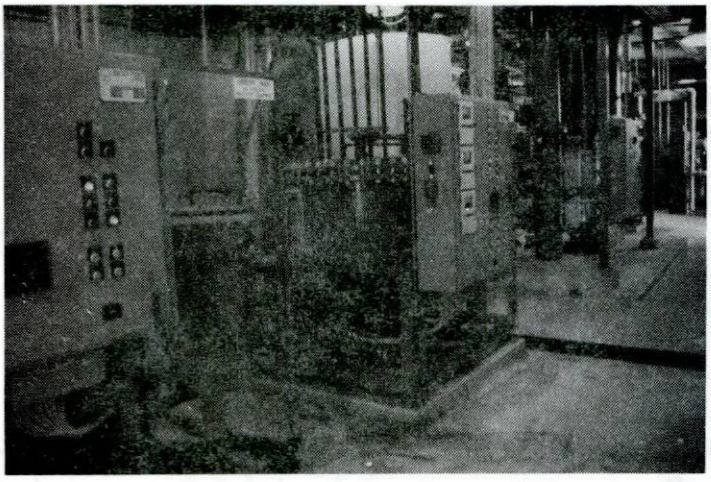

Fig. 5: (L to R) APU, DCU and evaporator at a large extrusion operation.

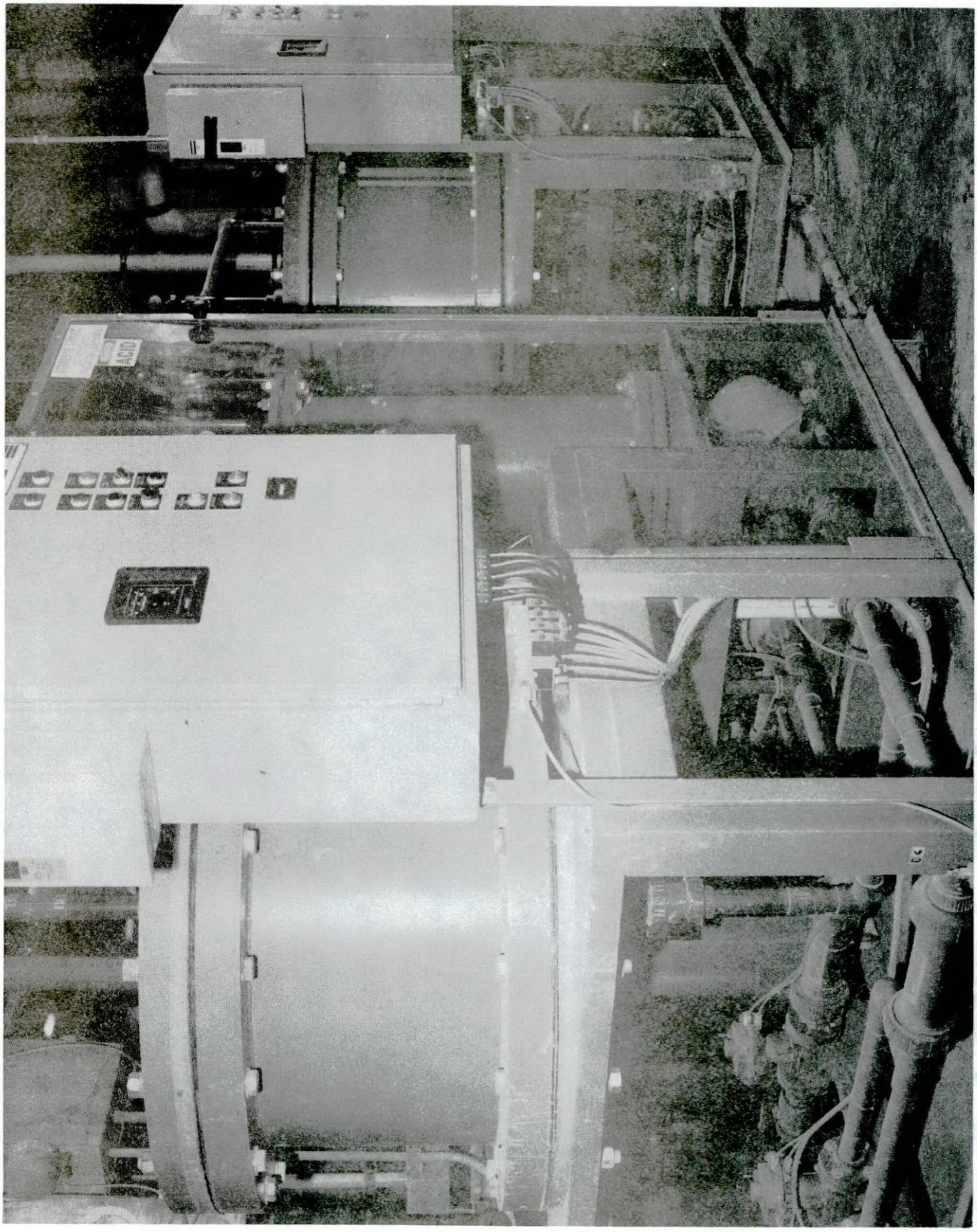

Fig. 6: APU's installed at Production Plating.

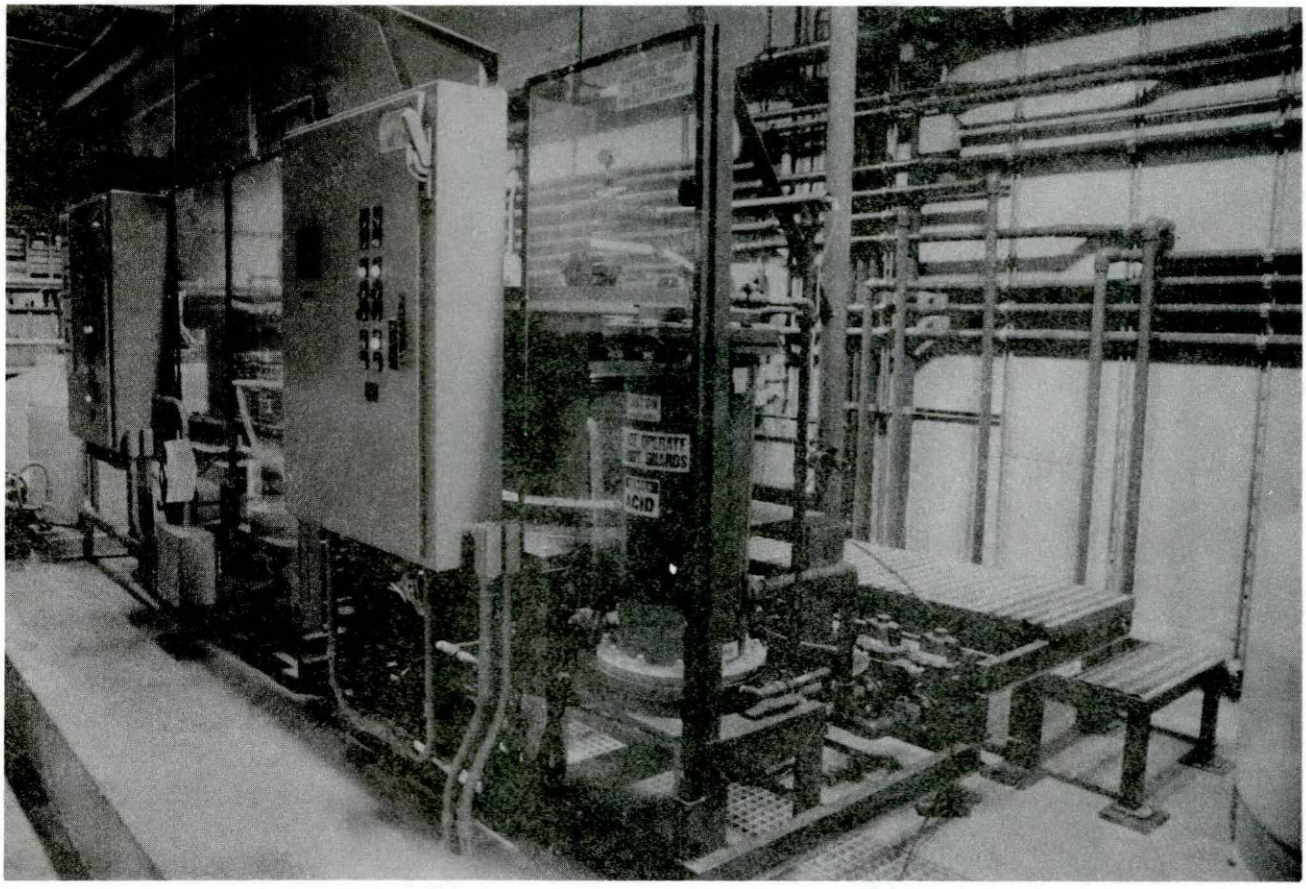

Fig. 7: (L to R) DCU and APU at General Extrusions.

G-2

# Light Metals Finishing II
# Session G

## Impact of Formation Time and Current Density on Barrier Anodizing Quality

Dr. S. K. Doss and G. A. Condas
IBM Corp.
San Jose, CA

# IMPACT OF FORMATION TIME AND CURRENT DENSITY ON BARRIER ANODIZING QUALITY

S. K. Doss and G. A. Condas
IBM San Jose, CA.

## Abstract

Barrier anodizing of aluminum over a wide range of voltages and current densities was studied. An empirical relationship was found between current density and barrier formation times ($t_1$) that allows the worker to lower the formation time; $t_1 = C\ V/J$, where V and J are the barrier's formation voltage and initial current density, respectively. This relationship was later derived based on Mott's equation and an ion drift model. It was also shown that large formation times led to a deterioration (roughening/etching) of the barrier, which could be avoided by increasing the initial current density.

## Introduction

While conventional, sulfuric acid anodizing of aluminum produces a porous, mechanically weak film, barrier anodizing produces a hard, non-porous structure. One of the primary differences of this process, as compared to sulfuric acid anodizing, is that the electrolyte is neutral and non-film (oxide) dissolving. The process tends to self limit at thicknesses of approximately 1000 nM. In the conventional, porous variety of anodizing there is no effective limit to barrier thickness. It tends to be jointly proportional to anodizing time and current density.

Barrier anodizing can be divided into two regions (see Fig. 1).[1] The majority of the barrier growth occurs in Region I. This region is characterized by a constant current density and a voltage which raises linearly with time. In Region II, when barrier growth to a thickness d is completed, the voltage remains constant and the current density rapidly decays, asymptotically approaching a low constant value. A characteristic time, $t_1$, separates Regions I and II. In this paper we primarily studied Region I in an attempt to produce various barrier thicknesses in as short a time as possible.

## Experimental

The process requires a bath of 3% by weight of neutralized tartaric acid and a constant current dc power supply. The acid is neutralized to $6 \leq pH \leq 8$ with addition of ammonium hydroxide. The power supply is able to supply up to 35 amps and had an upper voltage limit of 300V. High purity Al (99.99%) and AA 5086 (AlMg) substrates were machined by high-speed, diamond tool lathes to a surface smoothness of a peak to valley topography of about

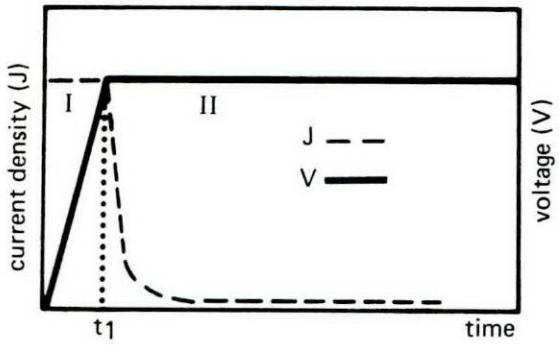


Fig. 1 Current density and voltage relationships with time in barrier anodizing. $t_1$ is the barrier "formation" time.

0.1 μM. Before anodization the substrates were hand scrubbed with a cotton cloth in a concentrated detergent, rinsed in tap water, followed by de-ionized water. An ellipsometer was used to determine the resulting barrier film thicknesses at the formation times ($t_1$) and at longer anodization times (10 $t_1$ and 100 $t_1$).

The surface topography of barriers formed at different formation and voltages and anodizing times, as well as with different current densities were studied. A Cambridge, Model 600 SEM at magnification factors of 5K and 10K was used for these studies.

## Results

The thickness to voltage ratio was first determined, so that one could relate voltage to barrier thickness, and to see if it is a function of time and/or voltage. Table I indicates the experimentally determined thickness as a function of applied voltage at formation times ($t_1$) and at times (10 $t_1$ and 100 $t_1$). The The data indicates a fairly constant relationship between thickness and formation voltage over a range of voltages. Table I also indicates that this thickness to voltage ratio hardly changes at times greater than $t_1$, implying insignificant growth in Region II.

Barrier growth was also studied as a function of current density (0.043, and 0.25 A/cm$^2$). For each current density, various forming voltages (50, 150, 200 and 250V) were applied to pure aluminum and the AA5086 (Al ≥ 95.5%) alloy. The formation times, $t_1$, (the time at which the current density begins to rapidly drop for each applied voltage) for each barrier layer were also determined. As a consequence, an empirical relationship between formation times ($t_1$) and current density for each formation voltage or thickness was found for a given barrier thickness, as shown in Fig. 2. One sees that t can be made as small as one desires, as long as one has adequate current density. These results are also shown in Table II. The graphical representation of Fig. 2 and Table II indicates the following

TABLE I: EXPERIMENTALLY DETERMINED THICKENSS VOLTAGE RATIOS FOR THE AA5086 AlMg SUBSTRATE AT VARIOUS VOLTAGES AND TIMES. INITIAL CURRENT DENSITY WAS 0.024 A/cm$^2$.

| TIME | VOLTS | THICKNESS | THICKNESS/VOLTS |
|---|---|---|---|
| $t_1$ | 100 V | 1400 nM | 1.4 nM/volt |
| $t_1$ | 150 V | 2184 nM | 1.46 nM/volt |
| $10xt_1$ | 150 V | 1953 nM | 1.30 nM/volt |
| | | Average | 1.38 nM/volt |
| $t_1$ | 250 V | 3304 nM | 1.32 nM/volt |
| $10xt_1$ | 250 V | 3567 nM | 1.43 nM/volt |
| $100xt_1$ | 250 V | 3600 nM | 1.44 nM/volt |
| | | Average | 1.39 nM/volt |

Overall Average: 1.39 nM/volt

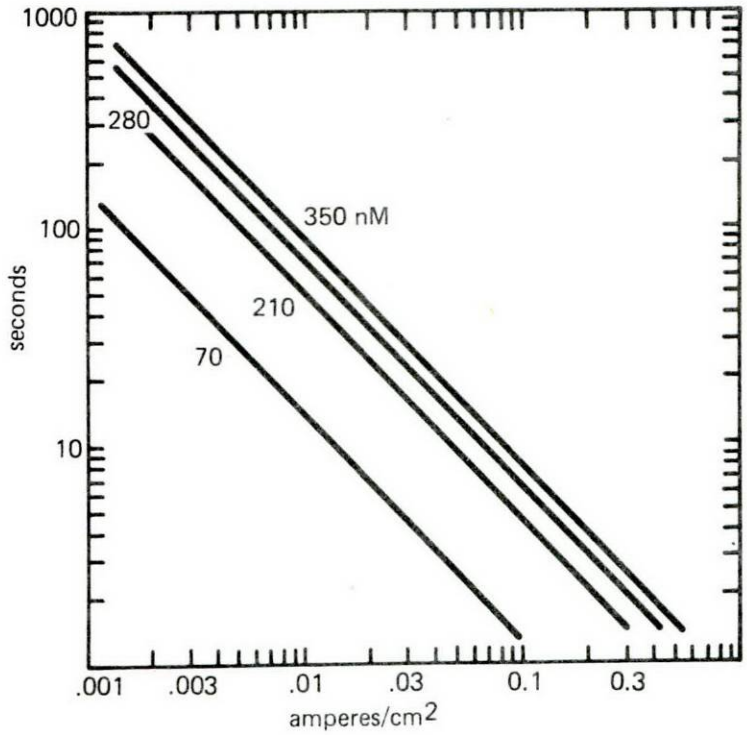


Fig.2 The empirical relationship between formation time, $t_1$, and initial current density, J, for barriers of various thicknesses on pure aluminum substrates.

inverse relationship between $t_1$ and J, as well as a linear relationship between $t_1$ and V:

$$t_1 = CV/J \qquad (1)$$

where C is approximately constant, whose value is in Table II. That is, for each forming voltage even though the current density change by almost 3 orders of magnitude, the value of C changes by less than a factor 1.4.

Although Fig 2 is for pure aluminum, Table II indicates that the time, current density values for the aluminum alloy are almost identical.

TABLE II: EXPERIMENTALLY DETERMINED FORMATION TIMES AS A FUNCTION OF VOLTAGES AND CURRENT DENSITIES

| J (A/cm$^2$) | V (volt) | d(nM)* | $t_1$ (sec) | C (A sec/volt cm$^2$) |
|---|---|---|---|---|
| Pure Aluminum | | | | |
| 0.003 | 50 | 70 | 48.0 | $2.9\times10^{-3}$ |
| | 150 | 210 | 175.0 | 3.5 |
| | 200 | 280 | 240.0 | 3.6 |
| | 250 | 350 | 300.0 | 3.6 |
| 0.043 | 50 | 70 | 3.0 | $2.6\times10^{-3}$ |
| | 150 | 210 | 11.0 | 3.2 |
| | 200 | 280 | 15.0 | 3.2 |
| | 250 | 350 | 19.5 | 3.4 |
| 0.254 | 50 | 70 | 0.55 | $2.8\times10^{-3}$ |
| | 150 | 210 | 1.7 | 2.9 |
| | 200 | 280 | 2.4 | 3.0 |
| | 250 | 350 | 3.3 | 3.3 |
| 5086 AlMg Alloy | | | | |
| 0.003 | 50 | 70 | 49.2 | $3.1\times10^{-3}$ |
| | 150 | 210 | 189.0 | 4.0 |
| | 200 | 280 | 258.0 | 4.3 |
| | 250 | 350 | 336.0 | 4.3 |
| 0.043 | 50 | 70 | 3.0 | $2.6\times10^{-3}$ |
| | 150 | 210 | 11.0 | 3.2 |
| | 200 | 280 | 16.0 | 3.4 |
| | 250 | 350 | 22.0 | 3.8 |
| 0.254 | 50 | 70 | 0.57 | $2.9\times10^{-3}$ |
| | 150 | 210 | 1.8 | 3.0 |
| | 200 | 280 | 2.6 | 3.3 |
| | 250 | 350 | 3.7 | 3.8 |

*Calculated from Table I ( 1.4 nM/volt)

The effect of anodization time, after a film has been formed, on the surface topography of the barriers was also studied; Fig. 3 and 4

show SEM photographs of these surfaces. A comparison of Fig. 3 (10 min) with Fig. 4 (60 min) of barriers of the same thickness show the increase of surface deterioration (etching) with long anodization times. Fig. 5 and 6 also show an increase of surface roughness with formation time.

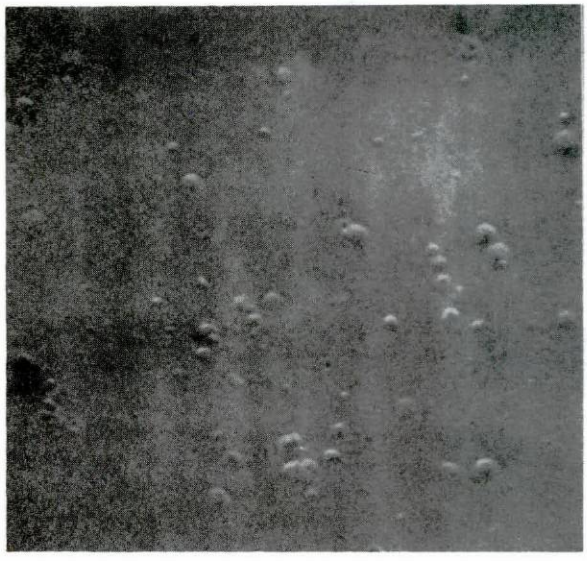

Fig. 3 SEM photo of barrier formed with 100 V and J = 0.30 A/cm$^2$, t = 10 min, 10KX.

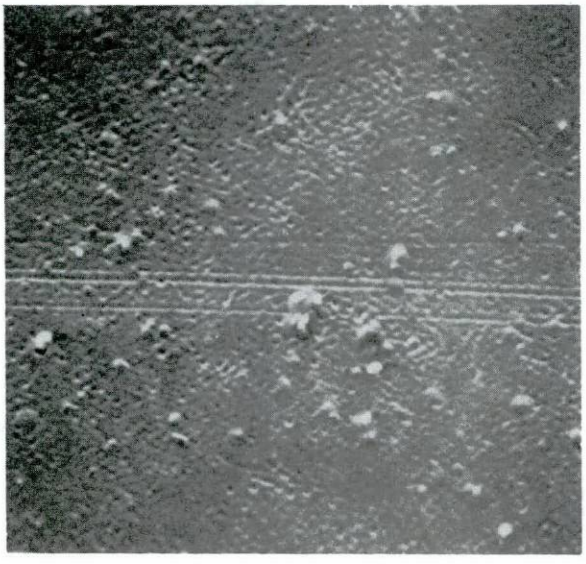

Fig. 4 SEM photo of barrier formed with 100 V and J = 0.30 A/cm$^2$, t = 60 min, 10KX.

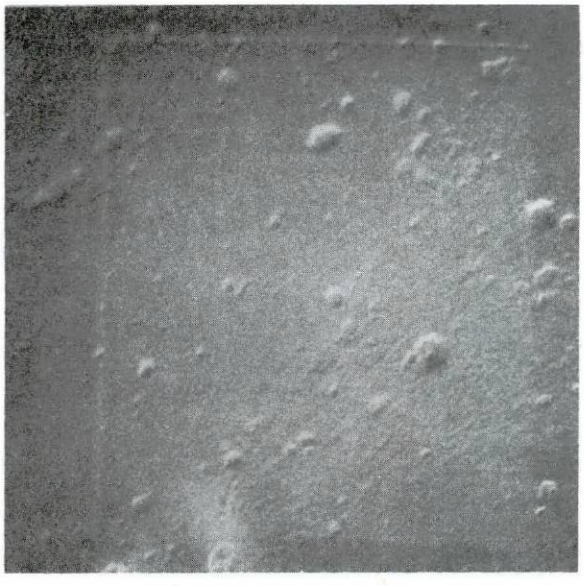

Fig. 5 SEM photo of barrier formed with 50 V and J = 0.023 A/cm$^2$, $t_1$ = 5.9 sec, 10 KX.

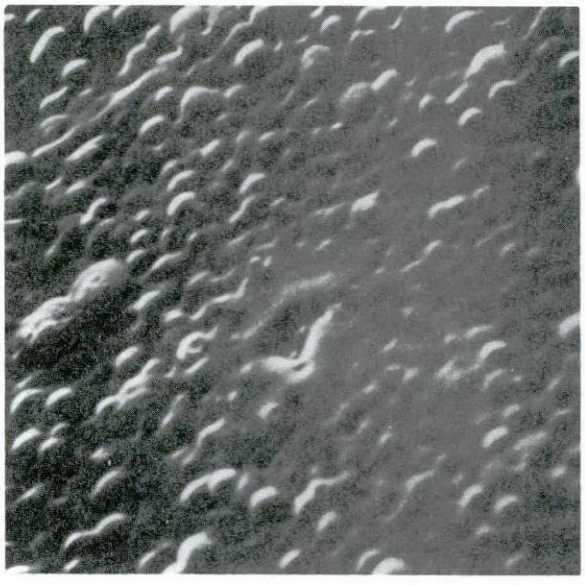

Fig. 6 SEM photo of barrier formed with 225 V and J = 0.023 A/cm$^2$, $t_1$ = 35.2 sec, 10KX.

The increase of current density was seen to have a significant effect on improving surface quality. This is seen in Fig. 7 and 8 for the AA5086 and in Fig. 9 and 10 for the pure aluminum substrate.



Fig. 7 SEM photo of barrier at 250 V and J = 0.171 A/cm2, 5KX.

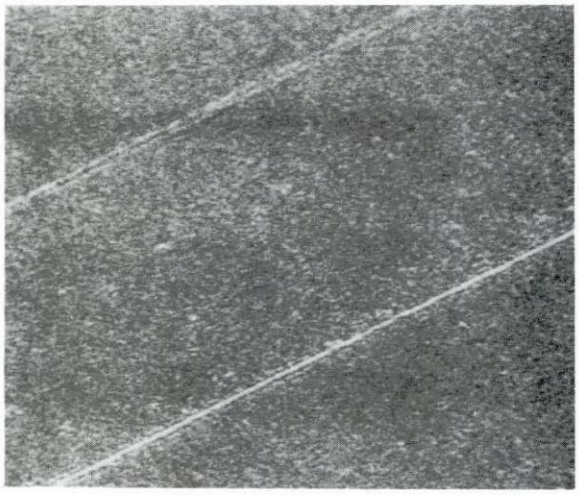

Fig. 8 SEM photo of barrier at 250 V and J = 0.254 A/cm$^2$, 5KX.

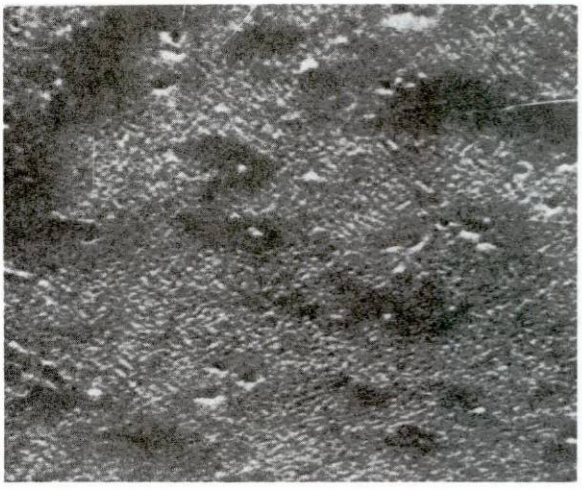

Fig. 9 SEM photo of barrier formed at 250 V anf J = 0.171 A/cm$^2$, 5KX.



Fig. 10 SEM photo of barrier formed at 250 V and J = 0.254 A/cm$^2$, 5KX.

## DISCUSSION

A justification of the empirical equation relating formation time ($t_1$), current density, J, and voltage, V, was found based on Mott's equation. [2] A form of Mott's equation will be used to describe the basic process :

$$J = A \exp (BV/d) \qquad (2)$$

where d is the barrier thickness and A and B are constants. We see from this equation that for a constant J, d/V is constant. Also due to the exponential nature of this equation d/V changes little over a range of J values. Hence, let

$$d/V = W \qquad (3)$$

The physical model of barrier formation can be described as aluminum ions propagating through the barrier under the influence of the electric field created by the applied voltage:

$$J = n q v \qquad (4)$$

where n, q, v are the ion density, charge and average drift velocity, respectively, of the ions under the action of the electric field.

The drift or formation time of a barrier, $t_1$, can then be represented as follows, where d is the barrier thickness and k is a constant:

$$t_1 = k \, d/v \qquad (5)$$

Hence, from equations 3 and 4:

$$t_1 = k \, n \, q \, W \, V/J = C \, V/J,$$

where $C = k \, n \, q \, W$.

Hence, we have demonstrated a reasonable derivation of the empirical equation 1, and the relationship of Fig. 2. Table II also indicates the validity of this derivation, showing the relative constancy of C, over a large range of values of J and V.

Concerning the deterioration of the barrier's surface with formation times, it is reasonable to assume that the longer it takes for the formation of a barrier the greater the number of defects that can be built into such a film. This was very apparent from Fig. 5 and 6. However, equation 1 now implies that shorter formation times cannot only be had with smaller voltages, but also with larger current densities. And this could explain the improvement in surface quality with increase in current density seen in Fig. 7 to 10. With regard to the surface deterioration with long anodization times (Fig. 3 and 4), electrolyte etching, after film formation, under the influence of an electric field has been seen by other workers. [3]

## SUMMARY

An anodizing process, called barrier anodizing, for aluminum was examined. It produces a tightly adhering, non-porous surface of particular importance. One has a very safe, non-corrosive bath (in contrast to sulfuric acid anodizing) and a very fast process. Of special interest is the "barrier formation" time process control equation (Eq. 1). It relates the

formation voltage with the initial current density. This control equation is extremely important and relevant in determining the time to effectively form the barrier, and its quality. The object being to make it as small as possible for good quality films. This equation conveniently marks the separation between Regions I and II of the process (Fig. 1). And it explains the very useful application of higher current densities for better quality barriers.

## REFERENCES


1. J. Diggle, T. Downie, C. Goulding, Chem, Reviews, 69, 365 (1969).

2. A. Charlesby, Pro. Phys. Soc., 66B, 317 (1953).

3. Y. Choo and O. Devereux, J. Electro-Chemical Soc., 122, 1645, (1975).

# G-3

# Light Metals Finishing II
# Session G

## Film Growth on Aluminum Alloys During AC Anodizing in Sulphuric and Oxalic Acid Solutions

Dr. J. Zahavi, H. Kerbel and O. Korothina
Israel Institute of Metals
Technion, Haifa, Israel

# FILM GROWTH ON ALUMINUM ALLOYS DURING AC ANODIZING IN SULPHURIC AND OXALIC ACID SOLUTIONS

J. Zahavi, H. Kerbel and O. Korotkina

Israel Institute of Metals
Technion, Haifa, Israel

## ABSTRACT

Studies are being made of A-C anodizing processes on aluminum commercial alloys in sulphuric and oxalic acids at constant AC voltages. Special attention is given to the effect of intermetallic second phase particles dispersed in these alloys on AC film growth and properties.

AC film topography, structure and composition were characterized through electron microscopy techniques such as scanning electron, microscope (SEM), replica and transmission electron microscope (TEM) and electron probe microanalyzer (EPMA).

Porous A-C film thickness increased with anodized time, electrolyte temperature and concentration and anodizing voltage on all the aluminum alloys used in this work. Intermetallic compounds dispersed in the aluminum alloy matrix incorporated into the anodic films during their formation and thus affected film composition and properties. AC and DC films were compared as regards to their anodizing efficiency growth rate, structure and sealing efficiency.

## INTRODUCTION

Recently[1-5] alternating current (AC) anodizing processes have gained considerable importance, especially in forming passive thick porous anodic films on commercial aluminum alloys including so called "difficult alloys" (for instance, high copper and silicon wrought or cast alloys) which actually are difficult to anodize under DC anodizing conditions[6,9].

Several investigators[1-4] have studied various variables associated with aluminum alloys AC anodizing processes such as type of electrolytes, electrolyte concentration and temperature, agitation, current density, anodizing time and voltage. The effects of dispersed intermetallic second phase particles in aluminum alloys on anodic film growth and properties have been studied rather extensively under DC anodizing[6-9] compared to AC anodizing[5]. The presence, the type and distribution of intermetallic constituents in aluminum alloys were found to be determining DC anodic film growth, film structure, film properties and film stability through their incorporation, oxidation or dissolution during film formation[6-9].

The present work therefore aimed at studying the formation of A-C porous thick anodic films on commercial aluminum alloys (Al-1100, 2024, 5052, 6061, 7075) containing various dispersed intermetallics rich in iron, copper, silicon, magnesium and zinc[7,10]. Particular attention is devoted to the behavior of these intermetallic constituents and especially to their incorporation into the growing film under A-C anodizing conditions and to their effects on film structure, composition, stability and properties.

## EXPERIMENTAL PROCEDURE

Commercial aluminum alloys designated with AA numbers as Al 1100-H14 (commercial pure aluminum), 2024-T3, 2024-To (aluminum-copper alloys), 5052-H32 (aluminum-magnesium alloys), 6061-T6 (aluminum-magnesium-silicon alloys), and 7075-T6 (aluminum-magnesium-zinc alloys) were used for AC anodizing in this work.

The alloys were in the form of flat sheets and specimens were cut into working area of 20x15x1 mm and a narrow tab.

Specimens were degreased in trichloro-ethylene, etched in 10% HF for 4 min., washed in distilled water, immersed in $HNO_3$:$H_2O$ 1:1 solution for 30 sec., washed in distilled water and then electropolished in 20 volume per cent (v/0) 70% $HClO_4$ in ethanol at 8 to 12 A/dm$^2$ for 5-10 min. at -10°C to -15°C and rinsed with jet of ethanol.

A-C anodized coatings were formed on four specimens (total anodizing area of 28 cm$^2$), two on each electrode simultaneously in 150-250 g/l sulfuric acid at 15°C-25°C and 30-90 g/l oxalic acid at 15°C-45°C at constant A-C effective voltage of 20-30V and 30-90 V respectively. Anodizing times of 15-150 min were used to obtain thick porous films (in the range of 5-40 μm) in which sections could be prepared for examination by various microscopy techniques such as optical, scanning electron microscope (SEM), transmission electron microscope (TEM) and electron probe microanalyzer (EPMA).

Agitation of the electrolyte solution was conducted by glass rod stirrer while its temperature was kept within ∓0.5°C of the required value by a thermostatic bath with cooling coils operating in the range of -10°C to +80°C. A stabilized A-C power supply of 10 A, 200 V was used for anodizing. Coating sealing processes were also carried out making use of a sealing solution containing 8 g/l boric acid and 6 g/l nickel acetate. Sealing times were up to 120 min.

Kinetic film growth under potentiostatic A-C anodizing was studied by recording effective current density vs. anodizing time curves together with measuring film barrier thickness and total thickness.

Film structure topography and composition including the presence of intermetallics were characterized through electron microscopy by direct transmission of film ultrathin cross section[11], replicas, SEM and EPMA of film surface and cross section.

## RESULTS AND DISCUSSION

### Anodizing, Kinetics and Film Growth

Effective current-time curves for potentiostatic A-C anodizing of aluminum alloys in sulphuric, oxalic and mixtures of sulphuric and oxalic acids as shown in Figs. 1,2 and 3 respectively were found very similar to curves obtained for DC formation of porous anodic films[12].

Fig. 1 shows typical current density-time curves obtained during AC anodizing of aluminum alloy Al2024-T3 at constant potential of 23 V in 170 g/l sulphuric acid solution without (Fig. 1A) or with additions of 10 g/l oxalic acid (Fig. 1B) at 15°C. Initially, the measured current reached a minimum

value after which it increased and remained at fairly constant value around 0.3 Amper (Fig. 1).

Typical current-time curves for A-C anodizing of Al 2024-T3 alloy at constant potential in oxalic acid solutions at various concentrations ranging from 30 g/l to 90 g/l. Typical current-time curves obtained during AC anodizing of Al 2024-T3 in various concentrations of oxalic acid solutions at constant potential of 75 V are shown in Fig. 2.

Increase in electrolyte concentration and temperature resulted in increase of the current fairly constant values. These values ranged from about 2,5 A to 4,0 A (Fig. 2A) and 3,5 A to 5,5 A (Fig. 2B) when the electrolyte temperature increased from 25°C to 35°C in 30 g/l and 60 g/l of oxalic acid solution respectively. Furthermore, upon increasing the electrolyte temperature from 15°C to 45°C at oxalic acid concentration of 90 g/l the current value increased from about 0.2 A to 1.7 A (Fig. 2C).

Figure 3 shows typical current-time kinetic curves obtained during A-C anodizing of Al 2024-T3 in oxalic acid solutions containing sulphuric acid additions at constant potential. Basically, the curves obtained were found very similar to curves obtained for AC anodizing either in pure sulphuric or oxalic acid solutions. Initially the current reached a minimum value after which it increased and remained at fairly constant value which was found to be around 0.2 A when 10 g/l $H_2SO_4$ was added to 60 g/l or to 30 g/l of oxalic acid solution (Fig. 3).

The basic behavior of the AC current-time curves indicated the formation of thick porous anodic films while current fluctuations probably indicated the presence of break-down-repair processes under some extreme anodizing conditions.

Film Growth.

A-C aluminum anodized film thickness increased steadily with anodized time in sulphuric acid (Fig. 4) oxalic acid (Fig. 5) or mixtures of sulphuric and oxalic acids (Fig. 6). Furthermore, increase in electrolyte temperature and concentration (Figs. 7,8) and anodized voltage (Figs. 9,10) resulted in film thickening reaching values up to 40 μm and 30μm in 170 g/l sulphuric acid and in 90 g/l oxalic acid respectively.

A-C Film Morphology and Composition

Typical SEM observations of surfaces of AC anodic films formed on various commercial aluminum alloys are shown in Fig. 11. These observations showed local dark sites (up to 10 μm across) with light rim distributed in film surface. These events indicated the presence of cavities in film surface resulted from second phase particles removal in the course of anodizing both in sulphuric acid and oxalic acid[5]. Furthermore, the cavities on the surface of these thick porous AC anodized films indicated that particles were embedded and retained in the films through their growth process on various commercial aluminum alloys such as Al 1100-H14 (micrograph not shown), Al 6061-T6 (Fig. 11A), Al 5052-H32 (Fig. 11B), Al 7075-T6 (Fig. 11C), Al 2024-%3 (Fig.11D) and Al 2024-To (Fig.11E). Second phase particles which were partly embedded in the film surface were dislocated from the surface as was observed previously in D-C anodizing .

Examination of cross sections of AC anodized aluminum alloy specimens by electron probe microanalysis (EPMA) revealed the presence and distribution of intermetallics in the aluminum matrix and through thickness of film formed in oxalic (Fig. 12) or sulphuric acid (Fig. 13).

The intermetallics appeared as bright local sites up to 10 μm in size in the various aluminum alloy cross sections (Fig. 13). These intermetallics contained primarily copper, iron, manganese, silicon as determined by X-ray images (not shown). Furthermore, the electron scanning images of specimen cross sections revealed dark sites distributed uniformly through film thickness and few in the alloy matrix (Fig. 13). These dark zones which were of the same shape and size (up to 10 μm) as the intermetallics in the aluminum alloy matrix, indicated the embedment of second phase particles into the AC anodic films during their growth processes either in oxalic acid (Fig. 12) or sulphuric acid (Fig. 13). Furthermore, these second phase particles were removed from film cross section through the procedure of preparing the cross section specimens leaving dark cavities in film cross section as observed for various aluminum alloys (Fig. 13). Moreover, the cross section micrographs showed that AC films on various aluminum commercial alloys were of uniform thickness, indicating that the presence of second phase particles did not substantially affect AC film growth processes compared to DC film growth, especially in so called "difficult alloys" such as aluminum-copper alloys[6]. EPMA analysis of AC film cross section revealed the presence of sulphur uniformly distributed in film formed in sulphuric acid solution[5].

## A-C Film Pore Structure

Direct transmission electrom microscopy (TEM) observations of ultrathin film cross sections showed the general porous structure as obtained in D-C film[13]. That structure comprises long straight pores of roughly circular section with scalloped barrier layer at the base (Fig. 14).

Porous structure of thin AC anodic film formed on pure aluminum in sulphuric acid was reported earlier[4]. Thick film porous structure maintained itself during thickening by growth through the barrier layer and dissolution of film at the pore bases for the various commercial aluminum alloys. Porous AC film growth, however, was associated with embedment of intermetallics as could be seen at the left hand side at the bottom of Fig. 14. The intermetallic particle appeared as a dark site at the interface metal film interface. Furthermore, typical TEM surface replica of AC porous film showed the presence of intermetallic particles at the surface (Fig. 15A) or the presence of cavities originally occupied by intermetallics which were removed during film growth (Fig. 15B).

Intermetallics in the size of 0.5 to 10 μm were entrapped in the AC thick porous films during their formation on various commercial aluminum alloys in sulphuric or oxalic acids. These particles did not modify or change film/electrolyte interface, film uniformity, thickness as well as film pore and barrier layer structure and morphology[4,5].

## A-C Film - Barrier Layer

Following the direct observation of film porous structure by TEM technique (Fig. 14) a schematic view of film cross section was evaluated as shown in Fig. 16. An electrical circuit (Fig. 16B) representing the mode and structure

of the porous film (Fig. 16A) takes in consideration film total thickness resistance, $R_o$, capacity, $C_o$, pore resistance, $R_1$, as well as film barrier layer resistance, $R_2$, and capacity, $C_2$.

Impedance measurements of porous films formed on various commercial aluminum alloys (used in this investigation) in sulphuric and oxalic acid solution at constant D-C and A-C voltages gave film barrier layer thickness (Fig. 17, Fig. 18). Barrier layer thickness was found to be of a constant value at constant AC or DC voltage independent of anodizing time (i.e. film growth) as shown for example in Fig. 17 for Al-1100 anodized in sulphuric acid. Barrier layer thicknesses of 8.7 Å/V and 7.6 Å/V were found for AC anodic films formed on Al-1100 and Al-2024 alloys respectively in sulphuric acid. These values were compared with values of 10.8 A/V and 8.8 A/V found for DC film formed on Al-1100 and Al-2024 respectively (Fig. 18). No substantial difference was found in barrier layer thickness in AC film[4,5] compared to DC film[13] formed under similar anodizing conditions. The embedment of intermetallic particles into AC film growth did not affect film barrier structure and its growth rate.

## Incorporation of Second Phase Particles into A-C Film Growth[5]

During the positive half-cycle period of alternating current anodizing, film growth and anodic processes occurred and were similar to those obtained during D-C anodizing. High anodic current density preferentially taking place at intermetallics free alloy surface zones resulted in a high rate film growth. Very low current densities (i.e., practically no film growth) took place at particles which were nonreactive compared with the aluminum matrix (iron rich constituents in commercial pure aluminum). Subsequently, the particles were electrically disconnected from the alloy matrix by film growth around them, which resulted in their embedment in the growing film. Furthermore, when more reactive intermetallic particles were present in the aluminum alloy (copper rich particles in aluminum-copper alloy), anodic processes of either film formation and dissolution or of direct increasing metallic cations in the electrolyte (copper ions when copper rich particles were involved).

During negative half-sycle period, "normal" film growth was stopped. Preferentially at particle sites, a higher rate of cathodic reactions took place than at filmed surfaces that were particle free. These cathodic reactions involved the reduction of hydrogen ions (primarily when nonreactive particles were present, such as iron rich particles) and the cathodic deposition of metallic cations (when reactive particles were present such as copper rich particles) preferentially on particle sites. In a subsequent positive half-cycle period, film growth resumed at particle-free zones where the cathodic deposits on the reactive particles (copper deposits on copper rich particles, for example) were oxidized or dissolved, resulting in retaining their original size and shape. Consequently, these particles became embedded in the growing A-C film in a mode similar to the nonreactive ones as discussed above.

## A-C Film Sealing Processes.

Thick porous anodic A-C films formed on various commercial aluminum alloys in this investigation were thereafter sealed in nickel acetate 6 g/l with

boric acid 8 g/l solution at ph = 6 and solution temeprature of 95°C.

Sealing efficiency was evaluated from film impedance measurement at various frequencies before and after sealing (Fig.19). Pore resistance (Fig. 16B) before sealing, $R_{1u}$, was found from impedance measurement at frequency of 1000 cycle/sec, while pore resistance after sealing $R_{1s}$ was found at frequency of 100 cycle/sec (Fig. 19). Sealing efficiency was defined as the ratio of pore resistance after sealing, $R_{1s}$, to pore resistance before sealing, $R_{1u}$, (Fig. 20). Sealing efficiency of A-C thick porous anodic film increased with sealing time while Al-1100 alloy exhibited higher efficiency compared to Al-2024 under practically the same conditions (Fig. 20).

## A-C Film-Energy Consumption

In evaluating the efficiency formation of A-C thick porous anodic films a comparison was conducted with formation efficiency of D-C thick porous films. AC and DC anodizing processes were conducted on Al-1100 in sulphuric acid solutions for 30 min at the same constant voltage of 19.1 Volts. The amounts of charge passed per unit area per film unit thickness were calculated (Table 1) and these values indicated anodizing efficiency.

TABLE 1: Anodizing efficiency of AC and Dc film formation on Al-100 alloy in 130 g/l sulphuric acid at 18°C.

| Operating Conditions | | | A. Min | Anodized Surface $cm^2$ | Film Thickness | $\frac{A.Min}{cm^2 \mu m}$ |
|---|---|---|---|---|---|---|
| Type of Current | Voltage V | Anod. Time min. | | | | |
| D.C. | 19.1 | 30 | 28.0 | 29.70 | 29 | 0.0323 |
| D.C. | 19.0 | 30 | 28.75 | 29.50 | 29 | 0.0336 |
| D.C. | 19.1 | 30 | 18.0 | 13.75 | 35 | 0.0374 |
| A.C | 19.2 | 30 | 11.44 | 27.60 | 11 | 0.0377 |
| A.C. | 19.2 | 30 | 11.74 | 27.60 | 11 | 0.0387 |

Anodizing efficiencies ranged from $3.23 \times 10^{-2}$ to $3.74 \times 10^{-2}$ $\frac{A \cdot Min}{cm^2 \cdot \mu m}$ for DC anodizing compared to $3.77 \times 10^{-2}$ to $3.87 \times 10^{-2}$ $\frac{A \cdot Min}{cm^2 \cdot \mu m}$ for AC anodizing (Table 1). Practically, the efficiency of AC anodizing of aluminum alloys was found to be the same as in DC anodizing of aluminum alloys.

## CONCLUDING REMARKS

Following previous studies[1-5], the contribution of this study was to show the formation of thick porous A-C anodic films on commercial aluminum alloys (commercial pure aluminum, aluminum-copper, aluminum-magnesium, aluminum-magnesium-silicon, aluminum-magnesium-zinc alloys) with special attention to the effects of second phase particles dispersed in the alloys.

Under AC anodizing conditions incorporation of intermetallics into growing thick porous films and their retention in the films were observed in all the commercial aluminum alloys investigated in this work including so called "difficult alloys" (difficult to anodize under D-C conditions) such as aluminum-copper or aluminum-magnesium-zinc.

These A-C films were found of uniform thickness, homogeneous cross section structure including at metal/oxide and oxide/electrolyte interfaces.

A-C film thickness increased with anodizing time, electrolyte temperature and concentration, anodizing voltages reaching values of several tens of microns.

A-C film pore and barrier layer structure were very similar to D-C film resulted in practically the same sealing efficiency processes as well as to the same formation efficiency as defined in this study.

REFERENCES


1. J.M. Kape, Metal Finishing Journal, Vol 20, pp. 80-85 (April 1974).
2. J.M. Kape, Trans. Inst. Met. Finish., Vol 55, pp. 25-30 (January 1977).
3. D.A.L. Nickler and D.R. Gabe, Surface Technology 7, 353-359 (1978).
4. F. Sacchi and G. Paolini, Trans. Inst. Met. Finish., Vol.40, pp. 228-241 (1963).
5. J. Zahavi, H. Kerbel and O. Korotkina, J. Electrochem. Soc. 129, 7, 1572 - 1579 (July 1982).
6. J. Herengel and P. Lelong, Metal Finishing Journal, pp. 20-23 (January 1958).
7. J. Cote, E.E. Howlett and H.J. Lamb, Plating, pp. 484-496 (May 1970).
8. G.C. Wood and A.J. Brock, Trans. Inst. Met. Finish. 44, 189 (1966).
9. J. Zahavi, A. Zangvil and M. Metzger, J. Electrochem. Soc. 125, 3, 438-444 (1978).
10. F. Keller, G.W. Wilcox, M. Tosterud and C.J. Slunder, Metals and Alloys, pp. 219-225 (July 1939).
11. R.C. Furneaux, G.E. Thompson and G.C. Wood, Corrosion Science, 18, 853-881 (1978).
12. T.P. Hoar and J. Yahalom, J. Electrochem. Soc. 110, 614 (1963).
13. J.P. O'Sullivan and G.C. Wood, Proc. Roy. Soc. (London) A 317, 511 (1970).

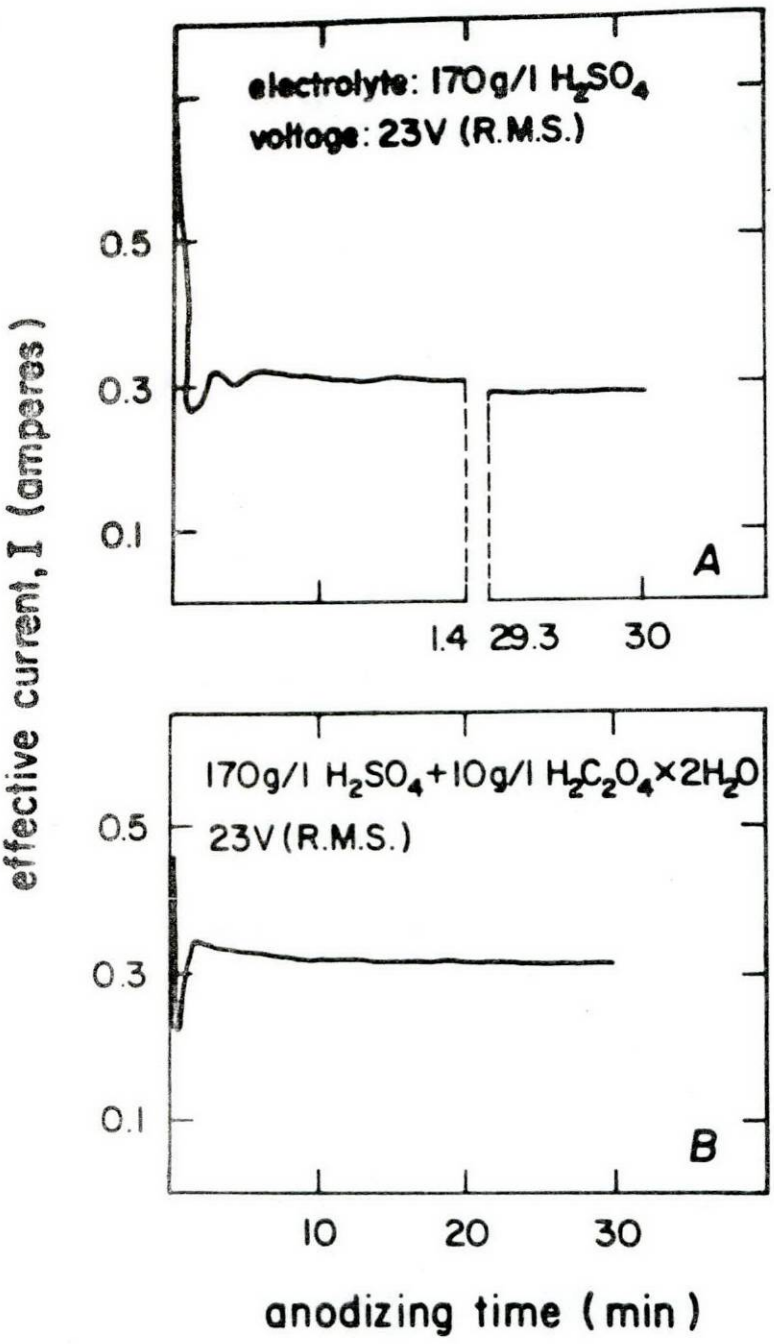


Fig. 1: Dependence of anodizing current on anodizing time of Al-2024-T3 alloy at constant A-C voltage of 23 V(RMS).
A. Sulphuric acid at 15°C
B. Sulphuric acid with addition of oxalic acid.

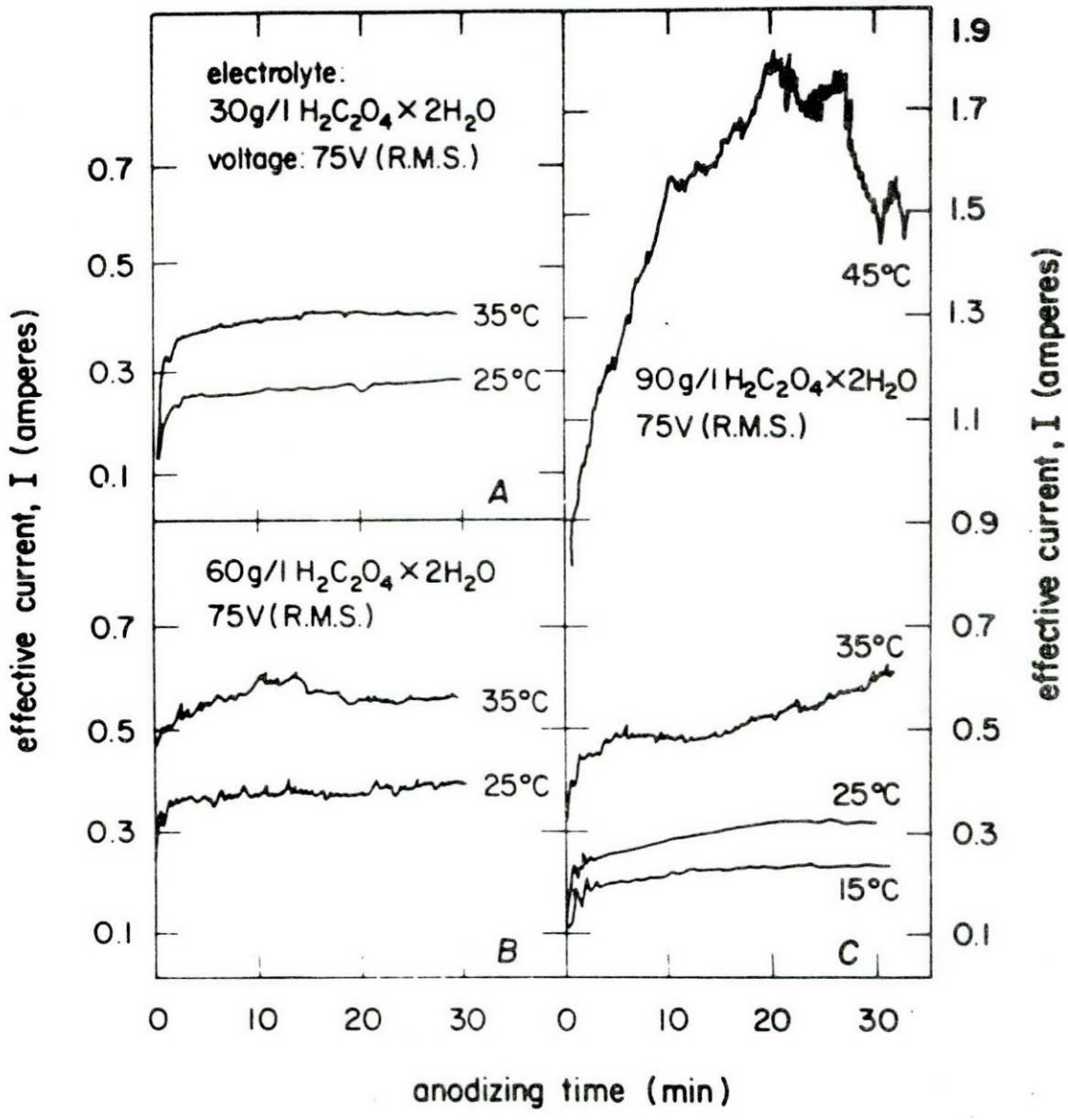


Fig. 2: Dependence of anodizing current on anodizing time of Al-2024-T3 alloy at constant A-C voltage of 75 V(RMS) in oxalic acid solutions.
A. Oxalic acid 30 g/l.
B. Oxalic acid 60 g/l.
C. Oxalic acid 90 g/l.

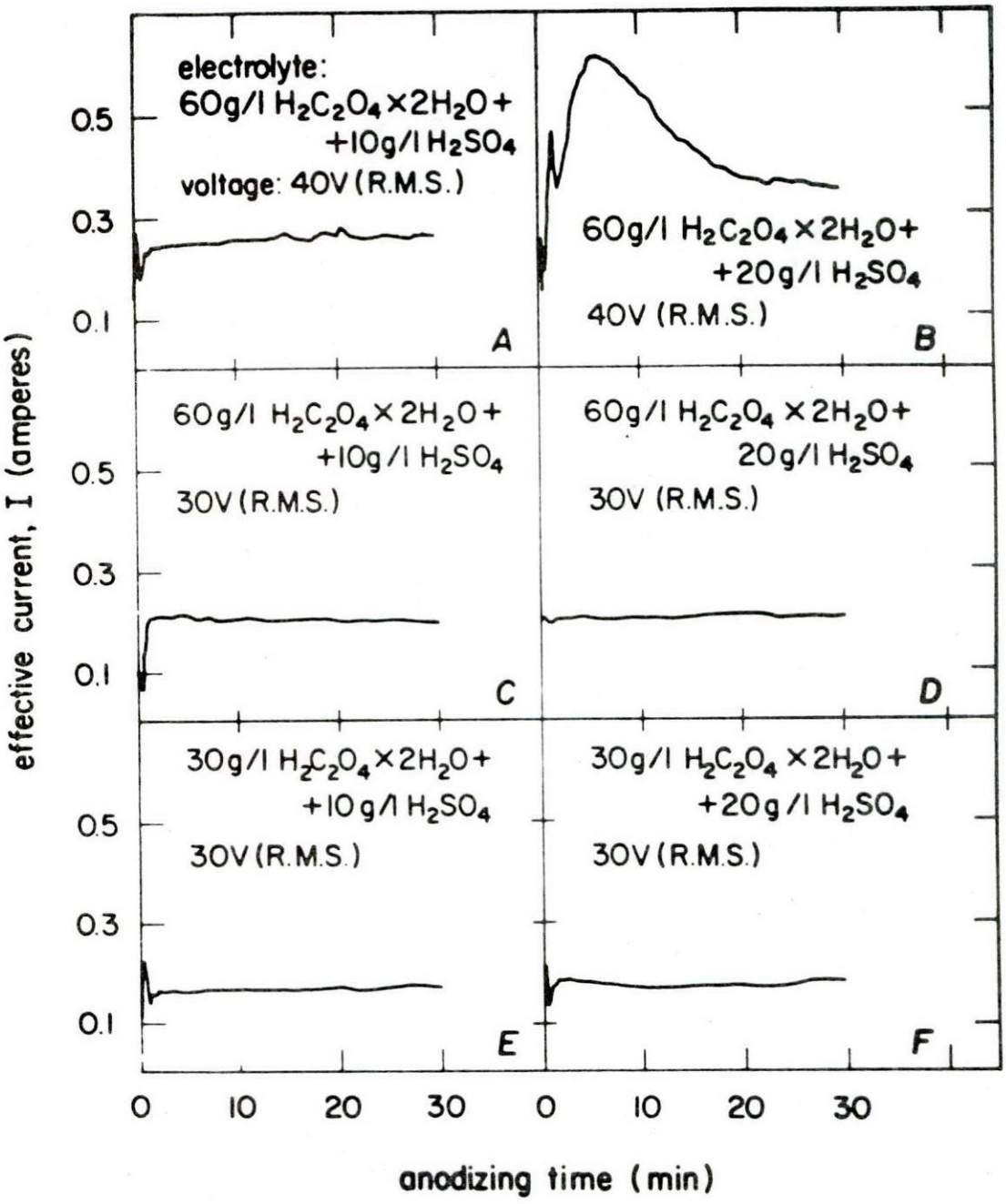


Fig. 3: Dependence of anodizing current on anodizing time of Al-2024-T3 alloy at constant A-C voltages in oxalic and sulphuric acids mixed solutions at constant temperature of 25°C.

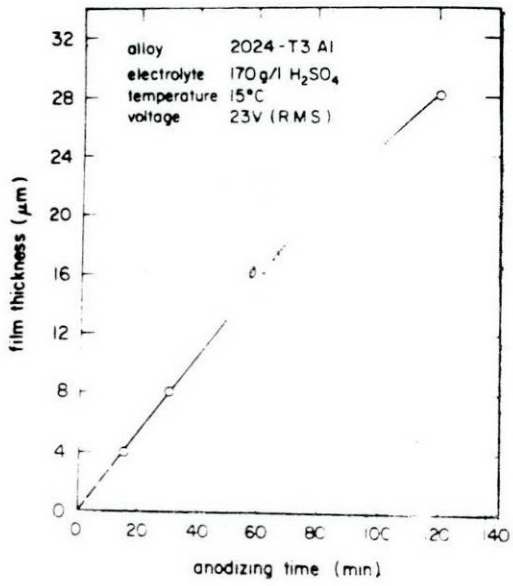


Fig. 4: Dependence of A-C film thickness on anodizing time of Al-2024-T3 alloy in 170 g/l sulphuric acid at 15°C and constant A-C voltage of 23 V (RMS).

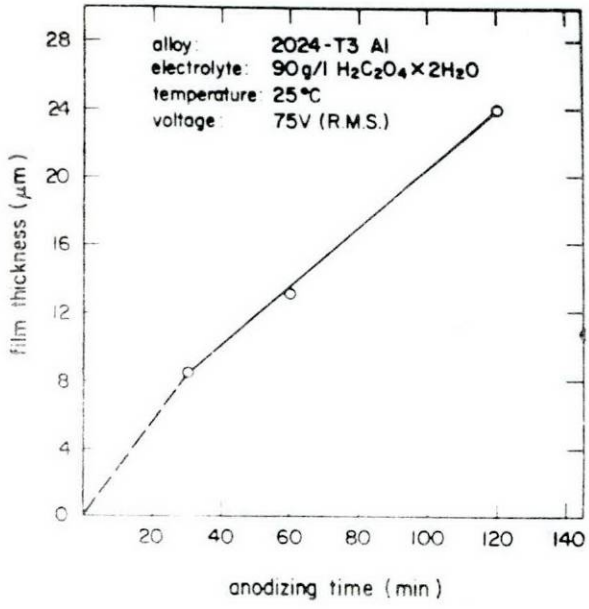


Fig. 5: Dependence of A-C film thickness on anodizing time of Al-2024-T3 alloy in 90 g/l oxalic acid at 25°C and constant A-C voltage of 75 V (RMS).

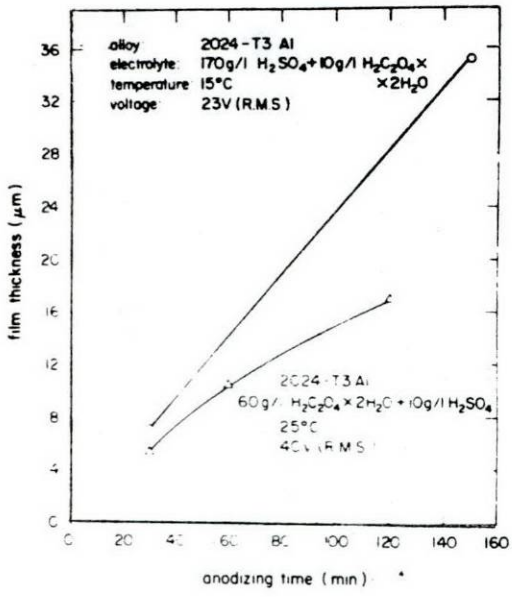


Fig. 6: Dependence of A-C film thickness on anodizing time of Al-2024-T3 alloy in solution mixture of 170 g/l sulphuric acid with 10 g/l oxalic acid at 15°C and constant AC voltage of 23 V(RMS).

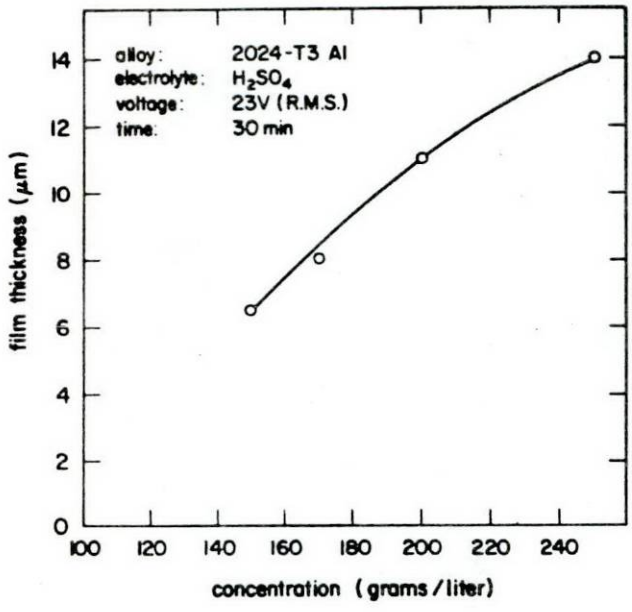


Fig. 7: Dependence of A-C film thickness on sulphuric acid concentration. Anodization was carried out on Al-2024-T3 alloy at AC constant potential of 23 V (RMS) for 30 min.

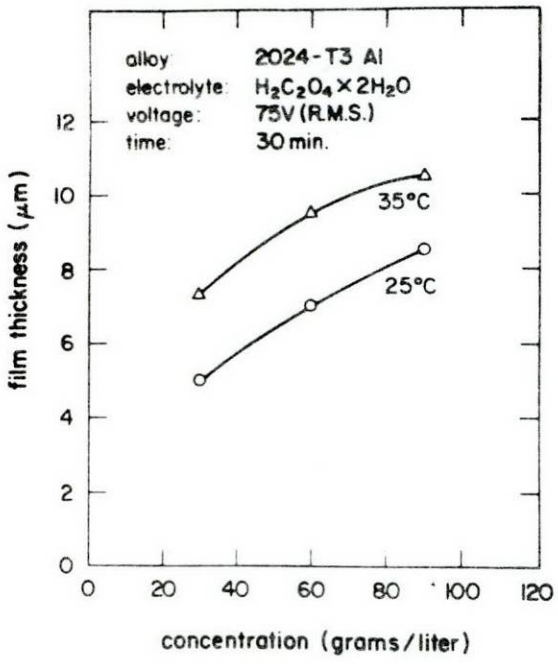


Fig. 8: Dependence of A-C film thickness on oxalic acid concentration. Anodization was carried out on Al-2024-T3 alloy at AC constant potential of 75 V(RMS) at 35°C and 25°C for 30 min.

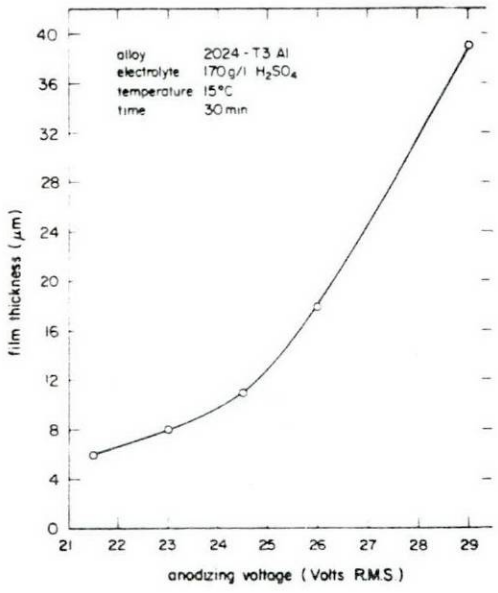


Fig. 9: Dependence of A-C film thickness on anodizing voltage. Anodization was carried out on Al-2024-T3 alloy in 170 g/l sulphuric acid at 15°C for 30 min.

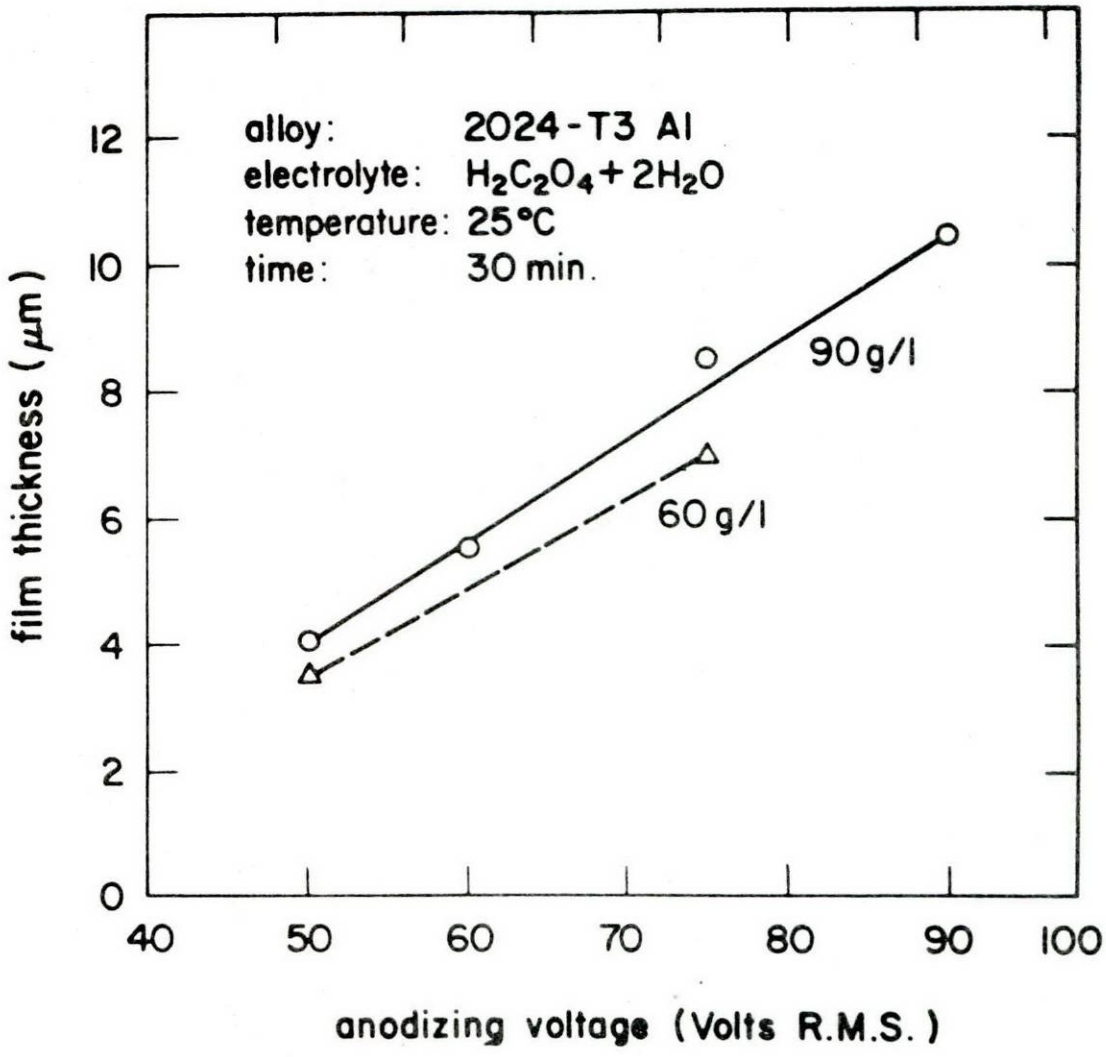


Fig. 10: Dependence of A-C film thickness on anodizing voltage. Anodization was carried out on Al-2024-T3 in 60 g/l and 90 g/l oxalic acid solutions at 25°C for 30 min.

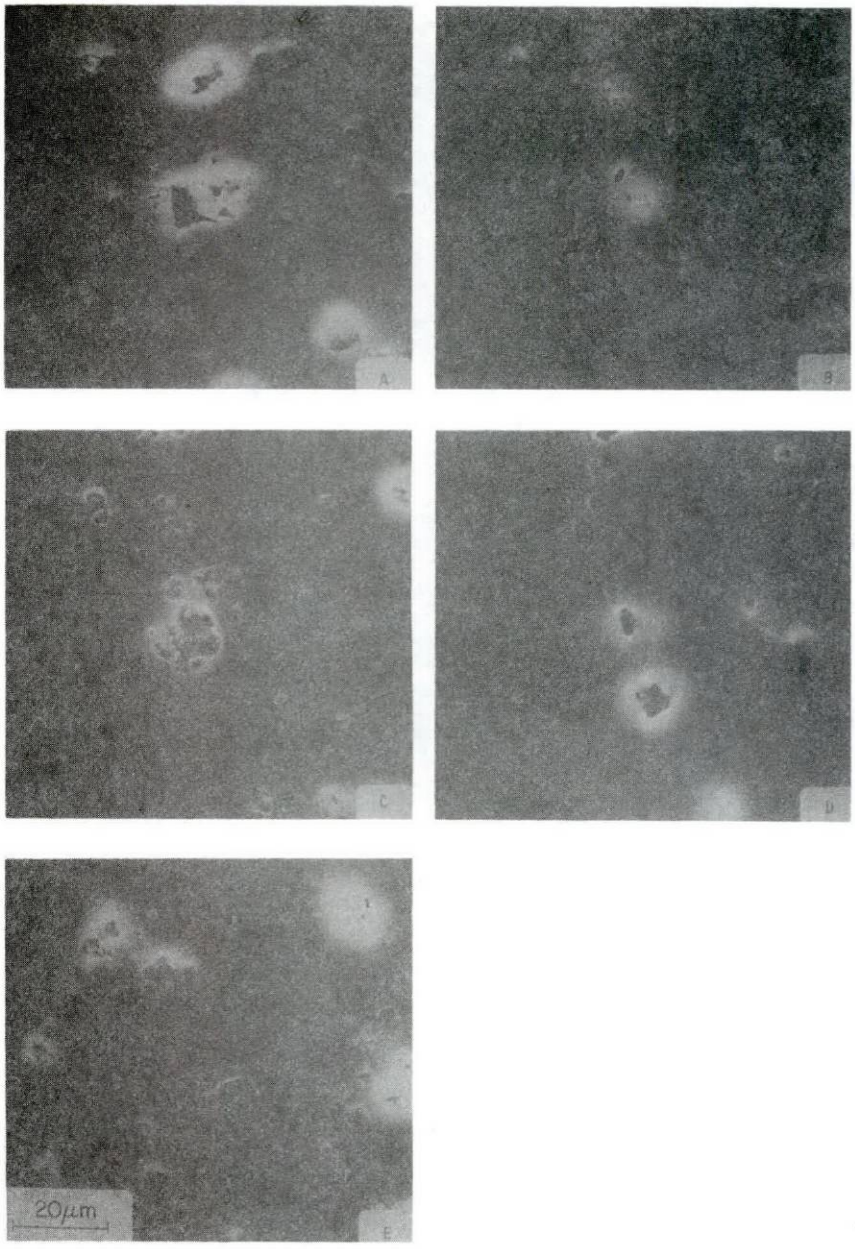


Fig. 11: SEM observations showing typical intermetallic cavities in A-C film surfac of anodized various aluminum alloys in 90 g/l oxalic acid at 25°C and at constant AC voltage of 75 V during 60 min.

A. Al-6061-T6; film thickness 20 µm.
B. Al-5052-H32; film thickness 35 µm.
C. Al-7075-T6; film thickness 22 µm.
D. Al-2024-T3; film thickness 13 µm.
E. Al-2024-TO; film thickness 16 µm.

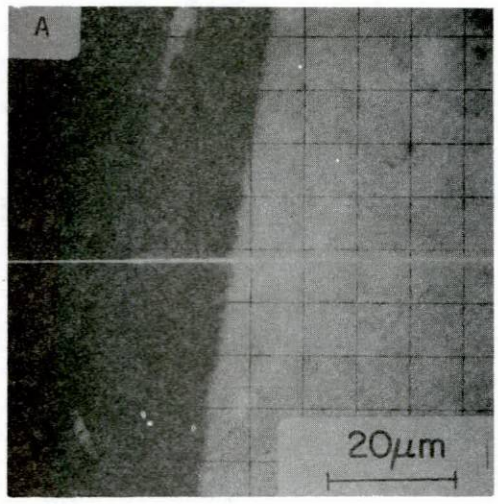


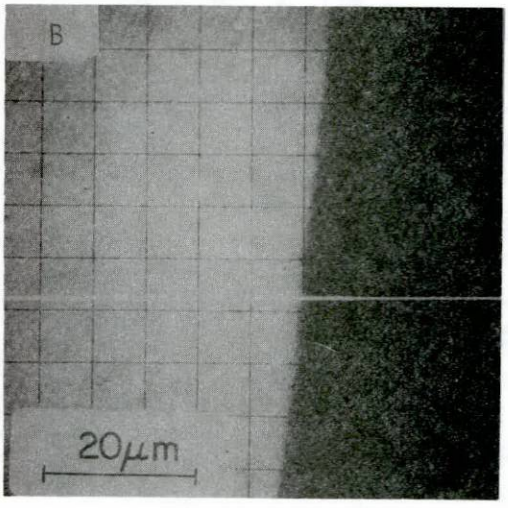


Fig. 12: Typical cross sections of aluminum alloys specimens anodized in 90 g/1 oxalic acid at 25°C and at constant AC voltage of 75 V during 30 min.
A. Al-1100-H14 alloy.
B. Al-5052-H32 alloy.

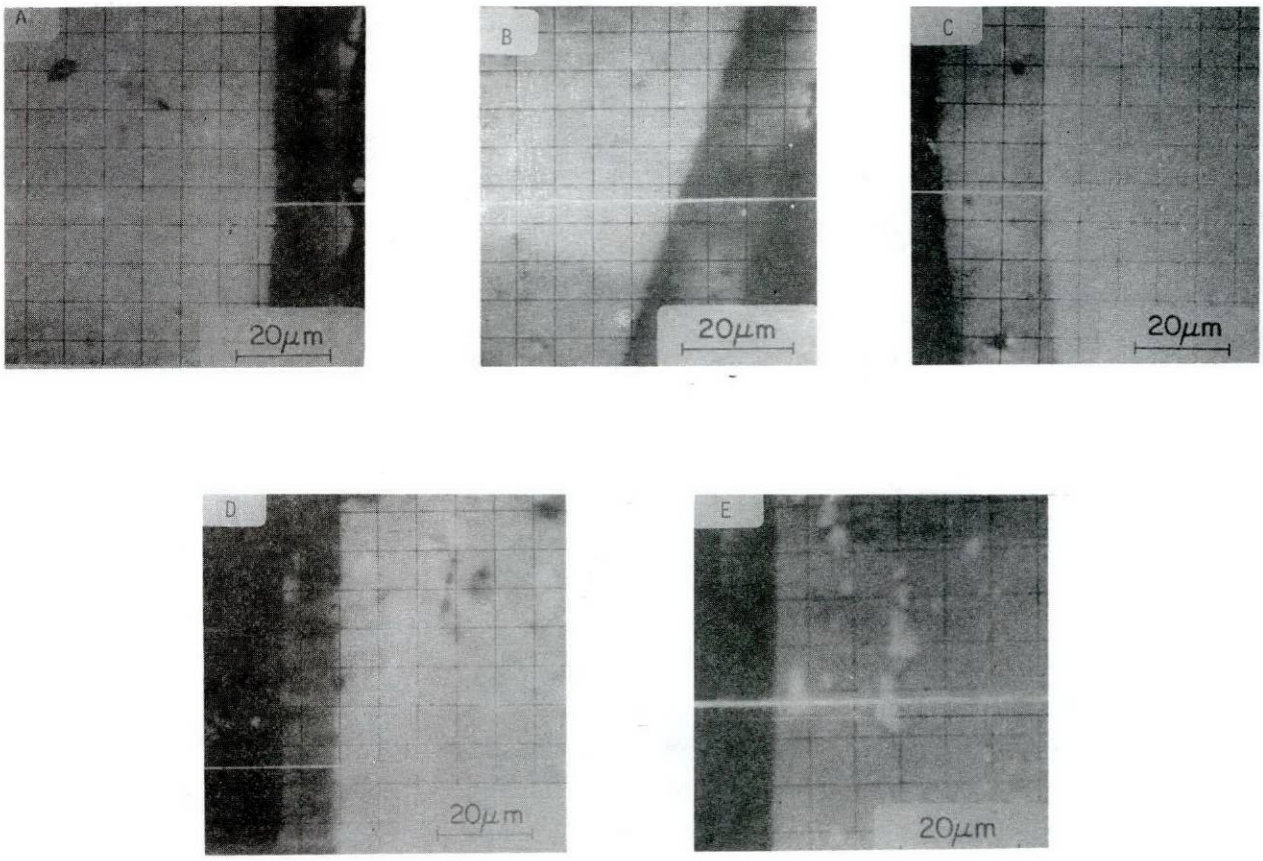


Fig. 13: Typical cross sections of aluminum alloys specimens anodized in 170 g/l sulphuric acid at constant AC voltage of 23 V for 30 min. EPMA observations.
A. Al-6061-T6 alloy.
B. Al-5052-H32 alloy.
C. Al-7075-T6 alloy.
D. Al-2024-T0 alloy.
E. Al-2024-T3 alloy.

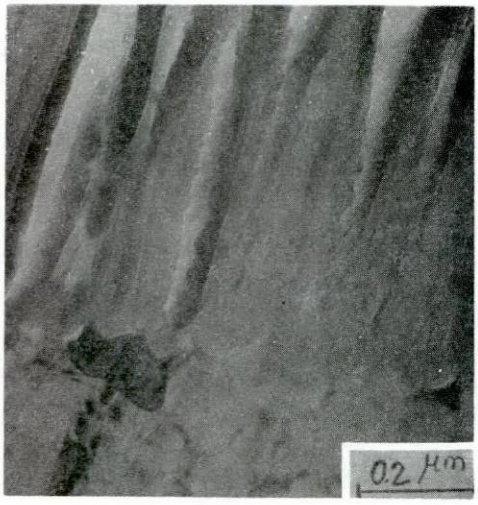


Fig. 14: Direct typical TEM micrograph of thick porous A-C film and aluminum alloy Al-1100-H14 substrate anodized in 90 g/l oxalic acid at 25°C and constant AC voltage of 75 V for 60 min.

Second phase particle (dark zone at the bottom of the left handside in the electron image) associated with porous film structure.

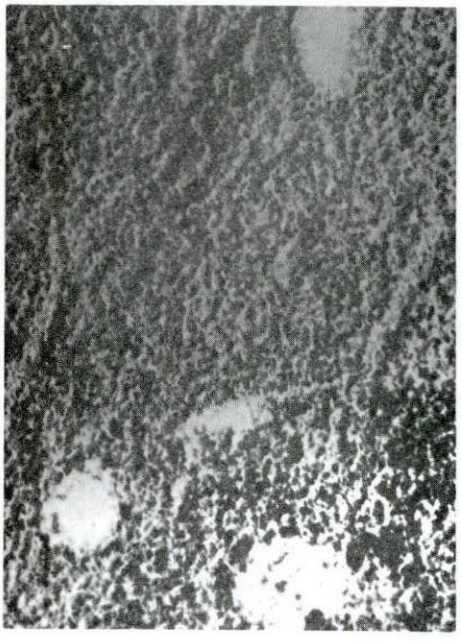

Fig. 15: TEM surface replica of A-C anodized Al-2024-T3 in 170 g/l sulphuric acid at 15°C and at constant potential of 23 V for 30 min.

Light sites indicating the presence of second phase particle at film surface.

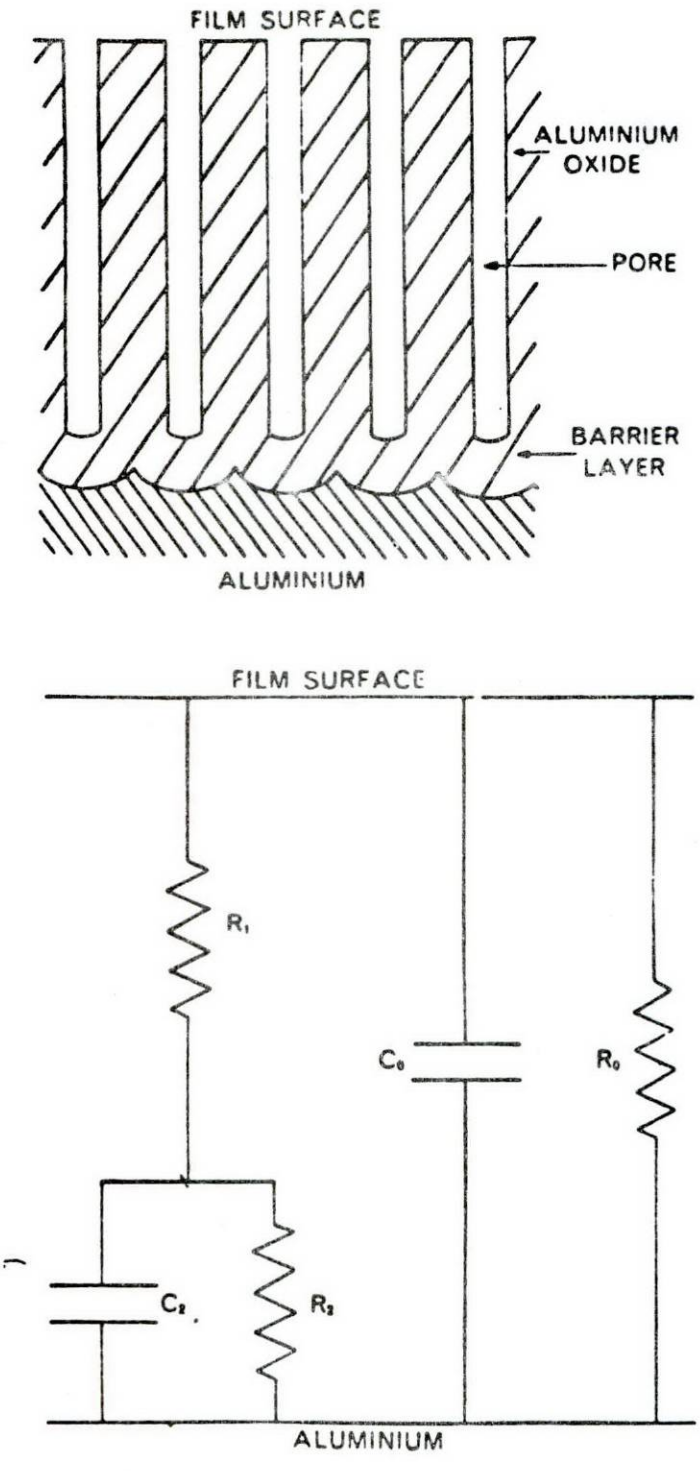


Fig. 16: Schematic description of porous thick A-C anodic film and its equivalent analog electrical circuit.

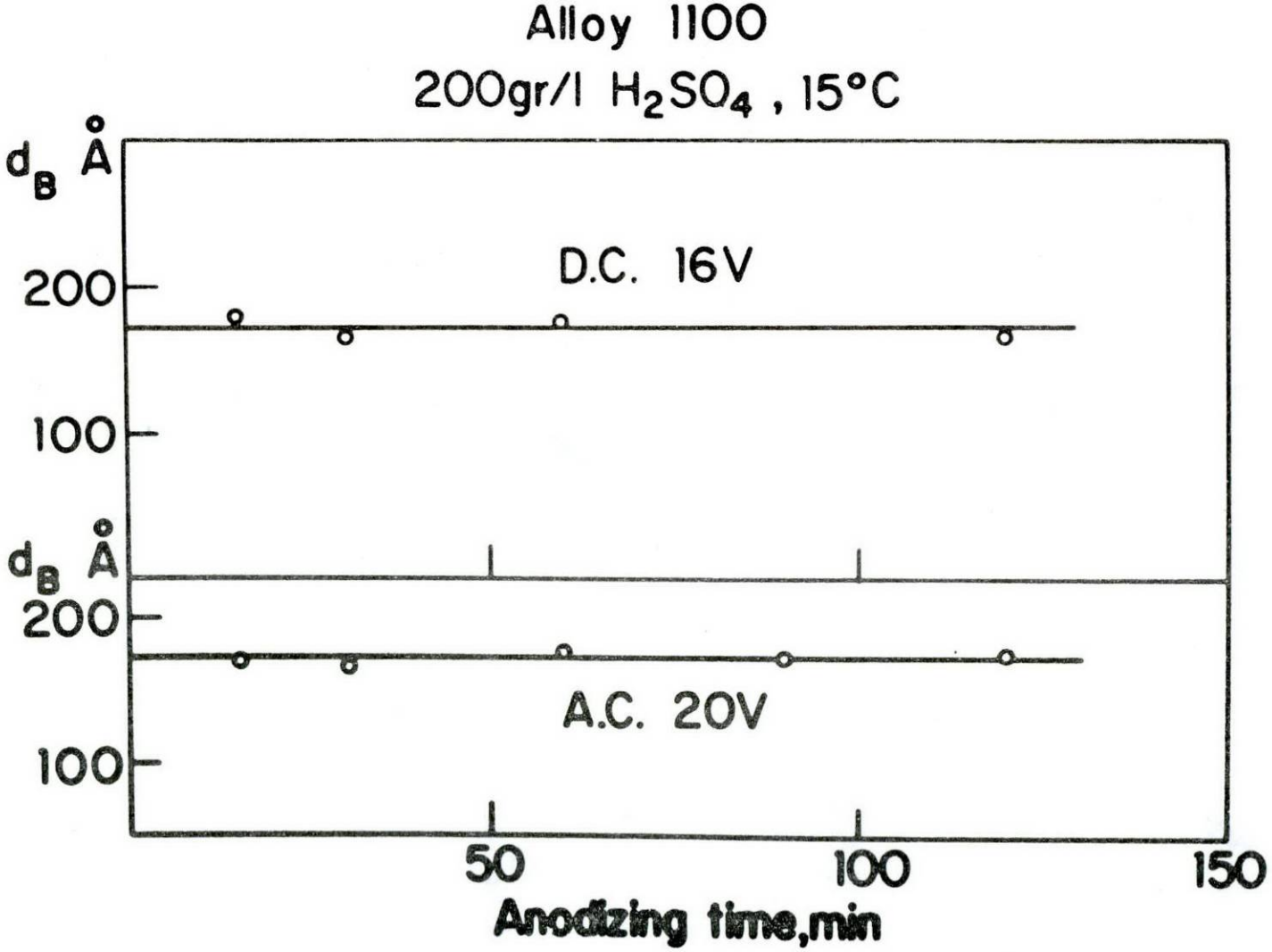


Fig. 17: Dependence of barrier layer thickness of DC and AC anodic films on anodizing time. Films were formed on Al-1100 in 200 g/l sulphuric acid at 15° C.

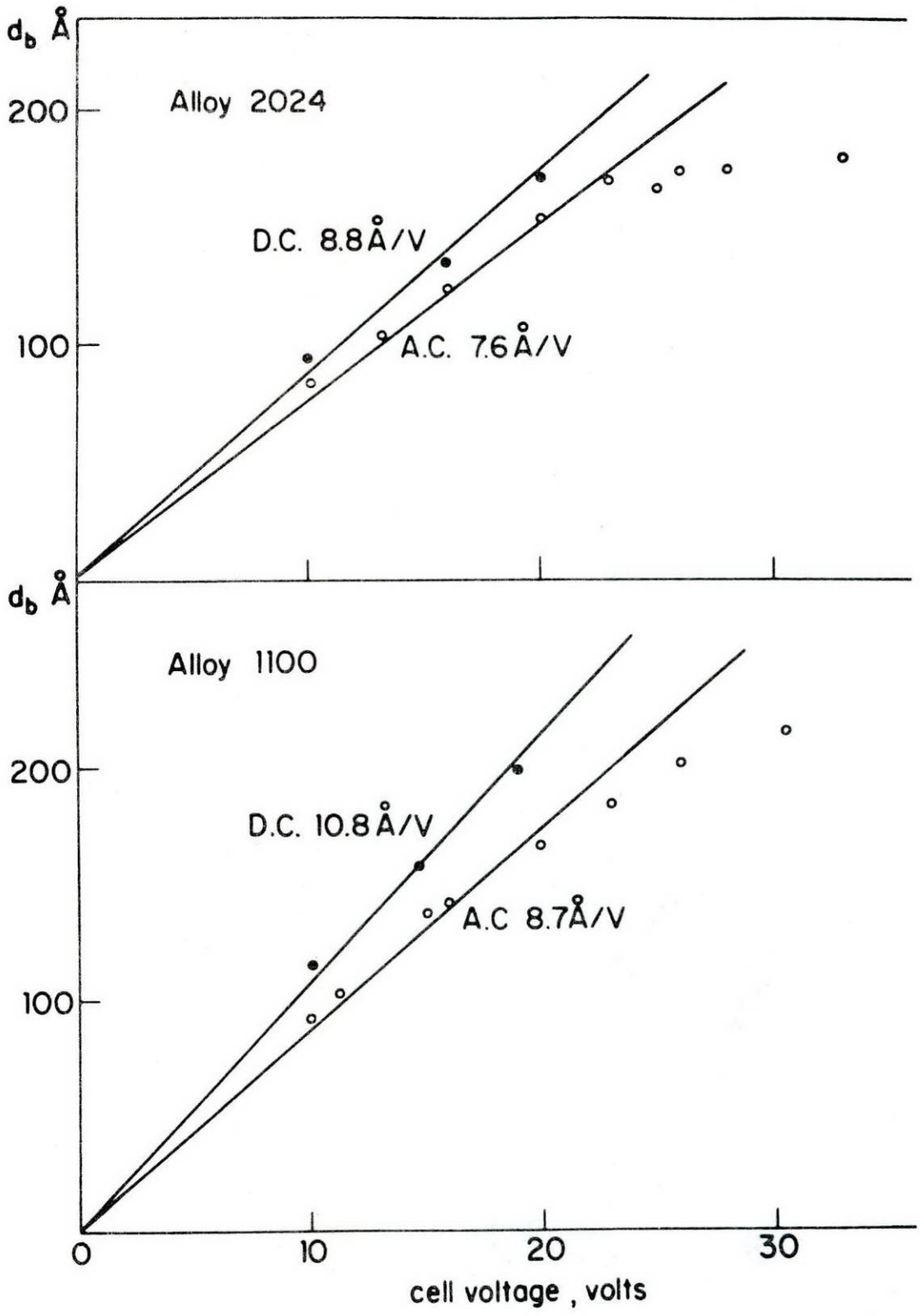


Fig. 18: Dependence of barrier layer thickness on DC and AC anodizing cell voltage for Al-1100 and Al-2024 alloys.

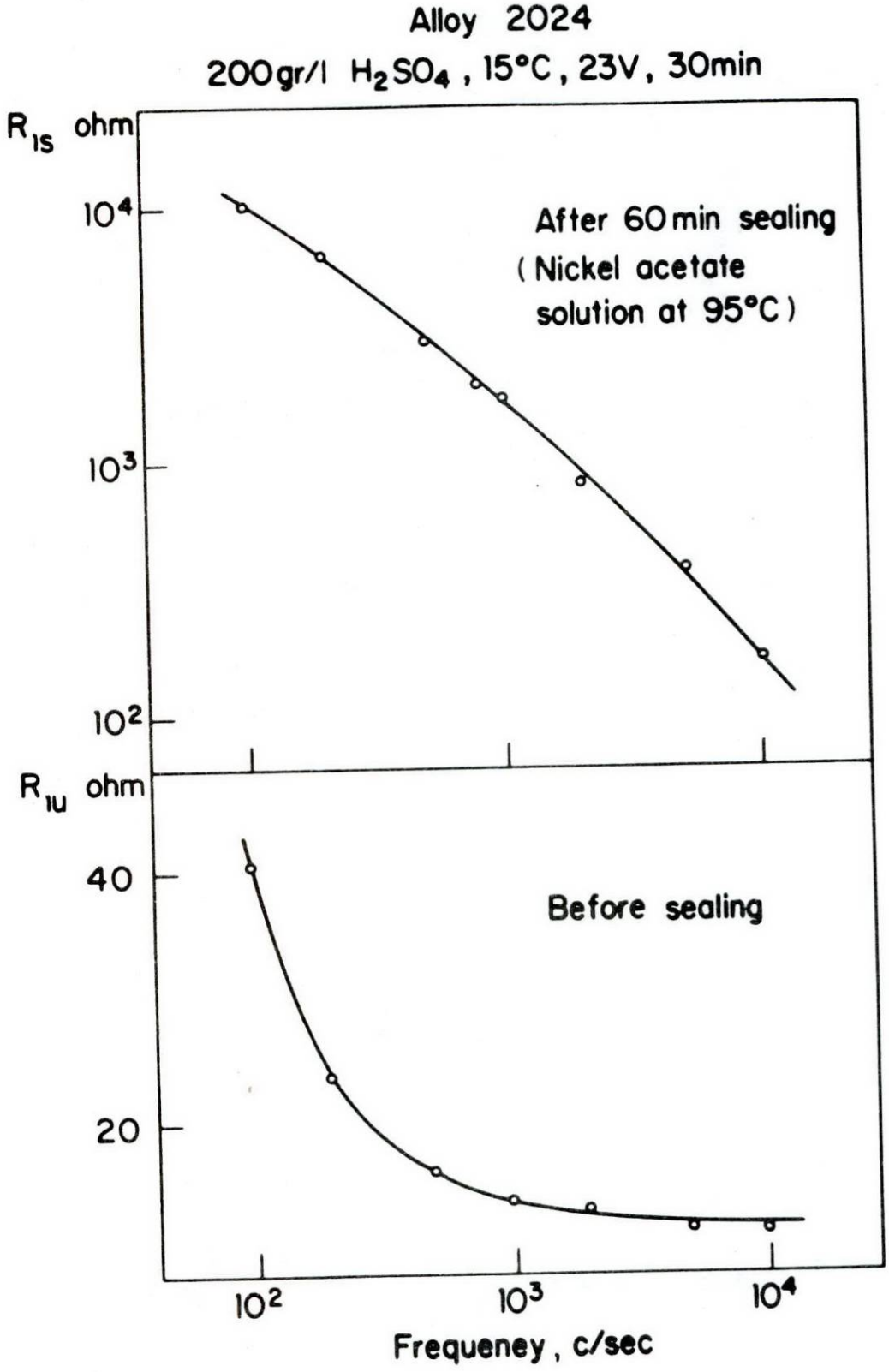


Fig. 19: Typical dependence of AC anodic film pore resistance before and after being sealed on impedance frequency measurement.

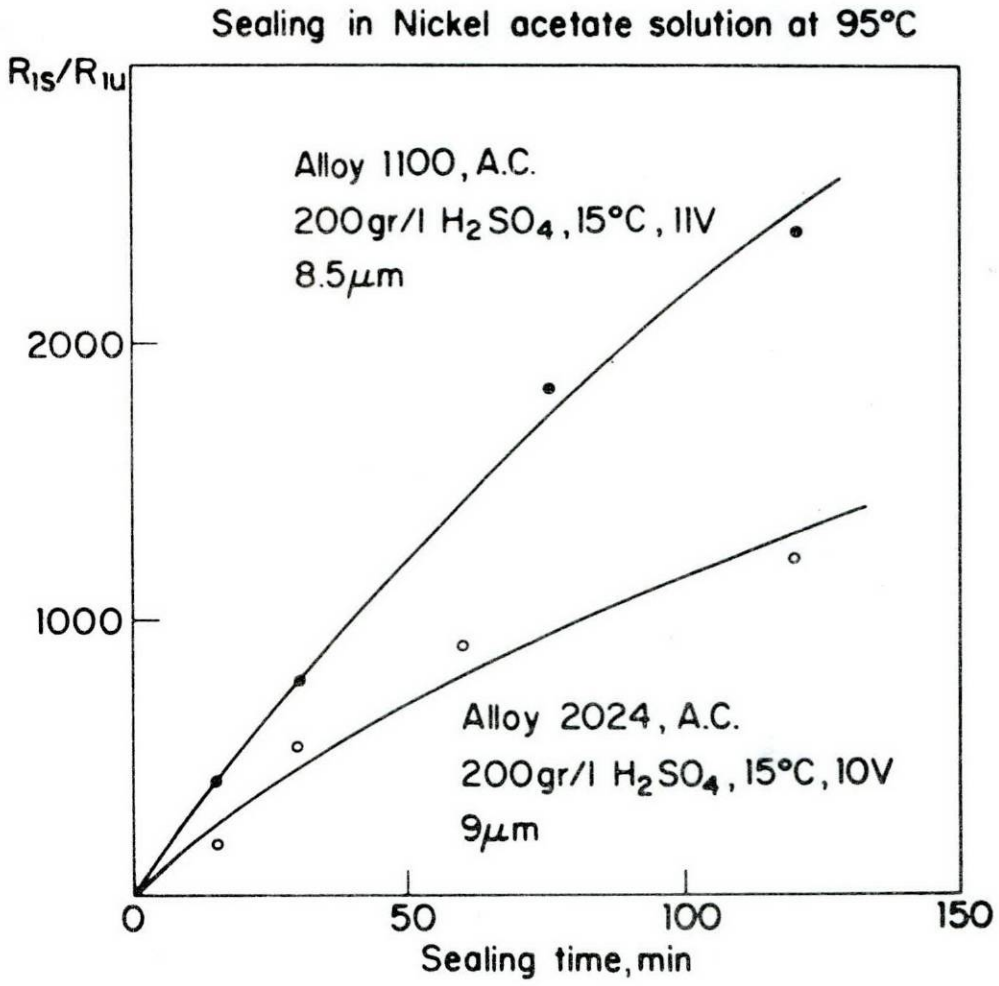


Fig. 20: Dependence of the ratio of sealed pore resistance to unsealed pore resistance on sealing time of A-C thick porous anodic films.

G-4

# Light Metals Finishing II
# Session G

## Corrosion Studies With The Rotated Aluminum Electrode (R.Al.E.)

Dr. W. E. Dalton
St. John's University
Jamaica, NY

# CORROSION STUDIES WITH THE ROTATED ALUMINUM ELECTRODE (R.Al.E.)

W.E. Dalton
St. John's University Jamaica, N.Y.

Introduction:

Despite the fact that chromate conversion coatings for aluminum[1] have been used since World War II, there is still some mystique as to their protective nature. It is believed that a redox reaction occurs with the formation of a passive film containing both trivalent and hexavalent chromium compounds.[2]

Potential measurements[3] indicate that the chromate bath is active and dissolves the natural oxide-film[4] on aluminum. Electrode potentials are of the order of -0.9V to -1.2V for treated samples measured in buffered aqueous solution (pH 6.5) as compared to -0.6V to -0.7V for untreated samples. This seemingly paradoxical phenomenon has led the author to look for a different mechanism in the passivity of aluminum by chemical treatment.

An oxidizing current is used here to play the role of chromate in a dip treatment. Fluoride and/or hydroxyl ions which are present in conversion baths depolarize the aluminum electrode at high negative potentials. The employment of the rotated aluminum electrode (R.Al.E.) helped to achieve reproducible i-E curves although zero current potentials did vary with pretreatment of the electrode.

Experimental:

A rotating aluminum electrode depicted in Fig.1 was found suitable for use. The electrode was so designed that an 1/8" diameter disc was exposed to the solution. The electrode was rotated primarily at 600 rpm by means of a Sargent synchronous motor. The electrode was mechanically cleaned with pumice and then rinsed with distilled water before each determination, unless otherwise specified.

Current-potential curves were run with an automatically controlled potentiostat as shown in Fig. 2. Except for the current decay curves, current readings were recorded after one minute at a given potential. All experiments were carried out at 25°C. Determinations were conducted in a 250 ml cell equipped with an inlet tube for the introduction of pure nitrogen to purge the solution of oxygen.[5] For the most part, measurements were run from negative to positive potentials. Reported potentials refer to the saturated calomel electrode (S.C.E.)

Results and Discussion:

The aluminum electrode is highly polarizable, the passivity of the metal being attributed to a film of aluminum oxide on the surface. Electrode potentials of aluminum measured by electrochemical techniques do not agree with the values calculated from thermodynamic data.[6] This can be realized by the fact that the anodic reaction at an aluminum electrode differs from the cathodic reaction[7] and the potential, therefore, does not correspond to that of a reversible system.

In Fig.3 it can be seen that fluoride ions exert a depolarizing effect on the R.Al.E. producing a fairly steep slope of the i-E curves near the zero current potential. The oxide-film is apparently permeable to fluoride ion forming a complex[8] according to the following equation:

$$Al_2O_3 + 12F^- + 6H^+ = 2AlF_6^{-3} + 3H_2O \qquad (1)$$

The onset of limiting current for fluoride ion concentration appears to be taking shape at -0.4V in curves A,C, and D, and the magnitude of the current varies with its concentration. The inception of a second anodic wave is evident between -0.6V and -0.7V, the subject of which is subsequently investigated in this paper. The surge in current at -0.2V in curve B is attributed to the permeation of $H_2$ through unprotective oxide-film and its resulting anodic oxidation.[9]

In Fig.4 there is approximately a 35% increase in limiting current for the electrode pretreated in alkali compared to the one that was just mechanically cleaned. (See curves A and B) It is believed that the production of $H_2$ at the surface from the former pretreatment[2] is responsible for this occurrence.[10] The Nernst potential for the oxidation of $H_2$ is reasonably close to the experimental value obtained here.

Theoretically- $E_{cell} = .059pH + E_{ref}$ (2)

$= .059(6.5) + 0.25V$

$= 0.63V$

Experimentally, the slope of the anodic wave is steep between -0.6V and-0.7V. This represents equal concentrations of oxidized and reduced species which in this case is believed to be the ratio of $[H^+]/[H_2]$. As one moves toward less negative potentials, limiting current for $H_2$ oxidation occurs and $[H_2]$ at the surface $\longrightarrow 0$. This is manifested by a decay in current on the plateau of the curve. A change in pH to higher values shows a shift in curves C and D to more negative potentials. Based on the Nernst equation, this is predictable for the oxidation of $H_2$.

In alkaline solution the oxide-film is permeable to hydroxyl ions which form the aluminate[11] complex as follows:

$$Al_2O_3 + 2OH^- + 3H_2O = 2[Al(OH)_4]^- \quad (3)$$

The complexing action of fluoride and hydroxyl ions thins down the pre-existing oxide-film on the R.Al.E. allowing the formation of $H_2$ electrochemically and chemically, the latter by the Al-$H_2O$ reaction[11] according to:

$$2Al + 3H_2O \longrightarrow Al_2O_3 + 3H_2 \quad (4)$$

In Fig.5 measurements taken in alkaline solution show well-defined limiting current regions. A threefold decrease in current is observed in curve A compared to curve B when the R.Al.E. is polarized from + to - potentials. This is attributable to the fact that there is no significant $H_2$ accumulation between -0.4V and -0.8V since it is oxidized at a faster rate than it is produced. Potentials of electrodes pretreated in alkali are 100 to 300 mv more positive than those that are mechanically cleaned. These are mixed potentials.[13] At such potentials the anodic reaction at the aluminum electrode differs from the cathodic reaction.

$$\text{(anodic)} \quad Al + 4OH^- \longrightarrow [Al(OH)_4]^- + 3e^- \quad (5)$$

$$\text{(cathodic)} \quad 2H_2O + 2e^- \longrightarrow H_2 + 2OH^- \quad (6)$$

$$\text{(overall balance)} \quad 2Al + 2OH^- + 6H_2O \longrightarrow 2[Al(OH)_4]^- + 3H_2 \quad (7)$$

Subsequent adsorption of $H_2$ by the electrode occurs.[14] The larger limiting current for the alkali pretreated electrode(See curve C) lends additional credance to a time-dependent process, the probable oxidation of $H_2$.

In Fig.6 the current-decay curves resulting from the oxidation of $H_2$ at various controlled potentials are shown. It was found that pH, electrode potential, and time of decay play a major role in forming a corrosion-protective oxide on aluminum. The electrochemical equivalent of a dip process was found to have the following limitations:

(a) pH range - 8.5 to 9.0

(b) Electrode potential range - -0.6V to -0.8V

pH values higher than 9.0 exert too strong a solvent action on the barrier oxide, and pH values between 6.5 and 8.5 require less negative potentials(-0.4V to -0.5V) to completely scavenge $H_2$. Such a potential range leads to the formation of unprotective anodic oxide-film.[15]

Salt spray[16] testing of polarized R.Al.E.'s revealed the following:

| | Controlled Potential | pH | Appearance | Hours to Corrosion |
|---|---|---|---|---|
| (1) | -0.4V | 6.5 | Visible film | 24 |
| (2) | -0.5V | 8.0 | Visible film | 48 |
| (3) | -0.6V | 8.5 | Gray surface | 96 |
| (4) | -0.7V | 8.7 | Polished surface | None after 250 |
| (5) | -0.7V | 9.0 | Polished surface | 1 pit after 200 |

Fig. 7 represents an experiment that was conducted to determine whether there is a relationship between extent of pitting and time of treatment in a typical chromate bath.[17] Aluminum foil samples( 1/2 by 1 ) were pretreated in alkali for different periods of time in order to charge the surface with $H_2$. After rinsing in distilled water, the samples were affixed to the shaft of a stirring motor and rotated at 600 rpm in the treatment bath. Each sample was removed at a different time and subjected to salt spray overnight to determine the extent of corrosion. There appears to be a correlation between the shape of the current-decay curves in Fig.6 and the pitting-time curves in Fig.7. In 8 minutes the curves tend to level off, probably indicating the complete oxidation of $H_2$. Salt spray data show little to no pitting after this treatment time.

In Fig.8 the time of treatment is held constant and rotation in alkali is varied. Again one can see the exponential nature of the process. A sharp increase in pitting is observed within the first few minutes followed by a gradual leveling off in 10 minutes.

Summing up, it is believed that efficient mass transport is the key to forming a corrosion protective barrier oxide. The removal of electro-oxidized hydrogen and pre-existing oxide-film at prominences by hydroxyl ions probably produces a surface polishing action; such a surface leads to lower reactivity.

Epilogue:

One of the objectives of this paper is to show that an applied negative potential can be substituted for chromate ions in a solution containing excess hydroxyl ions and produce a barrier oxide-film, such a film being capable of withstanding extensive salt spray testing à la conversion coating.

Another objective is to show that a relationship exists between the pitting of aluminum and the adsorption of hydrogen at the surface. The oxidation of hydrogen by chromate, which acts as an internal potentiostat, or the application of an external potential seems to be essential in producing a corrosion-resistant film.

Further research is needed to directly link hydrogen with the corrosion process. The author suggests that AC capacitance measurements and mass transport studies, with variations in rotational speed, may be the key to resolving the corrosion-protective mechanism. The use of ultrasonic agitation offers some promise in that one could go to larger aluminum samples to replace the R.Al.E. This may be a more practical approach in evaluating corrosion data.

The author has successfully used ultrasound to induce a passive film on elemental beryllium.[18,19]

References:


1. S. Wernick, R. Pinner, Surface Treatment and Finishing of Aluminum and its Alloys, R. Draper, LTD pp. 42, 43, 167, 168 (1956)
2. W. Pocock, Metal Finishimg, 53, 80 Dec. 1954 - Jan. 1955
3. K. Rajagopalan, J. Electrochem Soc., 106, 113 (1959)
4. R. Hart, Proc. Roy. Soc., (A) 236, 68 (1956)
5. I. Kolthoff, C. Sambucetti, Analytica Chimica Acta, (II) 21, 161 (1959)
6. W. Latimer, Oxidation Potentials, Prentice-Hall, Inc., New York, NY, (1952)
7. I. Kolthoff, C. Sambucetti, Analytica Chimica Acta, (I) 21, 17 (1959)
8. F. Haynie, S. Ketcham, Corrosion, 19, 407 (1963)
9. U. Evans, Corrosion and Oxidation of Metals, Edward Arnold, LTD p424 (1960)
10. G. Ewing, Instrumental Methods of Chemical Analysis, McGraw Hill Book Co., Inc., New York, NY, p42 (1954)
11. E. Gould, Inorganic Reactions and Structure, Henry Holt and Co., New York, NY, p450 (1955)
12. M. Hunter, P. Fowle, J. Electrochem Soc., 103, 482 (1956)
13. J. Petrocelli, J. Electrochem Soc., 99, 513 (1952)
14. B. Kolachev, Hydrogen Embrittlement of Nonferrous Metals, Israel Program for Scientific Translations, LTD pp. 103, 104, 105, 106 (1968)
15. F. Keller, M. Hunter, D. Robinson, J. Electrochem Soc., 100, 411 (1953)
16. A.S.T.M. Standard, B 117-57T (1958)
17. L. Spencer, Metal Finishing, 58, 59 (1960)
18. W. Dalton, U.S. patent 4,328,047 (1982)
19. W. Dalton, Plating and Surface Finishing, 70, 106 (1983)

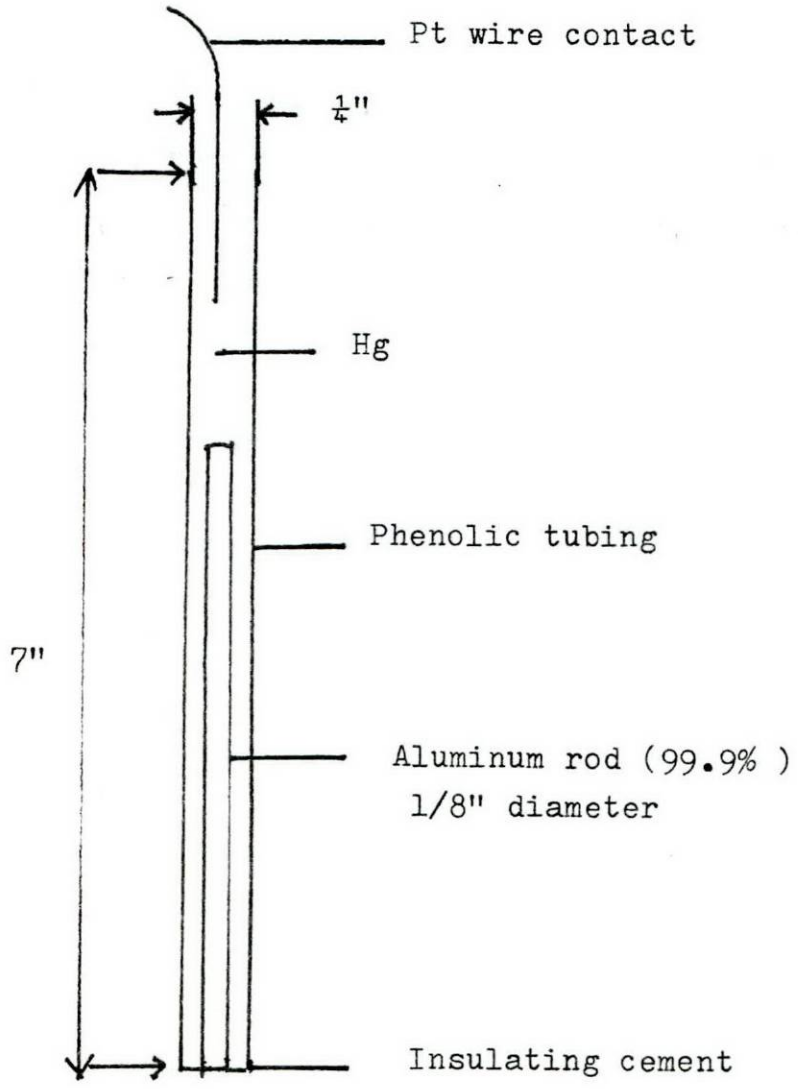


Fig. 1. The Rotated Aluminum Electrode

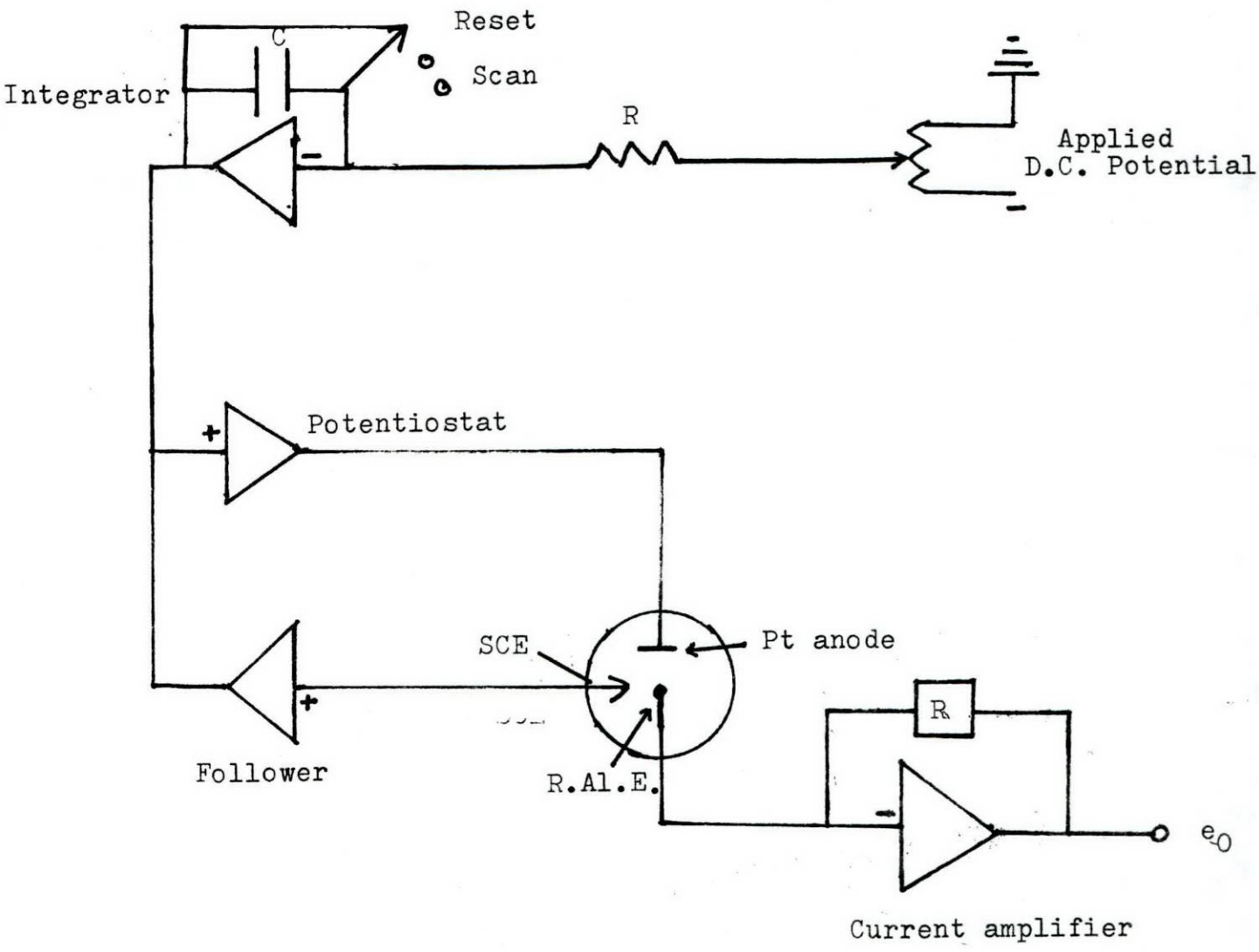


Fig. 2. Electrolytic cell and operational amplifier instrumentation for controlled potential experiments.

Fig. 3. Depolarization of the R.Al.E. by fluoride in media containing acetate buffer. A, 1. $10^{-3}$ NaF, pH 6.5; B, $1.10^{-3}$M NaF, pH 6.5 with $H_2$ bubbled into solution; C, $6 \cdot 10^{-3}$M NaF, pH 6.5; D, $7 \cdot 10^{-3}$M NaF, pH 6.5.

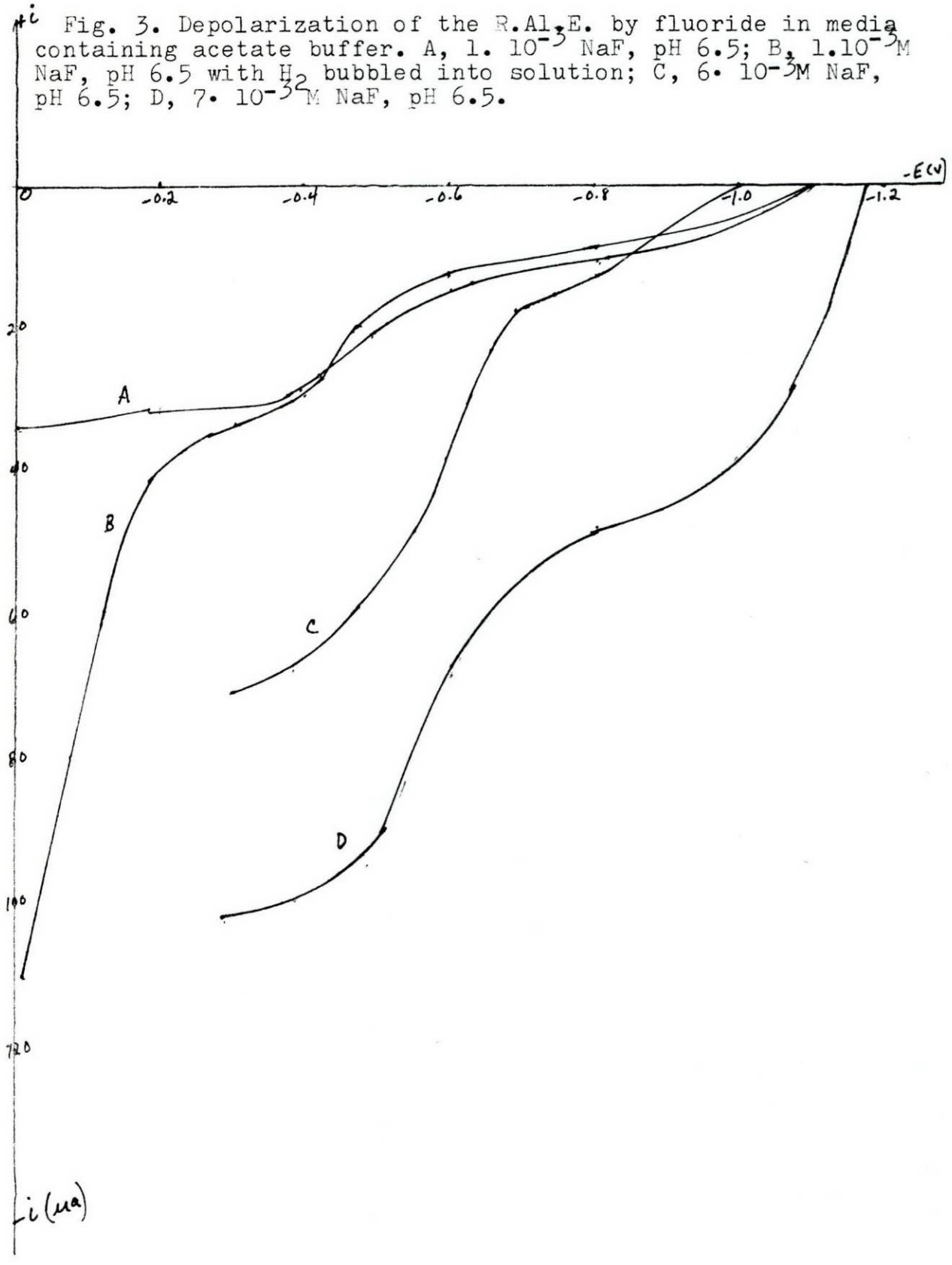

Fig. 4. Depolarization of the R.Al.E. as a function of pH and pretreatment. A, $6 \cdot 10^{-3}$M NaF, pH 6.5; B, $6 \cdot 10^{-3}$M NaF, pH 6.5, pretreated in 2M NaOH; C, alkaline solution, pH 9.0 containing bicarbonate buffer; D, alkaline solution, pH 9.5 containing bicarbonate buffer.

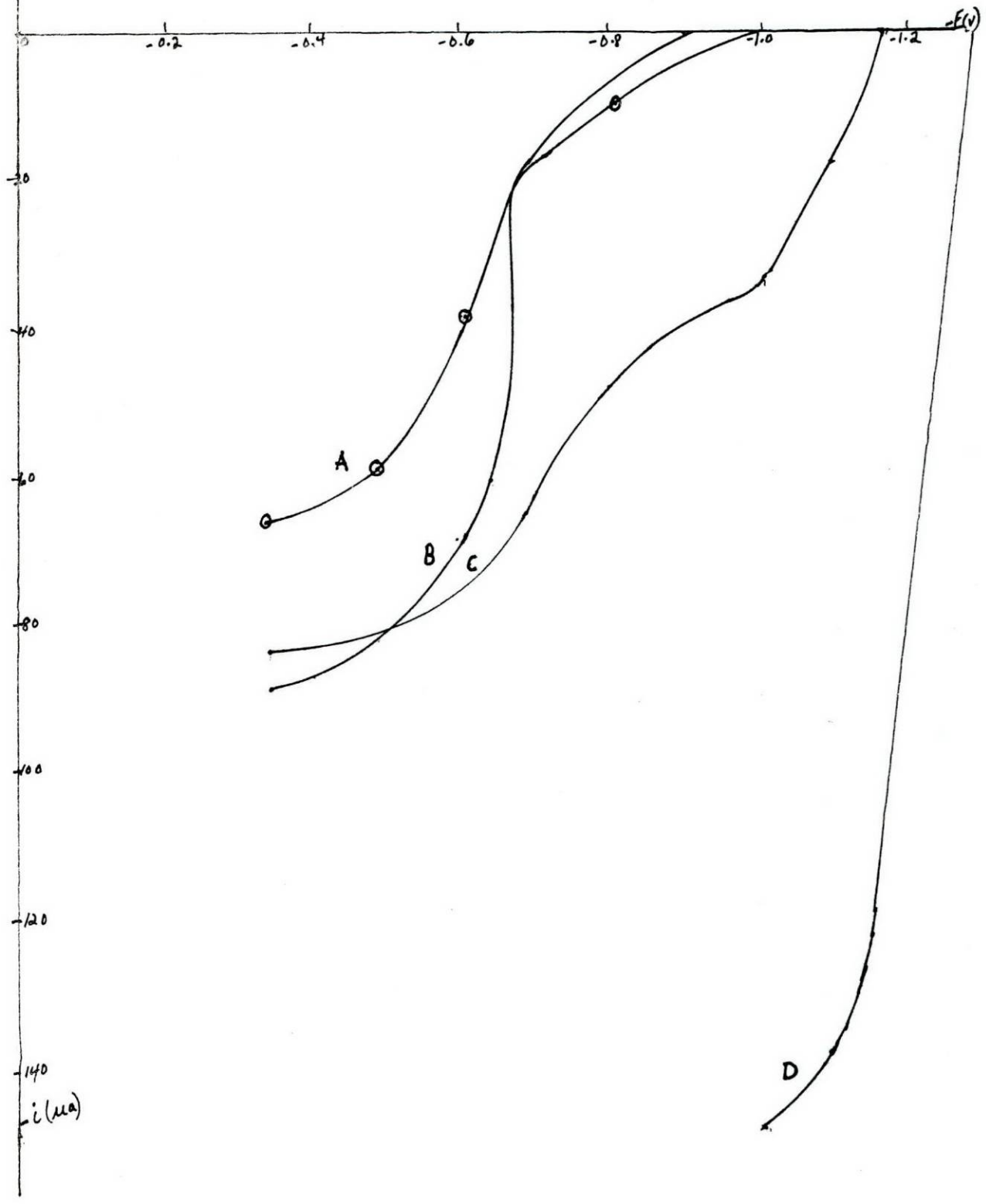

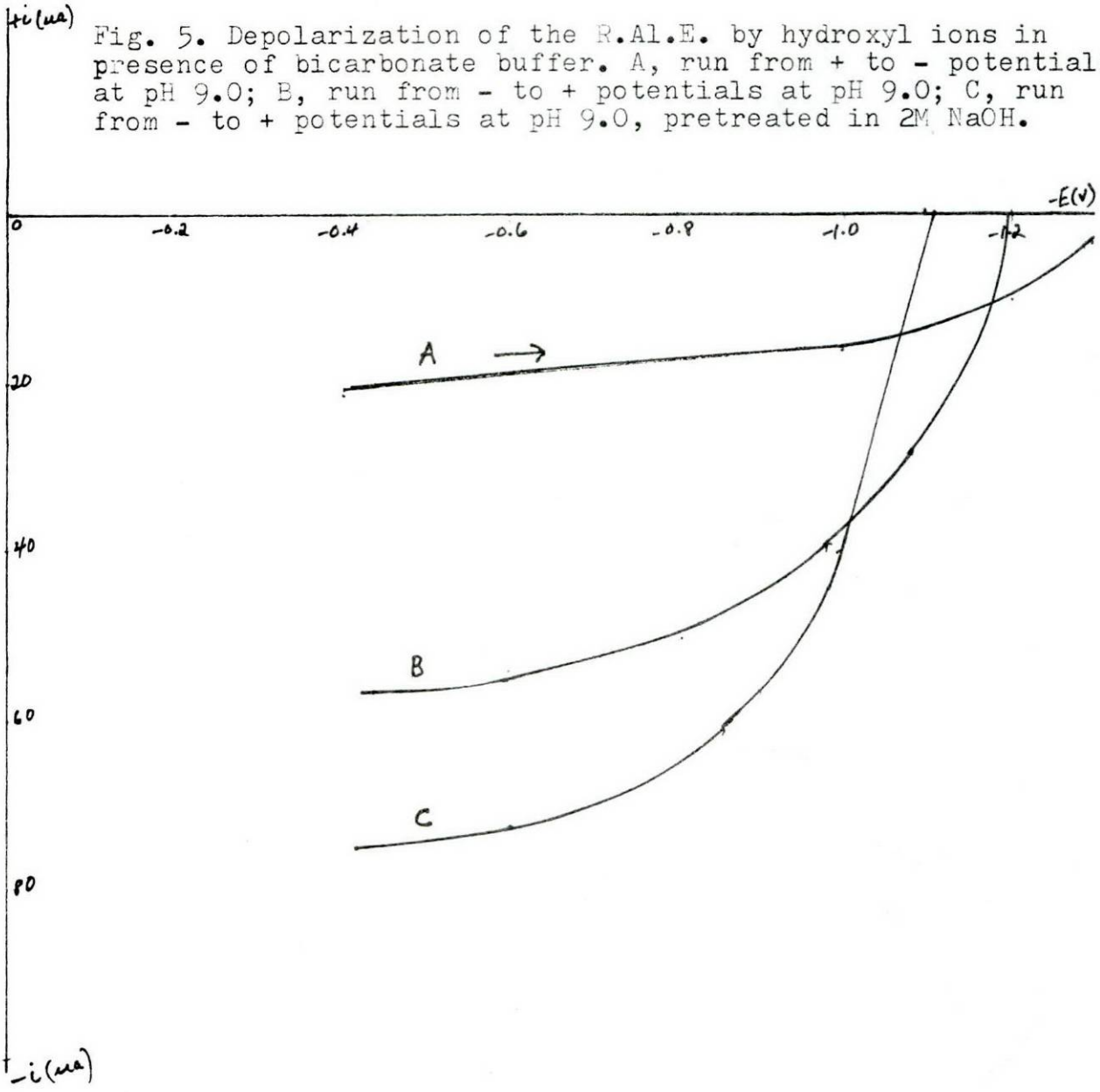


Fig. 5. Depolarization of the R.Al.E. by hydroxyl ions in presence of bicarbonate buffer. A, run from + to - potentials at pH 9.0; B, run from - to + potentials at pH 9.0; C, run from - to + potentials at pH 9.0, pretreated in 2M NaOH.

Fig. 6. Current-decay curves of R.Al.E. in alkaline solution (pH 9.0) at various controlled potentials after scanning from - to + potentials. A, -0.8V; B, -0.7V; C, -0.6V.

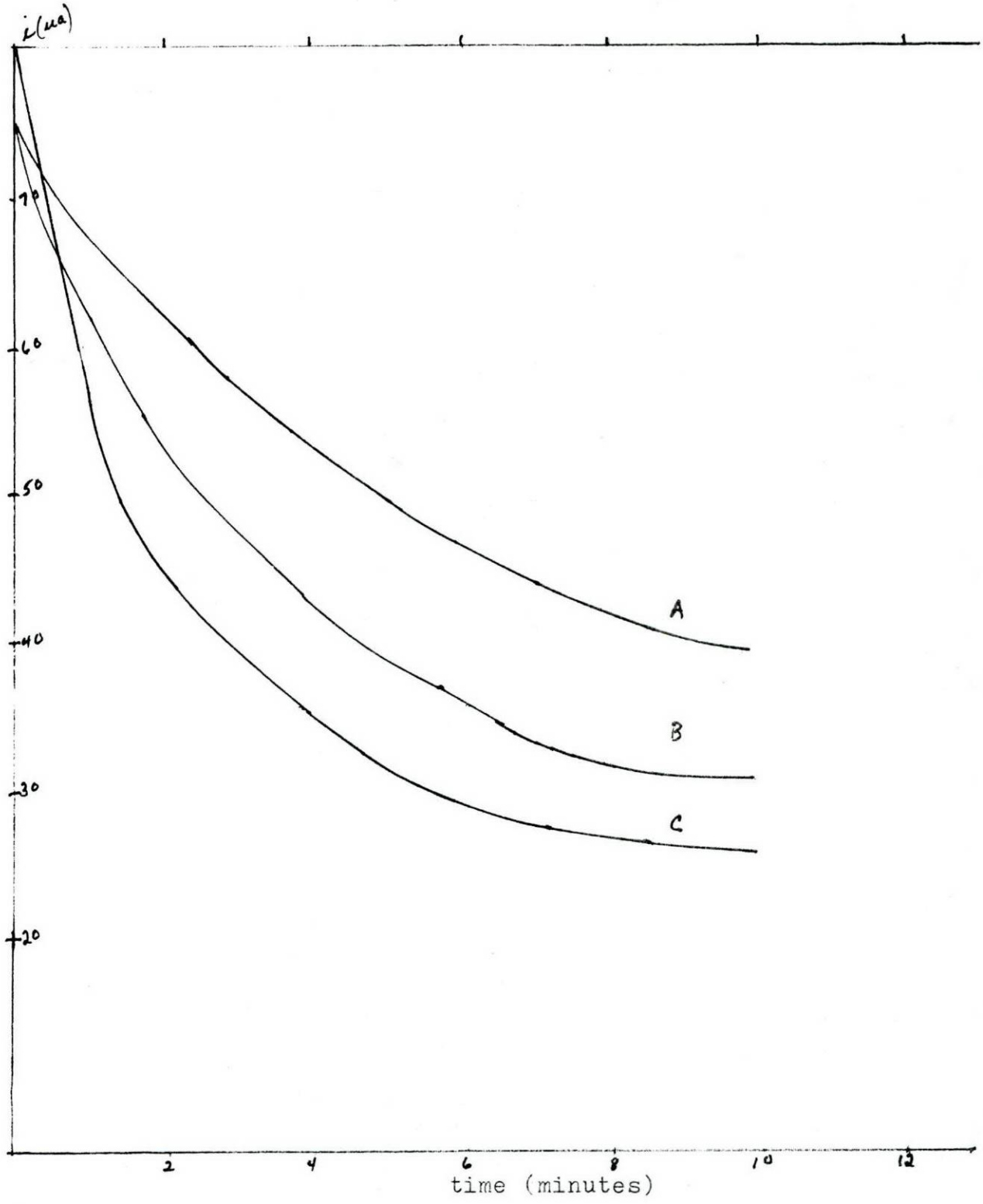

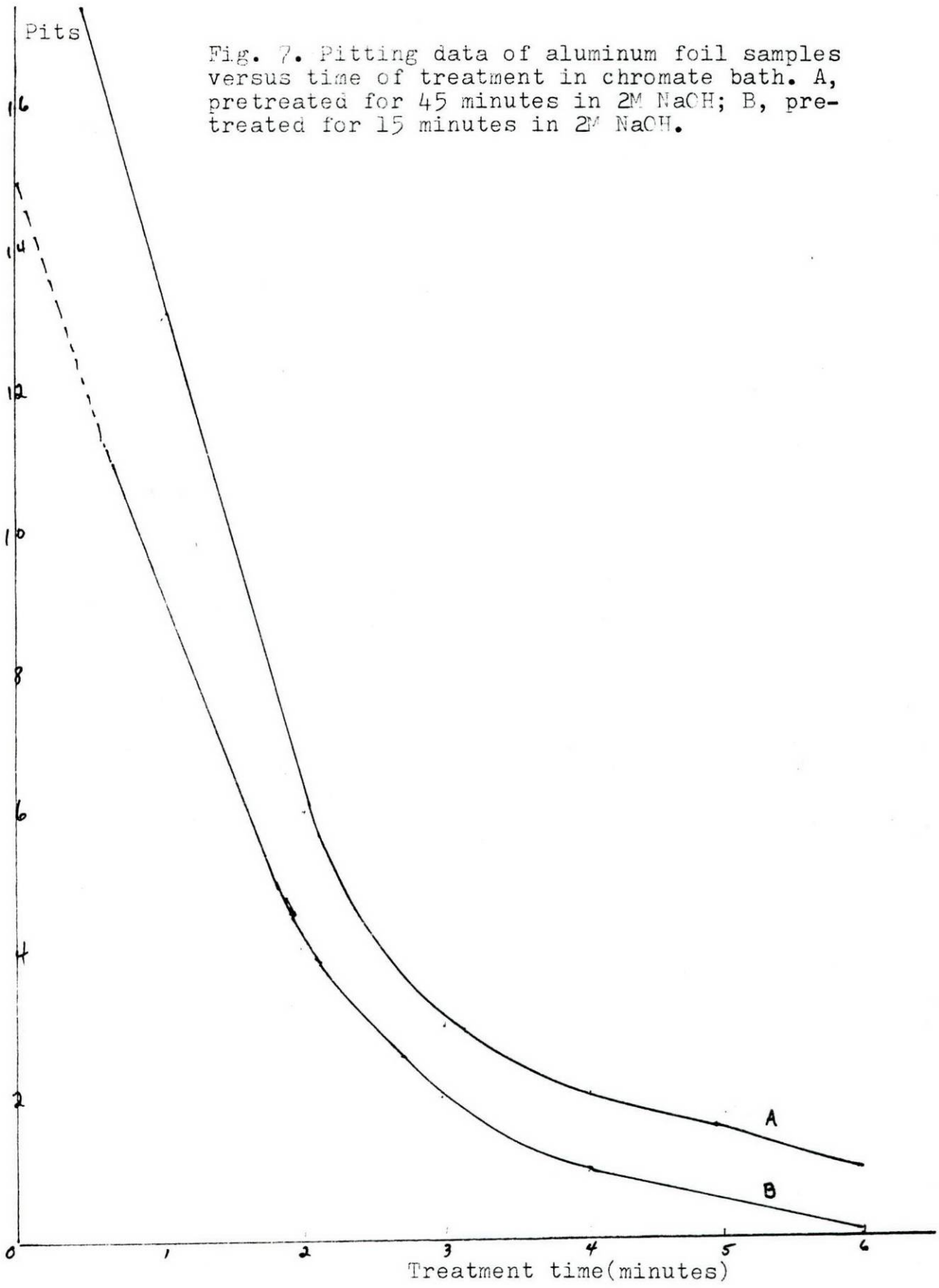


Fig. 7. Pitting data of aluminum foil samples versus time of treatment in chromate bath. A, pretreated for 45 minutes in 2M NaOH; B, pretreated for 15 minutes in 2M NaOH.

Fig. 8. Salt spray data of aluminum foil samples versus time of pretreatment in dilute alkali (pH 10). After rinsing, each sample was treated in a typical chromate bath for 10 seconds.

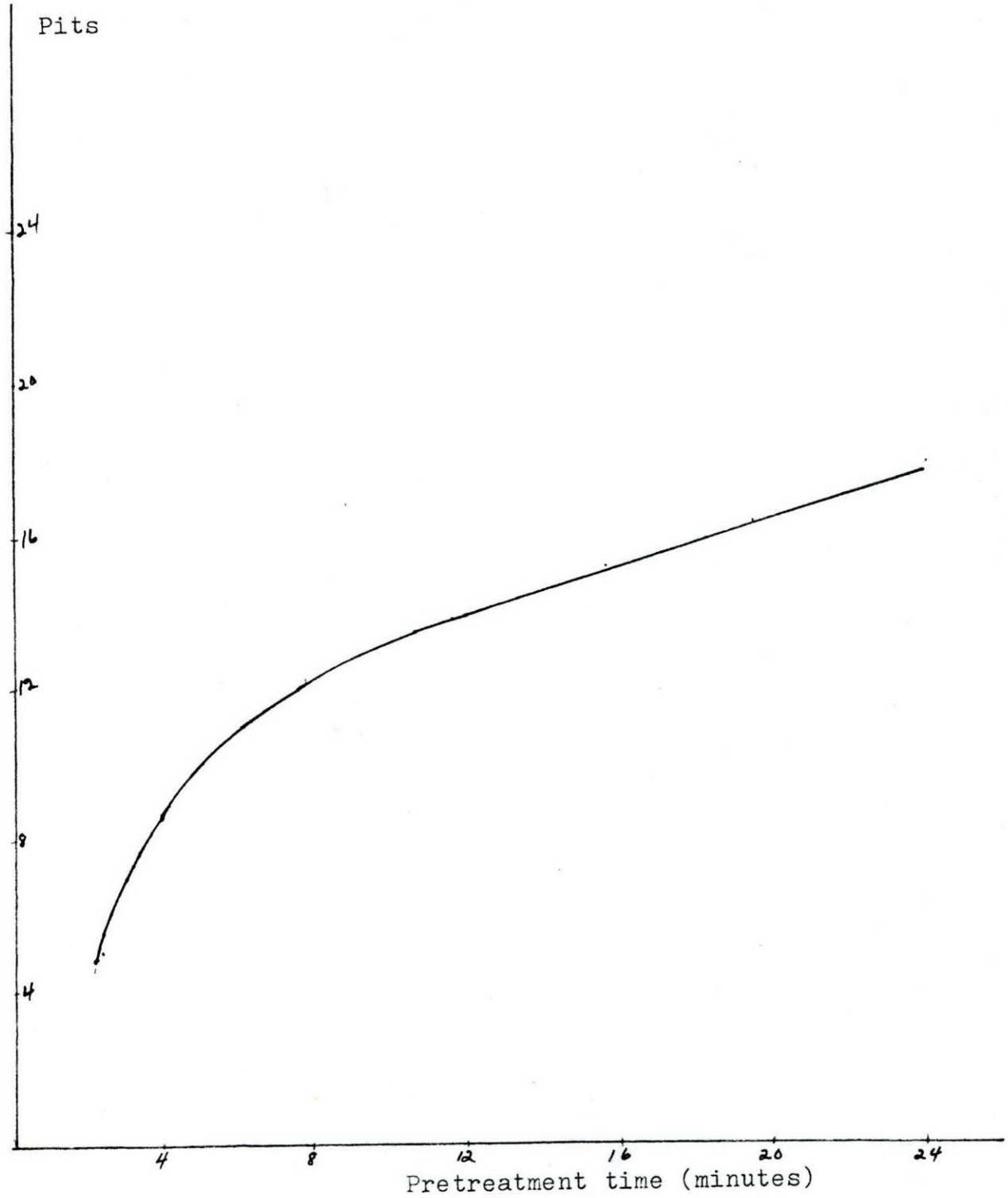

G-5

# Light Metals Finishing II
# Session G

## A Continuous Flow Caustic Etch Regeneration Process

Raymond J. Meyer
Aluminum Company of America
Alcoa Center, PA

# A CONTINUOUS FLOW CAUSTIC ETCH REGENERATION PROCESS

Raymond J. Meyer
Aluminum Company of America
Alcoa Technical Center
Alcoa Center, Pennsylvania 15069

The Caustic Etch Regeneration Process is a patented continuous flow system for controlling the composition of caustic etch solutions used for etching aluminum. But since it also drastically reduces chemical consumption and effluent waste solids, it becomes a resource conservation or recovery process.

To fully appreciate the effects of the recovery process requires insight into its mechanism and underlying principles. Prerequisite to the latter are some fundamentals and consequences of the caustic etch process as commonly practiced.

During etching, aluminum dissolves, combining with sodium hydroxide to form sodium aluminate as described by the reaction equation in Figure 1. As the etch solution is used, it becomes deficient in available NaOH and must be continually replenished to maintain consistent performance. Moreover, the etch solution becomes increasingly saturated with aluminum which eventually makes it useless; hence, it must be discarded. Because of this necessary practice, any commercial etching process is only 50 to 80 percent efficient with respect to caustic usage.

What is most significant is that all of the caustic used and all of the aluminum dissolved ultimately enters the effluent waste stream as depicted by the flow diagram in Figure 2. To maintain compliance with pollution control regulations, this alkaline waste water must be neutralized. Such treatment causes the dissolved aluminum to precipitate as colloidal aluminum hydroxide which creates a sludge upon dewatering of only 10 to 15 percent solids content. The economic consequence of this scenario will be put into perspective later.

The preceding picture is completely changed by the Caustic Etch Regeneration Process as summarized in Figure 3. In contrast to relative inefficient use of chemicals, this process can actually reduce NaOH consumption by about 80 percent. Of the other 20 percent, roughly 10 percent is inescapably due to dragout, and the remaining due to miscellaneous process variation. The composition and, therefore, the performance of the etch solution is stabilized through removal of aluminum as quickly as it is dissolved. Since aluminum is removed, there is no need for sequesterants. Last, since crystalline $Al(OH)_3$ is generated and removed from the system at its source, the overall quantity of effluent waste solids can be reduced by about 80 percent.

What makes this all possible is our successful exploitation of the propensity of dissolved aluminum to hydrolyze and precipitate from caustic solutions. As shown by the etching and hydrolysis reaction equations and

the overall process scheme in Figure 4, the sodium aluminate generated during etching is hydrolyzed to aluminum hydroxide, thereby liberating the NaOH which had been complexed during the etching (dissolution) reaction. Forcing this hydrolysis reaction to occur in an isolated environment permits reclamation of the regenerated caustic and is recycled to the etching operation. The crystalline aluminum hydroxide is removed from the system as an 80-90 percent solids content by-product.

The perspective drawing in Figure 5 illustrates the equipment and flowstreams fundamental to the Caustic Etch Regeneration Process. In essence, the process consists of a primary and an optional closed loop around the caustic etch tank. The optional circuit, consisting of a pump and an automatic backwashing tubular filter system, serves to remove etching smut (oxides and hydroxides of alloying constituents) and any other insoluble matter. This is useful if a relatively clean by-product $Al(OH)_3$ is desired; but the consequence will be an additional loss of caustic via backwashing. The reaction loop basically consists of a stirred reactor tank and an integral rotary drum vacuum filter. The reactor contains a slurry of aluminum hydroxide and etch solution. This dispersion of fine aluminum hydroxide crystalline particles throughout the bulk of the solution is instrumental in effecting continual nucleation of new insoluble crystalline particles of aluminum hydroxide and growth of older particles. The rotary drum filter separates the reaction slurry recovering the $Al(OH)_3$ by-product and the regenerated etch solution. The $Al(OH)_3$ by-product is dewatered to about 90 percent solids content upon separation; hence, its disposal is facilitated. The regenerated liquor is recycled to the etch bath.

The production facility required for this continuous flow process consists of essentially standard equipment; overall design, however, is critically dependent upon the rate at which aluminum is normally dissolved. Accordingly, each process facility must be custom built to satisfy the requirements of the particular etching operation. To give some perspective of scale, a typical etching operation in an extrusion anodizing line would need about 200 $ft.^2$ of floor space as shown in Figure 6 for a representative caustic etch regeneration system. The reactor would be about 10 ft. diameter by 8 ft. high with a volume of about 4000 gallons. The rotary drum vacuum filter would typically be 6 ft. diameter with about a 4 ft. face as shown in Figure 7. The associated vacuum pump, filtrate receivers, filtrate pumps, integral piping, and control panel are skid mounted as depicted in Figure 8, occupying about 40 $ft.^2$ of floor space. The surge tank also depicted in Figure 8 obviates the pulsed flow from the filtrate receiver/pump system. It is usually about 300 gal. capacity. The holding tank (used to store reactor liquor while replacing the drum filter cloth) is usually about 1000 gal. capacity (see Figure 6). Last, the optional smut filtration system as typified in Figure 9 occupies about 40 $ft.^2$ floor area.

Figure 10 considers a case example of an extruder/anodizer that anodizes, uses an integral color process, and a two-step anodizing process on a total of twenty-two million feet of aluminum extrusions per year.

While there are three plant locations currently employing this process, we do not have information available that is comparable to this example. Therefore, the information presented here covers a hypothetical case set up to completely cover all of the economic factors that should be addressed. The example is not fictitious, however, in that it represents computer developed information from an actual plant survey on a facility as just described.

The first section compares caustic usage with and without the caustic recovery system. The combined use of caustic for etching and die cleaning with the recovery system is 213,103 pounds per year. With the recovery of caustic, the system does become acid rich even with an acid recovery system, therefore the requirement of 21,123 pounds of caustic per year for acid neutralization. This means that only a total of 234,226 pounds of caustic is required rather than 1,002,258 pounds in a year's time without the caustic recovery system.

The same analysis for sulfuric acid is given in the second section using an acid recovery system. Acid recovery is needed in order to benefit from caustic recovery, or too much additional caustic will be required just for acid neutralization. Although the value of acid is less than caustic, the use of acid recovery also reduces the amount of acid produced in this case by about 890,000 pounds per year.

The third section in this figure covers aluminum hydroxide generation. A waste sludge of 8,755,472 pounds, which contains mostly water, is generated in a year without caustic and acid recovery, while with the recovery system, 1,175,609 pounds of aluminum hydroxide is generated in a nearly dry powder form (10% moisture) and it has some commercial value.

The fourth section covers overall reduction percentages in neutral effluent suspended solids, solids hauled to land fill, effluent dissolved solids, acid usage, and caustic usage as a result of employing the recovery systems.

Figure 11 describes the economic impact resulting from the reductions described in pounds in the previous figure through the use of caustic recovery.

Savings in caustic purchases in a year are $76,803 based on a unit cost of $200 per ton. Sulfuric acid savings in a year are $29,340 based upon $66 per ton. Then the elimination of etch additives, waste haulage, and die cleaning bath disposal effect annual cost savings of $12,000, $55,428, and $9,000 respectively. With an estimated annual operation cost for the recovery system at $38,000, the total savings through the use of caustic and acid recovery is $144,571. With a capital outlay for recovery at about $275,000 to $300,000, this represents a payback of about two years in simple economic terms. No attempt has been made to consider depreciation, interest, fluctuations in material costs, etc. I will be happy to entertain any questions regarding this presentation.

Figure 1

# CAUSTIC ETCH PROCESS

## REACTION:

$$2Al + 2NaOH + 2H_2O \rightarrow 2NaAlO_2 + 3H_2 \uparrow$$

## EFFECTS:

Aluminum Dissolved

NaOH Complexed by Aluminum 1.48 to 1.0

NaOH Utility of 50 to 80%

NaOH Consumed:

Dragout = 8 $\pm$ 4%

Discard = 92 $\pm$ 4%

Amorphous $Al(OH)_3$ Waste

Figure 2

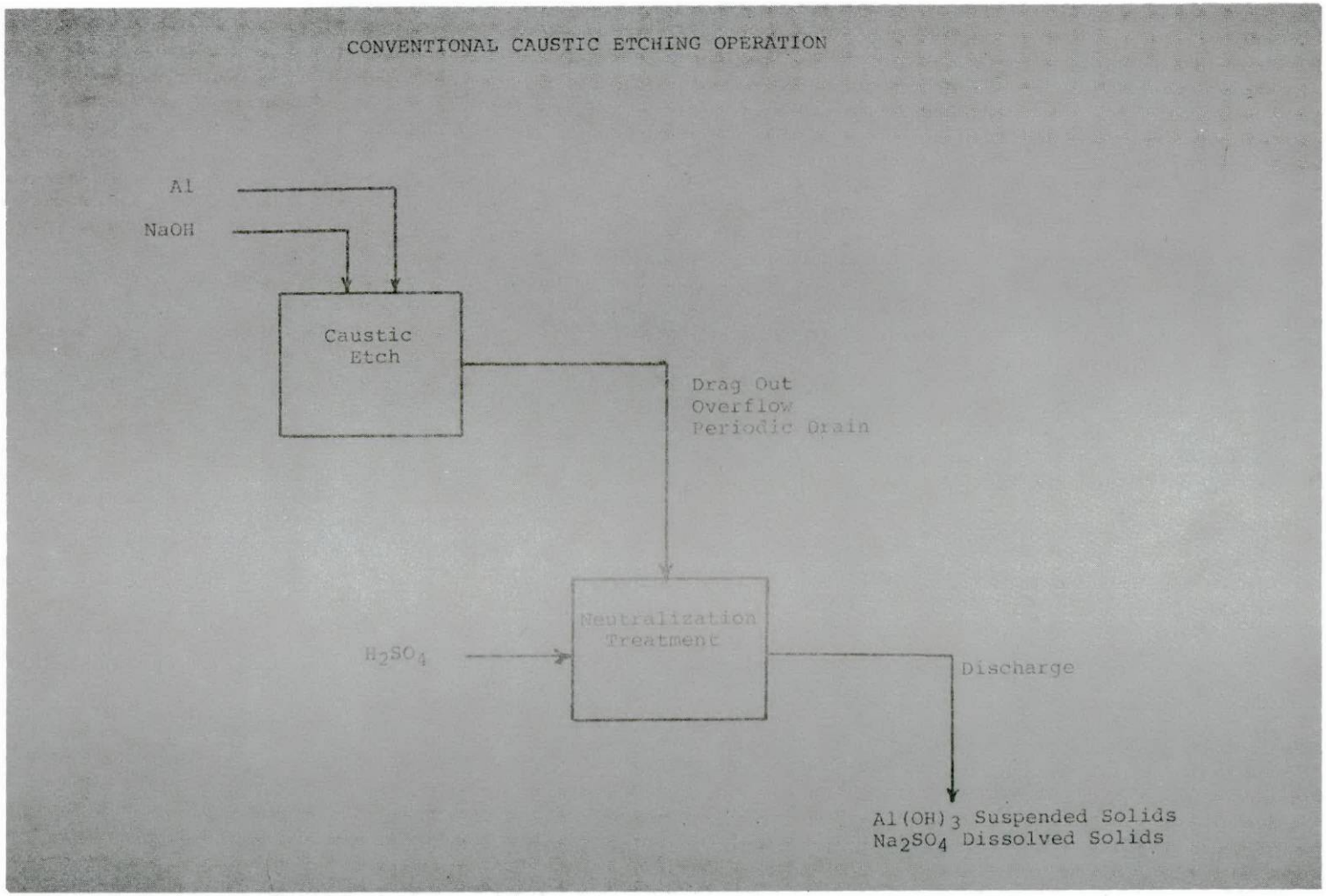
CONVENTIONAL CAUSTIC ETCHING OPERATION
Al
NaOH
Caustic Etch
Drag Out
Overflow
Periodic Drain
Neutralization Treatment
$H_2SO_4$
Discharge
$Al(OH)_3$ Suspended Solids
$Na_2SO_4$ Dissolved Solids

Figure 3

# CAUSTIC ETCH REGENERATION PROCESS

## REACTION:

$$NaAlO_2 + 2H_2O \rightarrow NaOH + Al(OH)_3$$

## EFFECTS:

- Reduces NaOH Consumption
- Eliminates Sequesterants
- Maintains Etch Composition
- Reduces Effluent Waste
- Crystalline $Al(OH)_3$ By-Product

Figure 4

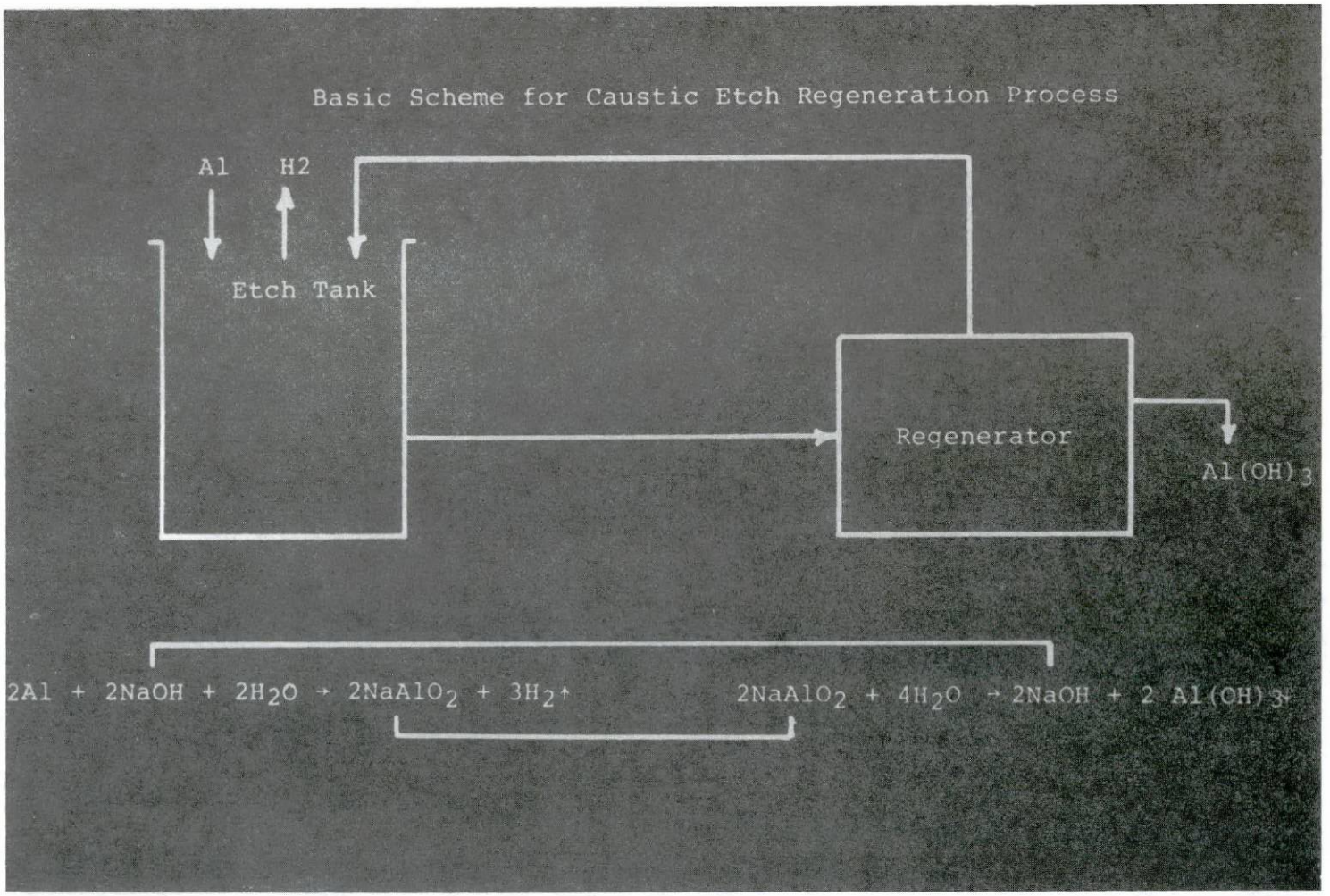
Basic Scheme for Caustic Etch Regeneration Process
Al
H2
Etch Tank
Regenerator
Al(OH)3
2Al + 2NaOH + 2H2O → 2NaAlO2 + 3H2↑
2NaAlO2 + 4H2O → 2NaOH + 2 Al(OH)3↓

Figure 5

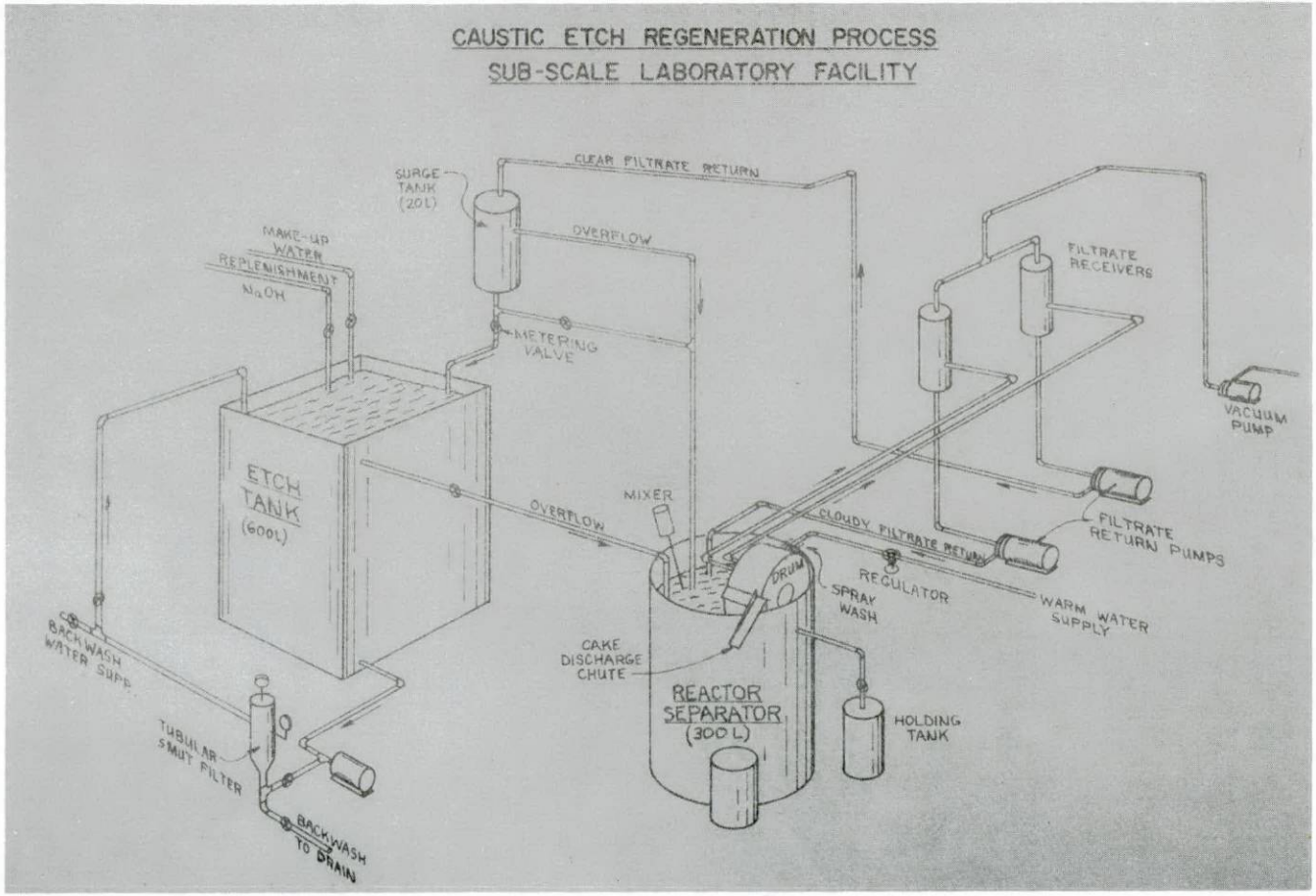
CAUSTIC ETCH REGENERATION PROCESS
SUB-SCALE LABORATORY FACILITY
SURGE TANK (20L)
CLEAR FILTRATE RETURN
OVERFLOW
MAKE-UP WATER REPLENISHMENT
NaOH
METERING VALVE
FILTRATE RECEIVERS
VACUUM PUMP
ETCH TANK (60OL)
MIXER
OVERFLOW
CLOUDY FILTRATE RETURN
FILTRATE RETURN PUMPS
DRUM
REGULATOR
SPRAY WASH
WARM WATER SUPPLY
BACKWASH WATER SUPP
CAKE DISCHARGE CHUTE
REACTOR SEPARATOR (300 L)
HOLDING TANK
TUBULAR SMUT FILTER
BACKWASH TO DRAIN

Figure 6

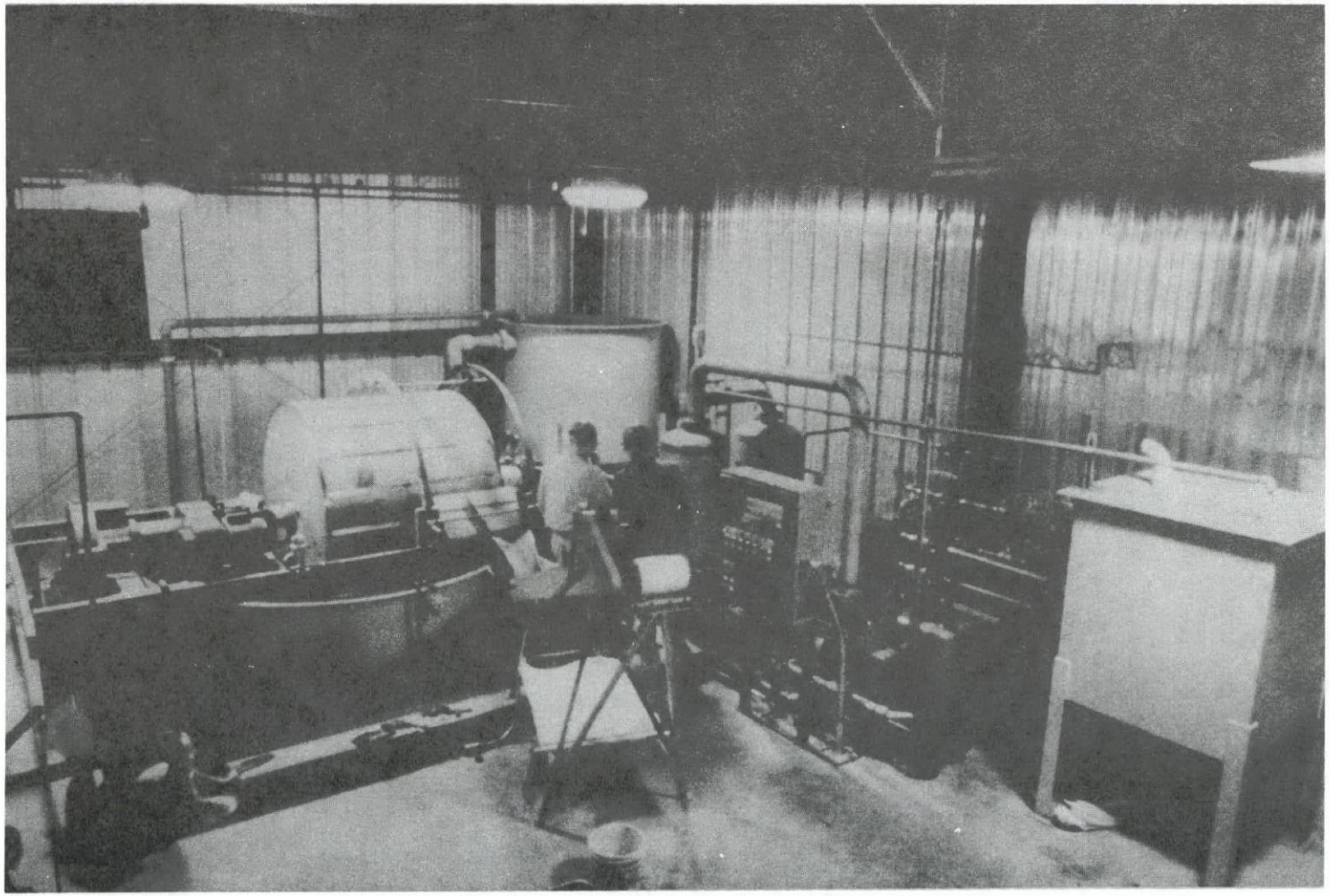

Figure 7

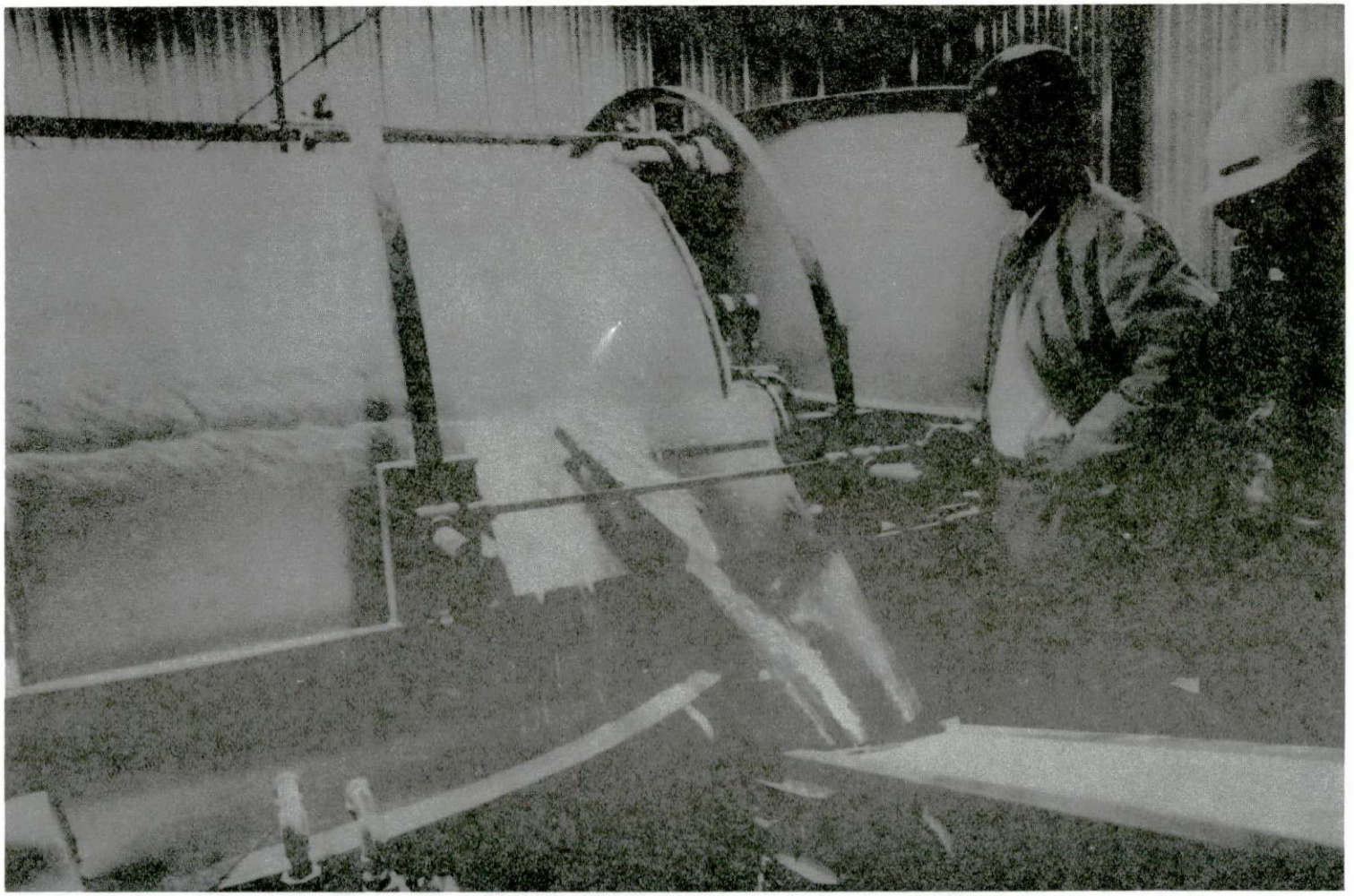

FIG 8

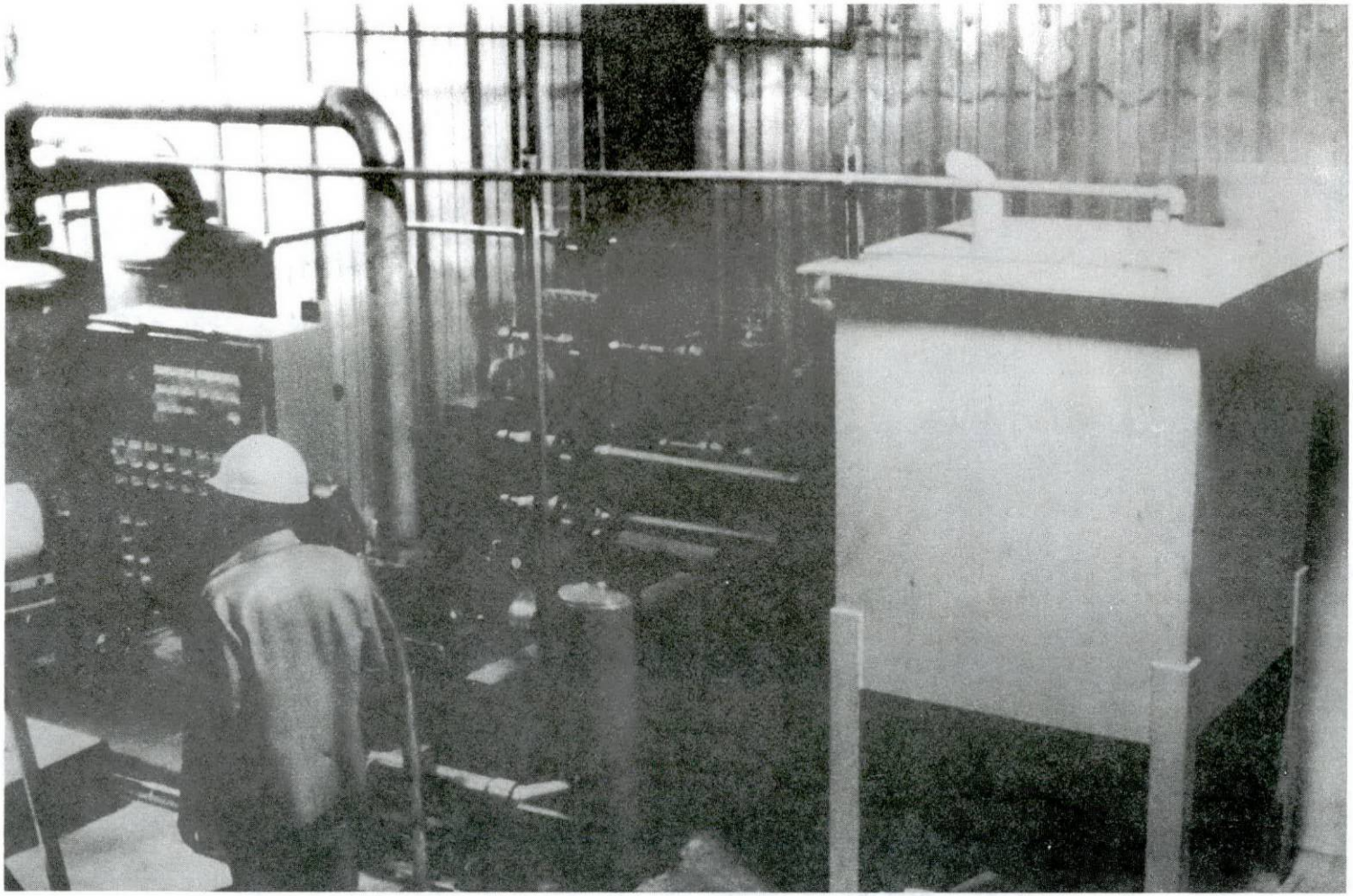

Figure 9

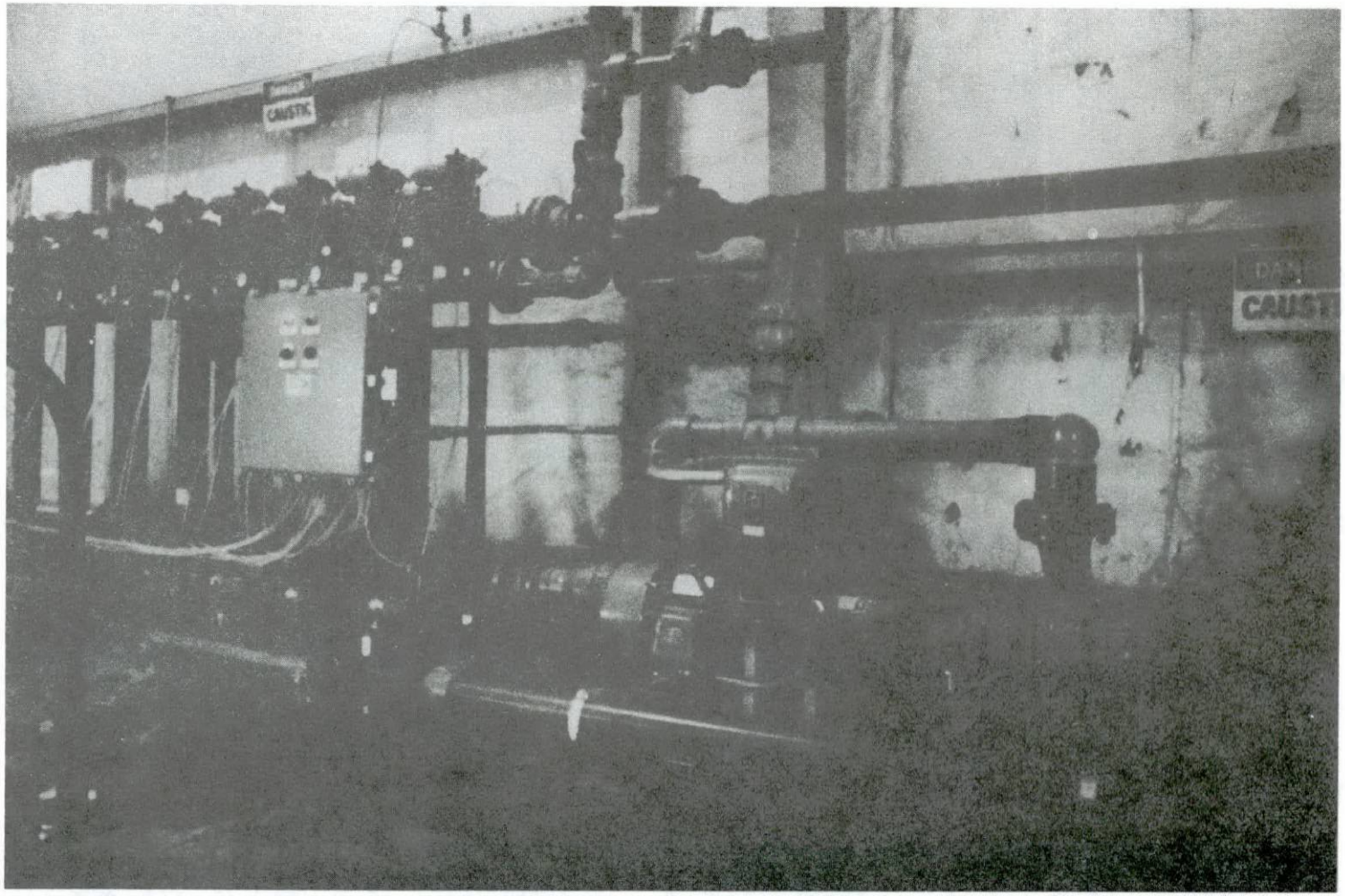

FIGURE 10

## CASE EXAMPLE
## FOR EXTRUDER/ANODIZER PROCESSING 22 MILLION $FT^2$/YR

| | POUNDS / YEAR | POUNDS / YEAR |
|---|---|---|
| NaOH for etching | 960017 | 213103 |
| NaOH for die cleaning | 42240 | |
| NaOH for waste treatment | 0 | 21123 |
| TOTAL NaOH USAGE | 1002258 | 234226 |
| $H_2SO_4$ for anodizing | 686589 | 216484 |
| $H_2SO_4$ for alum. concentrator regen. | 111680 | 70444 |
| $H_2SO_4$ for waste treatment | 377751 | 0 |
| TOTAL $H_2SO_4$ USAGE | 1176020 | 286928 |
| $Al(OH)_3$ Solids in neutral effluent | 1313321 | 305562 |
| Waste sludge produced @ 15% solids | 8755472 | 2037077 |
| $Al(OH)_3$ by product @ 90% solids | 0 | 1175609 |
| Overall reduction in neutral effluent suspended solids | — | 76.7% |
| Overall reduction in waste solids hauled to landfill | — | 63.3% |
| Overall reduction in effluent dissolved solids | — | 75.6% |
| Overall reduction in $H_2SO_4$ usage | — | 76.6% |
| Overall reduction in NaOH usage | — | 76.6% |

FIGURE 11

# CASE EXAMPLE
# ECONOMIC IMPACT

| | DOLLARS / YEAR |
|---|---|
| Reduced NaOH purchases (@$200 / T) | $ 76,803 |
| Reduced $H_2SO_4$ purchases (@$66 / T) | 29,340 |
| Elimination of etch additives | 12,000 |
| Reduced waste haulage (@$20 / T) | 55,428 |
| Elimination of spent die cleaning bath disposal | 9,000 |
| Total reduction | 182,571 |
| Operating cost | 38,000 |
| Total savings | $144,571 |
| Pay back on capital expenditures (Without consideration for depreciation, interest, variations in material costs, etc.) | Approximately 2 years |

# G-6

# Light Metals Finishing II
# Session G

## New Chemical Polishing Process of Aluminum Without the Use of Toxic Nor Nutritious Compositions and Fumes

Dr. Sakae Tajima
Environmental and Resources Research Institute (NRI),
Tokyo University and Agriculture and Tokyo City University,
Japan

# NEW CHEMICAL POLISHING PROCESS OF ALUMINUM WITHOUT THE USE OF TOXIC NOR NUTRITIOUS COMPOSITIONS AND FUMES

Sakae Tajima
Environmental and Resources Research Institute(NRI)
Tokyo University of Agriculture
and
Tokyo City University, Tokyo

## ABSTRACT

The conventional aluminum chemical polishing processes are based on phosphoric -(sulfuric)-nitric acids or ammonium bifluoride-nitric acid(Erftwerk Process mainly in West Germany). The former is popular since it results in polishing than brightening and rather tolerable for impurities and alloys. However,these solutions contain toxic and nutrtious compositions,evolving acidic fumes so that special care must be paid for neutralization,fume scrubbing,phosphoric acid recovery and recycles,waste disposal etc to comply with the recent strict regulations and the economy..Newly proposed chemical polishing solutions are based on sulfuric acid with addition of clathrate compounds,other metallic sulfates,inhibitors and in some cases surfactants. If required,the conventional phosphoric-nitric acid solutions may be gradually converted by adding new constituents, - further by supplementing sulfuric acid for the drag-out loss. The process is quite novel from the electrochemical point of view and from the modern Host-Guest chemistry. Of course,there may be still a room to be further improved.

## INTRODUCTION

Perhaps the oldest and comprehensive literature available in English for bright dipping may be the book by Hiorns (1882)(1) in which 1 measure of nearly exhausted aquafortis(nitric acid), 2 of water and 6 of hydrochloric acid, or 100 parts nitric acid, 1 part of common salt and 1 part of calcined soot are claimed to be useful to impart lustre to brass and similar articles. The author regards these two solutions as contradictory in principle; the reaction of the latter solution is so strong that the immersion time should be a few seconds. Later, the addition of sulfuric acid became popular for bright dipping for copper alloys except those containing tin or lead.
The most scientific paper together with discussions in English available to the author for bright dipping of copper and its alloys, Cd plate, Zn plate, Mg and Pb is the one by Soderberg (1945)(2) where he pointed out a theory of bright dipping, paralleling that for anodic brightening. Also he added: Larson(3) in 1934 already proposed 50% sulfuric acid, 36% nitric acid and 14% phosphoric acid, but no mention had been made for aluminum in this excellent presentation. We note the very active discussions were made by G. B. Hogaboom, C. L. Faust and other experts.

## CHEMICAL POLISHING IN PHOSPHORIC-NITRIC ACID BASED SOLUTIONS

A far as the author could be aware,the term 'chemical polishing' appeared in 1948(4). In this anonymous article, it is claimed that 'Metals that can be chemically polished successfully include brass, copper, nickel-silver, Monel, nickel and aluminum.----. Chemical polishing baths are mixtures of acids, the

basic onesbeing being phosphoric , nitric and acetic acids' The content of the paper and photos are all related to brass and Monel articles. 'Aluminum' appears once as the last word in the sentence referred to above. By checking the patent, no referece seemed to be made to aluminum. But this patent and the anonymous article are now thought to be the origin of the term 'chemical polishing'. The comprehensive book by Werneck and Pinner(1972)(5) made no reference to them. Instead,they refer to ALCOA(6) & Colonial Alloys(7) processes as the original phosphoric-nitric acid processes. Meahwhile,during the confusion of Post-War period,the Japanese were normally unaware of overseas literature until up to 1950. K.Hayasaka,quite independently in 1950,(5,8),patented a phosphoric-nitric acid mixture for chemical polishing of aluminum. According to him,he happened to find the solution while he was checking the polaization curves of aluminum electropolishing bath. His process was introduced in Japan for mass polishing of aluminum whisky caps and expanded to various articles including aluminum reflectors mainly supplied to Japan National Railway(JNR).
The addition of heavy metals ,typically Cu or Pb salt is a good idea since it displaces aluminum by local cell formation ,covering recessed area and promotes the dissolution of peaks, ,resulting in levelling action. But it is necessary to immerse in nitric acid to remove deposited copper or other smuts. According to the excellent comments by Hamlin(9), some time after immersion, a thin aluminum oxide must be formed and then it should be dissolved:

$$14\ Al + 10\ HNO_3 \rightarrow 7\ Al_2O_3 + 4\ N_2 + 2\ NO_2 + 5\ H_2O \quad (1)$$

$$Al_2O_3 + 6\ H_3PO_4 \rightarrow 2\ Al(H_2PO_4)_3 + 3\ H_2O \quad (2)$$

The over-all reaction is:

$$7\ Al + 5\ HNO_3 + 21\ H_3PO_4 \rightarrow 7\ Al(H_2PO_4)_3 + 2\ N_2 + NO_2 + 13\ H_2O \quad (3)$$

I quite agree with the formation of thin solid alumina films at the peaks. It can happen the simultaneous and/or alternate formation and dissolution take place over the entire surface.
However I sholuld like to add the common reactions:

$$Al + 3\ H_3PO_4 \rightarrow Al(H_2PO_4)_3 + 6\ (H) \quad (4)$$

$$2\ HNO_3 \rightarrow H_2O + 2\ NO + 3\ (O) \quad (5)$$

$$2\ NO + O_2(air) \rightarrow 2\ NO_2 \quad (6)$$

$$(H) + (H) \rightarrow H_2 \quad (7)$$

$$2(H) + (O) \rightarrow H_2O \quad (8)$$

$$2Al + 3\ (O) \rightarrow Al_2O_3\ (\text{thin solid film}) \quad (9)$$

since actually evolution of hydrogen is vigorous and NO is known to be easily oxidized to $NO_2$(red gas) in the air immediately. In order for aluminum to dissolve,electron acceptors are needed which are played by hydrogen ion etc. In this way,the toxic $NO_2$ gas and acid fume evolutionare vigorous and aluminum phophate (sludge) is gradually accumulated.

Chemical polishing is very simple and the throw is suitable for mass operations,but from above reasons,,neutralization, fume scrubbing equipment, recovery of rather high-priced phosphoric acid which also promotes the excess growth of inland sea,lake and river alga and weeds. Sludge disposal is becoming a serious problem, and much equipment is now in the market.
In order to solve the problem of red $NO_x$ gas evolution,the present author(10,11) proposed in 1952 the addition of urea which acts as reductant of $NO_x$ gas. The mist becomes transparent and $CO_2$, $H_2$,$N_2$ are evolved. The reaction is:

$$H_2N\text{-}CO\text{-}NH_2 + 2NO \longrightarrow 2\ N_2 + H_2 + H_2O + CO_2(H_2CO_3) \qquad (10)$$

Urea also acts as inhibitor but the demerit was that the polishing solution becomes more viscous,preventing the rinsing efficiency except in warm water. It seems this was the origin of using ammonium salts or amines as red $NO_x$ suppressor.
During and after the World War II,the author was engaged in electropolishing various metals and alloys without the use of perchloric acid as a young reserach chemist at the Materials Department of the Government Central Aeronautical Research Institute, Tokyo was in a blind condition from the world. After the War, I had very much interest in the progress achieved overseas and did my best to collect concerned literature during and after the War. Normally the foreign literatures were only become available around 1950 and we are really relaxed to see that the Japan's progress was non the less advanced as compared with those attained overseas. A comprehensive book on "Electropolishing and Chemical Polishing"(in Japanese) was published in 1952 (11)and also the Japanese progress in this field was introduced in U.S and German journals(11, 12).

## CHEMICAL POLISHING IN FLUORIDE -NITRIC ACID BASED SOLUTIONS

Another group of aluminum chemical brightening bath is based on the mixture of fluoride and nitric acid . This kind of process seems to be used mainly for high purity aluminum(Raffinal) and Al-Mg Alloy(Reflectal) in West Germany. Dr.Lattey,VAW,Bonn had shown the author one demonstration experiment. The process may be said to be rather brightening(micro-smoothing) than polishing(macro-smoothing) wherein the design of the article may be important though this is common for all electrochemical and chemical polishing processes. The two typical examples are:
(1) $HF\text{-}HNO_3$ System
This is represented by ALCOA bright dip(14)

| | | |
|---|---|---|
| HF | 1-5 % | |
| $HNO_3$ | 5 % | 90-100°C, 1-5 min. |

It is claimed to be adapted for treating many small articles due to its lower concentration and viscosity,resulting in lower drag-out loss.
(2) Erftwerk Process( 15,16,17)

| | | |
|---|---|---|
| $NH_4HF_2$ | 16 % | |
| $HNO_3$ | 13 % | |
| $Pb(NO_3)_2$ | 0.1-0 g/litre | 45-65°C, 15-30 sec. dipping |

Addition of Pb is similar to copper in phosphoric-nitric acid bath. The very low solubility of sludge(by-product) $AlF_3$(0.67 part in 100 part water at 20°C) will also be a problem. Nothing is heard of making cryolite for alumina reduction. Instead, ammonium cryolite $2NH_4F.AlF_3.1,5\ H_2O$ is also precipitated.

## NEW CHEMICAL POLISHING BATHS WITHOUT THE USE OF PHOSPHORIC,NITRIC NOR HYDROFLUORIC ACIDS AND TOXIC FUMES

Now we come to the processes newly proposed. As referred to above, aluminum chemical polishing solutions are mainly classified in 2 groups,i.e., phosphoric -(sulfuric)-nitric acids and hydrofluoric-nitric acids.
Due to the toxic and nutritious nature of these solutions, there is a strong need to develop a new process. At present,it seems,the effort is rather passive. A special session was planned at the recent AES Technical Conference in San Francisco,1982 on chemical polishing of aluminum, Papers were mostly devoted to fume scrubbing,recovery and recycle of phosphoric acid etc.
The solutons developed by the present author,based on his long experience in electropolishing,chemical polishing and anodizing since the World War II, are aimed to exclude the use of phosphoric,nitric or hydrofluoric acids.
As mentioned earlier,sulfuric acid has similar effects in various respects to phosphoric acid,but when we apply straight concentrated sulfuric acid,it attacks strongly mainly after withdrawal of aluminum from the solution of electro- or chemical polishing,leaving white compounds,mainly aluminum sulfate, on aluminum surface even if the aluminum is eventually brightened in the solution. In the case of chemical polishing,the situation is still worse.
But according to the author's experience and chemical common sense,there may be no other substitute for phosphoric nor hydrofluoric acid. Sulfamic is one possibility but its solubility is too low. Thus the author has tried to create a new idea to weaken the attack of sulfuric acid on aluminum and to eliminate the use of nitric acid. The basis for the new solutions are as follows:
(1) There is a possibility for sulfuric acid to play both roles of phosphoric acid and nitric acid(oxydant) when properly applied.
(2) Addition of metal sulfate,particularly magnesium sulfate to sulfuric acid to prevent the severe attack by considering the position of Al and Mg in the electrochemical series. Magnesium can not be an electron-acceptor for aluminum to corrode. It proved to be true that when Mg exists in appropriate amount,Al attack by sulfuric acid was greatly reduced. For Al-Mg alloys,excess Mg salt is not so favorable.
(3) The addition of clathrate compounds, based on modern Host-Guest chemistry, which absorb $H_2$, $NO_x$,$H_2O$, $H_2S$, $SO_2$ gases as well as cations and anions in their cages by Van der Waals forces and also have ion exchange capacity. In some clathrates,$Mg^{++}$ is the most difficult cation to be adsorbed luckily. The clathrate compounds have cages where above mentioned materials are trapped, depending upon the size of the cages. They also act as inhibitor. One of the typical model of clathrate is shown in Fig.1. The molecular size to be trapped is well known as calculated by Pauling and/or by Lennard-Jones. Examples of clathrate compounds will be described later.
(4) The use of inorganic inhibitors or multi-valent metal ions(as salt) which act as inhibitor by redox cycles, preventing pitting.

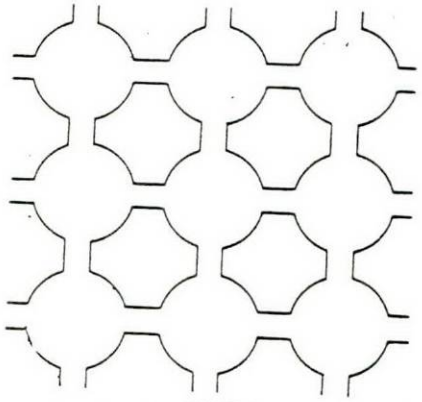

Fig.1 Typical Structure of Clathrates and Cages

Based upon these 4 principles, commercial pure Al, Al-Mg, Al-Mg-Si etc are polished excepting those containing Cu or Si in appreciable amount..
It is a great merit that $NO_x$, $H_2$, $H_2S$,,$SO_2$, etc are trapped in the clathrate, the solubilities of which in sulfuric acid are rather small at low temperature Accordingly , the conventional phophoric-nitric polishing solution can be gradually converted by supplimenting sulfuric acid for drag-out loss and by adding magnesium sulfate,clathrate etc wherein the existence of nitric acid gives no trouble. Instead,the existence of a small amount of nitric acid even gives favorable effects without evolving $NO_x$. and fumes.
The other merit is that the works to be treated can be held in the atmosphere for a minute or so before the temperature of the adhered solution is lowered, so that the polishing time can be matched with the running speed of the operation line(pre-treatment, rinsing, nitric acid dip if required, and anodizing etc. At the same time the drain of the adhered solution can be favorably recovered before rinsing.
Some examples of the new processes are given:
Example 1.

| | |
|---|---|
| Sulfuric acid(d= 1.65) | 1 litre |
| Magnesium sulfate($+7H_2O$) | 20 g |
| Inorganic clathrate compound | 5 - 10 g |
| Temperature | 80 - 110 °C |
| Immersion Time | a few to 5 min. |

As clathrate compound,we may recommend the by-product in our paper "Self-regulating High Temperature Anodizing with Full Utilization of Alkaline and Anodizing Waste", presented at the AES Milwaukee Technical Conference,1980,published in the Proceedings and also in AES official Journal(18). There are,of course, in the market similar synthetic or natural ones.
Since this solution contains neither phosphoric nor nitric acid and the hydrogen to be evolved seems mostly trapperd in the cages of the clathrate,there arises little acidic fumes except some moisture by rather high temperature. Further the existence of common sulfate ion,together with the effect of $Mg^{++}$,suppresses the excess dissolution of aluminum according to the solubility law.
The decrease in thickness is ca,5 micron (15 $g/m^2$) at about 105°C per minute, which is nearly equal or a little greater than by phosphoric-nitric bath for 1100Al For Al-Mg,,the loss is less. It is said that by Erftwerk process,the attack is stronger and 10 micron per minute(30 $g/m^2$) is reported(16).
Photo 1 shows the bycyle parts (Al 1100) before or after chemical polishing in this solution and Photo 2 shows the comparison of their insides.

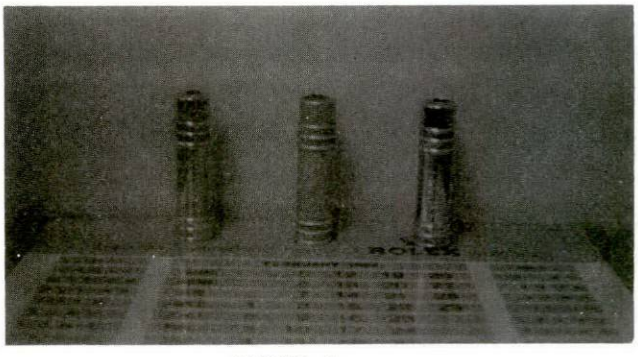

PHOTO 1




PHOTO 2

Example 2.

| | |
|---|---|
| Sulfuric acid(d= 1.60 ) | 1 litre |
| Ammonium alum | 20 g |
| Inorganic inhibitor and/or clathrate | 5 g |
| Temperature | 100°C |
| Immersion time | a few to 5 min. |

wherein the inorganic inhibitor reduces pits.

Example 3.

| | |
|---|---|
| Sulfuric acid(d= 1.65) | 0.8 litre |
| Phosphoric acid | 0.2 litre |
| Nitric acid | 2 ml |
| Magnesium sulfate(+ 7 $H_2O$) | 20 g |
| Inorganic clathrate compound | 20 g |
| Temperature | 100°C |

In this case also,the reaction is mild and the velocity can be controlled by temperature and the solution is applicable to aluminum alloys except those with appreciable Si.

When withdrrawn from the bath,the polishing reaction continues by adhered solution and enough time is available before rinsing. Since the solution contains a small amount of phosphoric acid and nitric acid,the composition corresponds to the intermediate stage for converting from conventional phosphoric-nitric bath to the newly proposed solutions. In this case, the ratio of sulfuric acid to phosphoric acid is too large to be usable without the new additions. Of course the existence of nitric acid has a beneficial effect upon polishing but gives no trouble since the decomposition compounds are trapped by co-existing clathrate. This composition is useful for mastering the new process.

Photo 3 and 4 shows a door knob made of Al-Mg polished by this solution. Please note that the recessed and intricate area is uniformly polished.

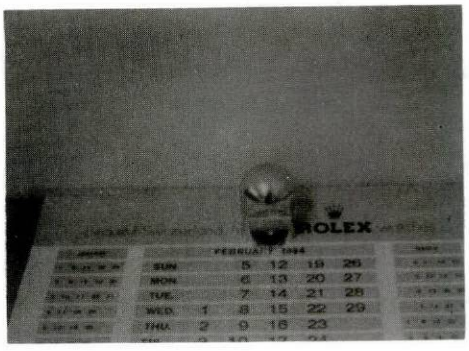


PHOTO 3

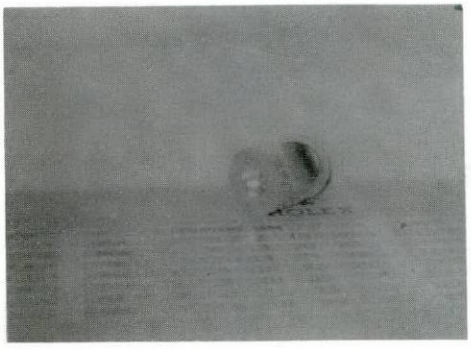

PHOTO 4

Example 4.

| | |
|---|---|
| Sulfuric acid(d=1.65) | 1 litre |
| Cobalt sulfate(+ 7 $H_2O$) | 30 g |
| Calthrate compound | 10 g |
| Temperature | 100°C |

Generally the trasition metals,particularly iron group metals such as Fe, Ni, Co etc which form multi-valent ions act as inhibitor by repetition of redox reaction and especially the addition of Co was found effective for aluminum. As is usually done,the addition of copper ion is also effective in the new

solutions,but the additional dipping in nitric acid is needed as usually done to remove copper and is not recommended in the new solutions except when it is needed to remove smuts accoring to the kind of alloys.

## FUNDAMENTALS

According to the author's experience and to that of Soderberg(2) referred to before,both during the World War II, electropolishing(anodic brightening) is done on the balance of metal activation and passivation processes, so is the case with chemical polishing. In the former,anodic potentialplays both roles, particularly anodic passivation(11.19),while in the latter,chemical activator and passivator and mild corrosion are needed as clearly shown by the combinationof phosphoric-nitric acids or hydrofluoric-nitric acids. In the case of the new process presently proposed, sulfuric acid acts both as activator and passivatorand the suppression of strong attack upon aluminum is controlled by magnesium sulfate , ,clathrate compounds,poly-valent metal ions and by some inhibitors. Surfactants are recommended to to wet the surface and to assist levelling and also to make easier the rinsing. However the surfactant must be stable in strong sulfuric acid. This kind of surfactant may be the one like alkyl-aryl sulfonate(soapless soap) which is,however,rather stable in the waste..
The over-all reactions are:

$$H_2SO_4 \longrightarrow H_2O + SO_2 + (O) \qquad (11)$$

$$H_2SO_4 \longrightarrow H_2S + 4(O) \quad \text{(side reaction)} \qquad (12)$$

$$R + SO_2 \longrightarrow R(SO_2) \quad \text{(R: clathrate)} \qquad (13)$$

$$R + H_2S \longrightarrow R(H_2S) \qquad (14)$$

$$2\,Al + 3(O) \longrightarrow Al_2O_3 \qquad (15)$$

Since the dissolution of clathrate compounds is not always easy at room temperature,so that when the temperature was lowered after the operation, a precipitate appears. Even during operation(temperature is maintained by the heat of dissolution reaction),these compounds happen to suspend in the solution,which give no trouble or even seem to assist smoothing by rubbing the aluminum surface.

Since the composition of the new solution is mainly sulfates,the dissolved Al will be precipitated as sludge together with clathrates,the extra care more than the conventional chemical polishing or anodizing may not be so much needed. However,it must be borne in mind that aluminum ion is known to be detrimental to plant growth excepting the tea group trees(the extract of which is known to contain aluminum and fluoride ions),since $Al^{+++}$ ions fix phosphate disturbing absorption by plants.

## CONCLUSION

It may be an exciting adventure to attempt to use sulfuric acid as basic acid in place of phosphoric or hydrofluoric acid. This attempt is entirely dependent upon the findings of the role played by magnesium and other sulfates,upon the modern concepts of "host-guest' chemistry and upon the effective use of inhibitors mainly to moderate the acid attack and to reduce pitting.

The process proposed is a substitute for hitherto undoubtedly used widely and recognized phosphoric-nitric acid based solutions which have a great merit still and have played an important role for a long time in aluminum finishing and in expanding its uses.
The new process has just attained the same effect without toxic nor nutritious problems. The process is still young and has much to be improved.
Meanwhile, hydrofluoric-nitric acid process is not used in Japan for aluminum, The situation seems the same in the United States. However, this system has found another new important role,i.e.,cleaning and finishing of semi-conductor metals.

ACKNOWLEDGEMENT

The author is grateful to Mrs.Dr. Michiko Shimura of the Tokyo City University for her cooperation,particularly in taking micrographic pictures and to Messers Kazuo Yokoyama and Yasuhiko Fujita for encouragement.
The author is also grateful to the Light Metal Educational Foundations (Keikinzoku Shogakukai),Osaka,Japan for the partial financial support.

REFERENCES

1. A.Hiorns, Metal Colouring and Bronzing,,First Edition,Mac Millan and Co..,1892,London
2. G.Soderberg, Trans. Electrochem. Soc., 88 297(1945). The manuscript received July 19,1945 and presented at the Symposium 'Before and After Plating',held at New York City,Oct. 24,1945, F.A.Lowenheim presiding.
3. L.O.Larson, US. Patent,1,984,534 Dec. 18, 1934.
4. Anonimous, Metal Finish. 47 Nov. 50(1949)
5. S.Wernick and R.Pinner, The Surface Treatment and Finishing of Aluminium and its Alloys, Vol.I ,Robert Draper Ltd., Teddington,1972(4th ed.)



PHOTO 5 as-rolled Al(1100) x400



PHOTO 6 chemically polished for 1 min in phosphoric-nitric acid solution x400



PHOTO 7 chemically polished for 1 min in the solution, Example 1. x400

6. Aluminum Co. of America, Brit. Pat. 625,834;659,747;US.Pat.2,650,157(31.12.1947)
7. Colonial Alloys Co., US Pat. 2,729,551
8. K.Hayasaka, Jap. Patent, 187067(1950)
9. M.E.Hamelin, Plating and Surface Finish. 47 Nov. 50(1983)
10. S.Tajima, Y.Kimura and T.Fukushima, Metal Finish. 51 Sept. 69(1953)
11. S.Tajima, 'Electropolishing and Chemical Polishing'(in Japanese) pp.323 Sangyo Tosho Publishing Co.,Tokyo, First Ed.,1952; 14, B81-126(1960)
12. S.Tajima,Metal Finish.,47 95(1949), ibid. 48 June 95(1950)
13. S.Tajima,Metalloberfläche 6, Heft 4-5,pp.54-58,73-75(1952)
14. S.Gelfman, City College Vector, 12 54,58,72,74(1948)
15. W.Helling, H.Neunzig, Aluminium 28 Heft 9, 289(1952)
16. R.Lattey, Metall, 7 Heft 15/16, 582(1953)
17. R.Lattey, and H.Neunzig,Metalloberfläche 9 Heft 7, A97(1955)
18. S.Tajima and Y.Umehara, Proc. 67th Annual Tech. Conf.E-4(Milwaukee,June 1980); Plating and Surface Finish., 68 Jan. 54(1981)
19. S.Tajima, 'Anodic Oxidation of Aluminum' in Advances in Corrosion Science and Technology(M.G.Fontana and R.W.Staehle,ed) Vol.1,pp.229-362, Plenum Press,New York(1969)


AMERICAN ELECTROPLATERS' SOCIETY